UC Santa Cruz
UC Santa Cruz Electronic Theses and Dissertations

Title

Accessory Proteins of the Melanocortin-4 Receptor Signaling System

Permalink

https://escholarship.org/uc/item/7mb5k26p

Author

Chen, Valerie

Publication Date

2020

Peer reviewed|Thesis/dissertation

University of California
Santa Cruz

Accessory Proteins of the Melanocortin-4 Receptor Signaling System

A dissertation submitted in partial satisfaction
of the requirements for the degree of

DOCTOR OF PHILOSOPHY

in

CHEMISTRY

by

Valerie Chen

June 2020

The Dissertation of Valerie Chen is approved:

_____
Professor Michael Stone, chair

_____
Professor Carrie Partch

_____
Distinguished Professor Glenn Millhauser

_____
Quentin Williams
Acting Vice Provost and Dean of Graduate Studies

Table of Contents

List of Figures

Abstract

Accessory Proteins of the Melanocortin-4 Receptor Signaling System

Valerie Chen

The melanocortin 4-receptor (MC4R) is a G-protein coupled receptor (GPCR) that is expressed in the hypothalamus and is essential for energy homeostasis. Mutations in MC4R are the most common monogenic cause of obesity. MC4R signaling is regulated by its agonist α-MSH and by its endogenous antagonist the agouti-related peptide (AgRP). AgRP's orexigenic effects are extraordinarily long-lasting. Additionally, several accessory proteins have been implicated in the regulation of MC4R. This dissertation focuses on two accessory proteins, syndecan-3 and the melanocortin receptor accessory protein 2 (MRAP2). Syndecan-3 is a cell-surface heparan sulfate proteoglycan that is hypothesized to increase the local concentration of AgRP at MC4R neurons. AgRP's prolonged orexigenic effects are dependent on positively charged residues outside of its inhibitor cystine knot (ICK) core. These positively charged residues are not required for MC4R binding or antagonism but are crucial for electrostatic interactions with heparan sulfate. Using AgRP peptides with varying positive charge in its non-ICK segments along with glycan arrays and feeding studies with AgRP-treated mice, we find that AgRP increases food intake and reduces energy expenditure. These actions are dependent on AgRP's positive charges and the AgRP variant that has the most protracted feeding response also has the greatest affinity

for heparan sulfate. These findings further support the role of syndecan-3 in facilitating AgRP signaling. MRAP2 increases α-MSH-induced MC4R signaling and also modulates several other hypothalamic GPCRs that regulate metabolism. MRAP2 is a single-pass membrane protein that forms highly unusual anti-parallel dimers. Despite MRAP2's important role in energy balance, very little is known regarding the molecular details that drive its unique structure and how this relates to its ability to modulate MC4R. Using a panel of MRAP2 variants, biochemical experiments reveal that MRAP2 dimerizes through its transmembrane domain. We also show that MRAP2 can form parallel dimers using a luciferase-based molecular complementation assay. Elucidating the functions and structures of MC4R's accessory proteins will not only further our understanding of GPCR signaling but also aid in the development of therapeutics aimed at modulating this complex signaling system.

Acknowledgements

I believe that obtaining a doctorate degree is almost impossible without a team of friends and family offering their time, kindness, and support. My friends have always been encouraging and supportive. I knew I could find comfort in them whenever I needed it and they were always there to lend an ear. I would have never been able to start my scientific career if it were not for the love and support of my family. I want to thank my mom for instilling the importance of education early on in my life as she would accompany me at the kitchen table for hours every evening to make sure my homework was completed on time. My dad has always been a role model when it came to hard work and perseverance. My parents taught me to always try my very best and that regardless of the outcome, to be proud of my efforts. Following this mantra has helped me through hard times in graduate school. I also want to thank my grandma for offering me her words of wisdom when I needed it and encouraging me to take a step back to see the bigger picture. Finally, my fiancé Michael has always believed in me and has helped me through many difficult times. His unwavering patience and support have been instrumental in this process. I truly believe that the support of my family and the sacrifices they made for me is why I had the opportunity to pursue my graduate degree.

Rafael Palomino, Jillian Miller, Eric Evans, and Kate Markham were all wonderful mentors when I joined the lab. You were all so patient with me and put up with all

my questions. The expertise that I gained when I first joined the lab was an important foundation for my graduate career and I wouldn't have been able to get this far without the help of the graduate students who came before me. Graham Roseman and I started in the lab at the same and Kevin Schilling joined shortly after. I'm thankful for the countless scientific discussions we've had and I'm so glad that we went on this journey together. You guys were both there whenever I needed someone to bounce ideas off of or to talk my results over with. Rachel Oldfield, Mark Wadolkowski, Tufa Assafa, and Francesca Pavlovici brought fresh ideas and positivity to the lab. I knew I could count on you guys for good conversations and advice about experiments. The past and current members of the Millhauser lab have always been such amazing scientists and people. I want to thank you all for making me laugh, listening to me ramble, and for being my friends.

During my time in graduate school, I've had the opportunity to mentor several awesome undergraduates: Matt Marquis, Ashley Wong, Tony Bruno, Laura Britt, and Shaneen Britton Acevedo. I appreciate you guys for all of your hard work and for keeping me motivated. I'm so proud of you all and am happy that I got to play a small role in your own scientific journeys.

I want to thank my advisor Glenn Millhauser for always keeping his office door open and being so supportive. Glenn taught me how to think independently, ask the right

questions, and how to communicate my research to others. He also gave me the

freedom to pursue research that was outside the scope of the lab. Thank you for

believing in me, even at times when I didn't believe in myself. I also want to thank

my committee members Michael Stone and Carrie Partch for their willingness to

help and their good advice. I'm so lucky to have to have been part of such an

amazing Chemistry department for both my undergraduate and graduate careers. I

will always remember my time here and am thankful for all the support over the

years.

The text of chapter 2 of this dissertation includes reprint of the following previously published material:

The co-author Jihuan Chen performed all animal-based feeding experiments and glycan arrays from chapter 2. The co-authors Pietro Paolo Sanna and Glenn L. Millhauser directed and supervised the research which forms the basis for chapter 2 of the dissertation.

Chapter 1

Introduction

The Melanocortin-4 Receptor

Hunger and satiety signals from peripheral tissues in the form of circulating hormones such as ghrelin, leptin, glucagon-like peptide 1, and peptide YY are integrated by the central melanocortin system in the hypothalamus and brainstem. The central melanocortin system, which acts as a rheostat for energy balance, is composed of neurons that produce neuropeptide Y (NPY), agouti-related protein (AgRP), and GABA, neurons that produce pro-opiomelanocortin (POMC), and neurons that express their downstream targets, the melanocortin 3 receptor (MC3R) and the melanocortin 4 receptor (MC4R). Food intake that is induced by ghrelin, a circulating orexigenic hormone produced by the gut, is mediated by AgRP/NPY neurons in the arcuate nucleus of the hypothalamus (ARC) [1–4]. Leptin, an anorexigenic hormone that is produced by adipocytes, is also sensed by neurons in the ARC. AgRP mRNA levels are decreased by leptin and stimulated by fasting while POMC mRNA is stimulated by leptin and reduced by fasting [5,6]. The signals from AgRP and POMC arcuate nucleus neurons are then relayed to downstream neurons of the paraventricular nucleus of the hypothalamus (PVH) that express MC3R and MC4R. Both MC3R and MC4R are involved in the regulation of energy homeostasis but the exact role of MC3R in food intake remains enigmatic and controversial, therefore, this dissertation will focus solely on MC4R. Central MC4R regulates satiety, energy expenditure, blood pressure, and growth. Recent work has shown that MC4R signaling involves several accessory proteins that are expressed in the ARC and in the PVH.
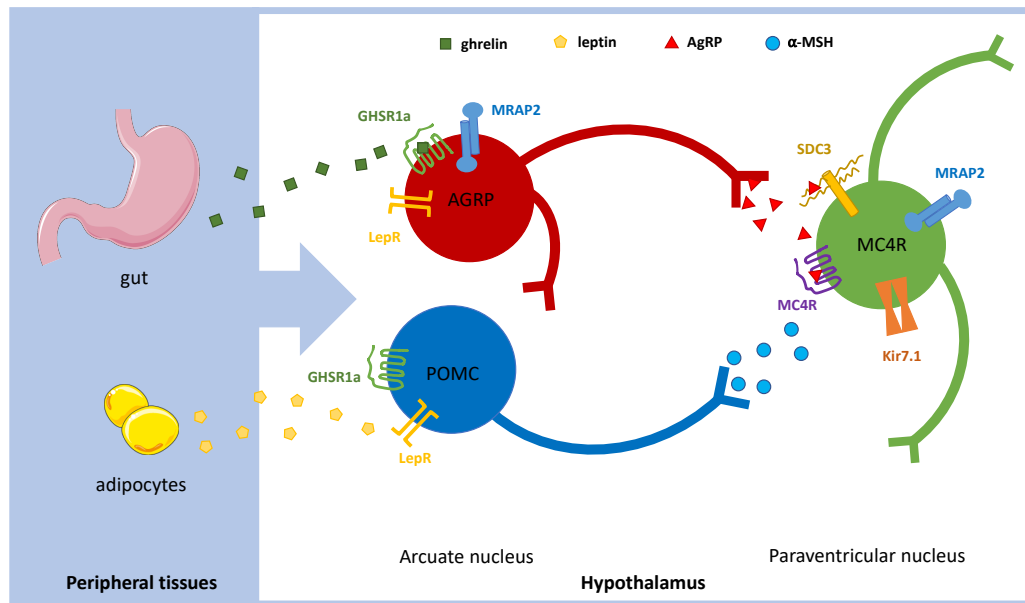
Figure 1 The central melanocortin signaling system. Circulating hormones from peripheral tissues such as ghrelin and leptin are integrated in the hypothalamus. AgRP and POMC neurons of the arcuate nucleus that express the leptin receptor (LepR) and the ghrelin receptor (GHSR1a) detect these peripheral feeding cues and modulate downstream MC4R neurons in the paraventricular nucleus. Several accessory proteins have been shown to regulate MC4R signaling such as syndecan-3 (SDC3), Kir7.1 (inwardly rectifying potassium channel 7.1), and melanocortin receptor accessory protein 2 (MRAP2).

There are a total of five melanocortin receptors that regulate a variety of physiological processes throughout the body. MC4R was first cloned using degenerate PCR and homology screening in 1993 and was found to localize in the brain [7]. Localization studies in adult rat brains showed that MC4R mRNA is present in the cortex, thalamus, hypothalamus, brainstem, and spinal cord [8,9]. MC4R is expressed predominantly in the hypothalamus, a critical center known to be important for feeding behavior and

energy homeostasis. In addition to the central nervous system where its functions are most well-studied, MC4R has also been found in the peripheral nervous system and in enteroendocrine L cells of the gastrointestinal system [10,11].

The human MC4R gene is intronless and codes for a 332 amino acid protein. MC4R's sequence is highly conserved and the identity of full-length mammalian and fish MC4R is approximately 67% [12]. MC4R, as well as the four other melanocortin receptors, are rhodopsin-like, class A G-protein coupled receptors (GPCRs). GPCRs are cell surface receptors that activate intracellular signaling pathways through downstream G-proteins in response to extracellular ligand binding. Through the widely accepted, classical view of GPCR signaling, α-MSH induced activation of MC4R through the Gα_s pathway results in an increase in cAMP and negative energy balance, whereas AgRP antagonism reduces levels of cAMP and results in positive energy balance.
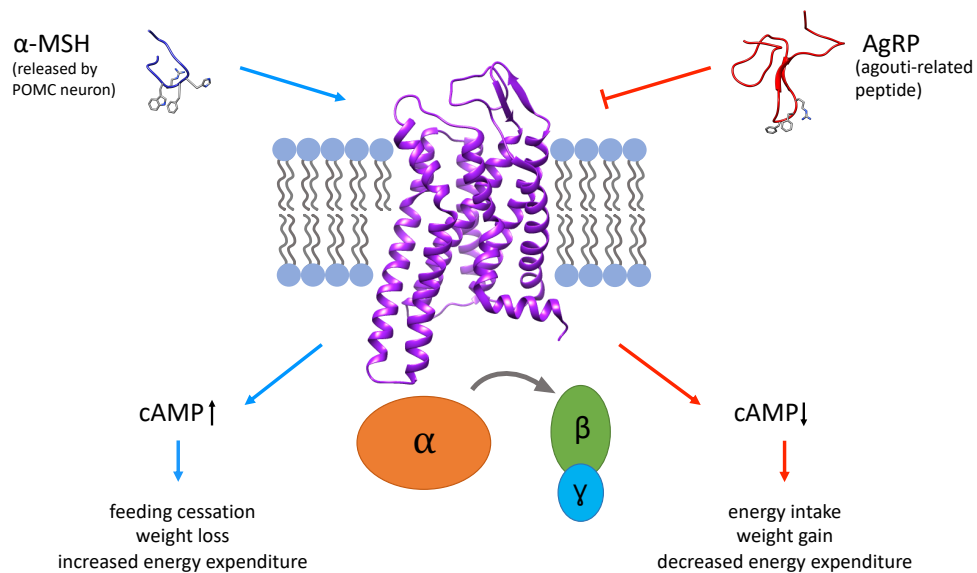
Figure 2 MC4R is a GPCR that is regulated by both endogenous agonist α-MSH and antagonist/inverse agonist AgRP. Classical MC4R signaling occurs through G_s signaling where receptor activation by α-MSH leads to an increase in intracellular levels of cAMP and a negative energy balance phenotype. AgRP inverse agonism decreases levels of cAMP and results in a positive energy balance phenotype. The model of MC4R is from Pogozheva et al. 2005[13].

Based on its atomic resolution structure, MC4R is distinct from other reported class A GPCR structures [14]. These structural differences are due to MC4R having a short extracellular loop 2 (ECL2), lacking the conserved disulfide bond that connects ECL2 to helix III that is present in other GPCRs, and having an unusual outward position of helix V. Additionally, crystallographic structural studies show that Ca^{2+} is a cofactor for ligand binding and the presence of Ca^{2+} increases the affinity and potency of MC4R's endogenous agonist, α-MSH. While MC4R does have four potential glycosylation sites, the biological significance of glycosylated MC4R is unknown.

POMC

Melanocortin peptides are derived from the gene encoding the prohormone pro-opiomelanocortin (POMC). POMC is first cleaved by prohormone convertase 1/3 which yields proACTH and ACTH. These cleavage products are then processed by prohormone convertase 2, resulting in the production ACTH (1-17) which is then cleaved by carboxypeptidase E. The resulting peptide is amidated by peptidyl α-amidating mono-oxygenase and is then finally acetylated by N-acetyltransferase to generate mature α-MSH [15,16]. In the hypothalamus, α-MSH is produced by POMC neurons in the arcuate nucleus of the hypothalamus and the commissural nucleus of the solitary tract of the brain stem. POMC-derived peptides are agonists at MC3R and MC4R. As with the other melanocortin receptors, treatment with melanocortin peptides α-MSH and ACTH leads to an increase in intracellular cAMP in MC4R-expressing cells [7].

One of the first signs that POMC-derived peptides played a role in energy homeostasis was in 1986 when Vergoni and colleagues injected ACTH(1-24) into the lateral ventricle of starved rats or into the ventromedial hypothalamus during the nocturnal feeding phase and an inhibition of food intake was observed in these rats[17]. More than a decade later, it was shown that mice lacking POMC are obese, have impaired adrenal development, and altered pigmentation [18]. In this study, when POMC null mice were

treated with peripheral α-MSH, 40% of the excess body weight was lost. Similarly, in humans, mutations in POMC leads to severe early onset obesity, adrenal insufficiency, and red hair [19]. Setmelanotide, a synthetic α-MSH mimic, has been shown to be successful for the treatment of obesity in patients with POMC deficiency as well as with patients with leptin receptor deficiency [20,21].

AgRP Structure and Function

A unique feature of MC4R signaling is that it is also regulated by an endogenous antagonist and inverse agonist, AgRP. This feature was first brought to light due to the unique obesity phenotype of mice with dominant mutations in the agouti locus, specifically the lethal yellow (A^y) and variable yellow (A^{vy}) alleles. The agouti gene encodes the agouti- signaling peptide (ASiP) (Bultman et al. 1992) and controls coat color in mice through antagonization of the melanocortin-1 receptor (MC1R) in the skin [22]. Heterozygous mice with the lethal yellow and variable yellow mutations have yellow fur, increased hepatic lipogenesis, and increased linear growth [23]. These mice are also obese, hyperinsulinemic, and have noninsulin-dependent diabetes. The A^y and A^{vy} alleles result in ectopic expression of ASiP, including in the brain where it antagonizes MC4R [22–24]. AgRP was first cloned due to its sequence similarity to agouti, specifically by the cysteine-rich C-terminal ends [25]. In human tissues, AgRP was found to be primarily expressed in the adrenal gland, subthalamic nucleus, and the hypothalamus. Additionally, AgRP expression was upregulated in leptin-deficient and

leptin receptor-deficient mice, suggesting that AgRP has a role in regulating food intake. This was further validated by Graham and colleagues in 1997 by isolating the AgRP gene and showing that overexpression of AgRP leads to obesity in transgenic mice [26].

Figure 3 Lethal yellow agouti mouse (Ay) Dominant mutations in the agouti allele result in ectopic expression of agouti, an endogenous antagonist of MC1R. Agouti antagonism of both MC1R in the skin and MC4R in the central nervous system results in a mouse that has yellow fur and is obese[27].

AgRP is released from neurons in the arcuate nucleus of the hypothalamus in response to energy deficit and is a potent antagonist and inverse agonist at MC3R and MC4R [28,29]. AgRP inverse agonism at these receptors leads to increased feeding and decreased energy expenditure [29]. Central administration of AgRP (83-132) induces food intake in animals for up to 7 days after injection [30]. Given AgRP's ability to stimulate long-term feeding and decrease energy expenditure, central melanocortin antagonism may have clinical benefit for treating cachexia, a wasting disease

associated with some cancers. Furthermore, AgRP has been shown to reverse the symptoms of cancer cachexia in animal models [31].

AgRP-induced feeding is longer in duration that all known feeding stimulators. As a result, several studies have been aimed at understanding the interplay between AgRP structure and its long-lasting orexigenic effects. Full-length AgRP is a 132 residue pro-protein that is post-translationally processed by pro-protein convertase 1/3 into its mature form AgRP(83-132) [32]. AgRP (83-132) contains five disulfide bonds, three of which form an inhibitor cystine knot (ICK) motif [33]. An AgRP variant that only encompasses this ICK core, AgRP(87-120), is sufficient for MC3/4R binding and antagonism [34]. However, regions of polypeptide flanking the ICK core are both highly conserved and necessary for prolonged AgRP-induced feeding.
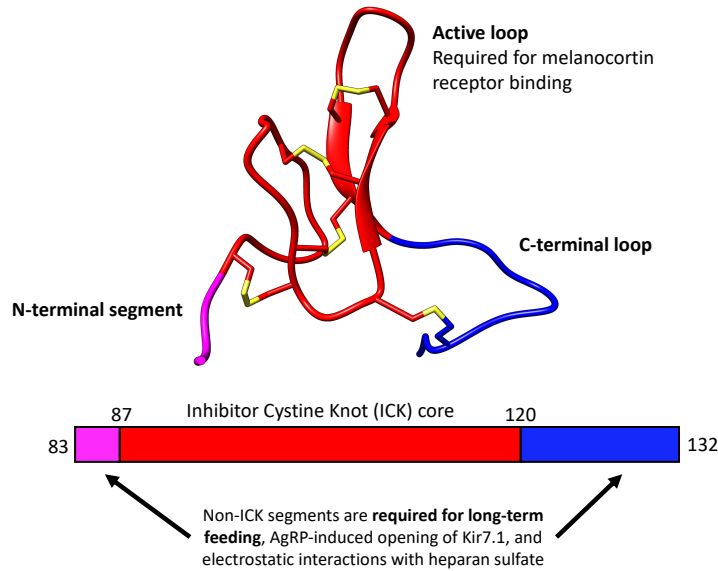
Figure 4 Nuclear magnetic resonance structure (Protein DataBank: 1HYK) of mature AgRP-WT(83-132) The inhibitor cystine knot (ICK) core is in red, the N-terminal segment is in magenta and the C-terminal loop is in blue. Disulfide-bonds are in yellow. The ICK core that contains the active loop is sufficient for MC3/4R binding and antagonism. However, the N-terminal segment and C-terminal loop that flank the ICK core are highly conserved and required for AgRP-induced long-term feeding.

Recent studies highlight the importance of AgRP's non-ICK sequence. AgRP (83-132), but not AgRP(87-120), has been shown to hyperpolarize MC4R neurons and decrease the frequency of action potential firing [35]. Additionally, central administration of AgRP peptides with varying charge in the non-ICK segments showed that positive charge density within the non-ICK segments is positively correlated with feeding and weight gain [34,36]. A peptide variant possessing additional positive charges, AgRP 4K, is able to enhance feeding in rats even beyond that of wild-type AgRP. In contrast, AgRP 4Q, a peptide with non-ICK charges removed, results in a weak 24-hour feeding response

that returns to baseline in just 2 days. The significance of AgRP's non-ICK segments can be largely explained by the presence of accessory proteins that modulate MC4R signaling. These accessory proteins will be the focus of subsequent sections in this chapter.

Mutations in MC4R and Metabolic Disease

The loss of MC4R results in late-onset obesity in mice and MC4R insufficiency in mice leads to hyperphagia, increased fat mass, dysregulated glucose homeostasis, and reduced energy expenditure [37–39]. As expected, the MC4R null phenotype is strikingly similar to the agouti obesity phenotype. An interesting feature of MC4R-deficiency is that that mice that are heterozygous for the MC4R null allele have an obesity phenotype that is intermediate to wild-type mice and mice that are homozygous for the mutant allele [37]. The haploinsufficiency of MC4R is also present in humans. In 1998, the first two obesity-causing frameshift mutations were discovered in two different patients, both resulted in truncated MC4R protein and both were heterozygous mutations [40,41]. Gene dosage effects are uncommon with GPCRs and most morbid obesity-causing mutations in humans are either homozygous and compound heterozygous mutations as seen with leptin, leptin receptor, and POMC gene mutations. Over 200 obesity-associated MC4R mutations have now been identified and it is now evident that mutations in MC4R are the most common

monogenetic cause of human obesity, accounting for approximately 5% of investigated obese patients [42–45].
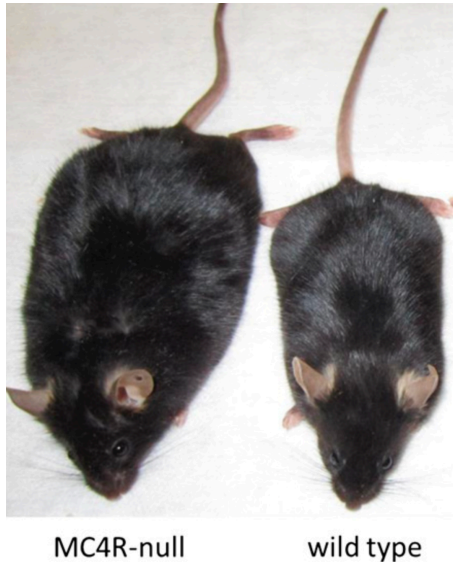
Figure 5 Loss of MC4R results in severe obesity in mice. Heterozygous mutations in MC4R are the most common genetic cause for obesity in humans [46].

MC4R-null   wild type

MC4R variants have been functionally characterized based on their surface expression, ligand binding, and ability to stimulate cAMP in vitro when transfected into mammalian cells. Based on these pharmacological studies, there are five classes of MC4R mutations [47]. Class I mutants are null mutations that result in defective protein synthesis or increased rate of degradation. Class II mutants are mutants that are improperly trafficked and retained in the ER, most likely due to misfolding. Class II mutants makes up the largest class of MC4R mutants. Class III mutants are properly trafficked to the cell surface but have defective ligand binding. This category also includes receptors that have enhanced inhibition by AgRP. Class IV mutants are

expressed at the cell surface, can bind ligands, but are defective when it comes to G_s signaling. MC4R has been shown to have a high level of constitutive activity, possibly through its own N-terminal domain acting as a tethered ligand [48,49]. MC4R mutants with decreased constitutive activity also fall under class IV. Finally, class V accounts for variants that have unknown defects. This classification system does not consider downstream effects such as desensitization and β-arrestin recruitment, alternative signaling pathways, or receptor signaling that is mediated by accessory proteins.

Alternative MC4R-signaling Pathways and Accessory Proteins

MC4R has long been known to signal through the G_s pathway, leading to increase levels of intracellular cAMP through activation of adenylate cyclase, which then activates protein kinase A. However, there are obesity-causing mutations in MC4R that do not result in impaired G_s/cAMP signaling [50]. There is now growing evidence for alternative MC4R-signaling pathways. GPCRs can also couple to G_q and G_{11}, which activates phospholipase C β (PLCβ) which hydrolyzes phosphatidylinositol phosphate (PIP2) into diacylglycerol (DAG) and inositol triphosphate (IP3). DAG activates protein kinase C (PKC) while IP3 signaling leads to Ca^{2+} release into the cytoplasm. The treatment of mouse MC4R-expressing cells with α-MSH results in an increase of intracellular Ca^{2+} [51,52]. The relevance of MC4R signaling through the $G_{q/11}$ pathway was further solidified by showing that PVH-specific loss of G_q and G_{11} leads to severe hyperphagic obesity, increased linear growth, and animals that no longer display

MC4R agonist-induced inhibition of food intake [53]. It has also been shown that AgRP induces β-arrestin mediated endocytosis of MC3R and MC4R and also activates the $G_{i/o}$ signaling pathway [54,55]. From these studies, AgRP not only antagonizes agonist binding and inhibits constitutive activity of MC4R but also reduces receptors levels at the cell surface and inhibits cAMP through $G_{i/o}$.

It is now apparent that melanocortin signaling is more complex than previously understood and cannot be explained simply by agonist/antagonist modulation of the Gαs pathway. There is neuroanatomical evidence that supports independent actions of α-MSH and AgRP. Specifically, POMC synapses target PVH dendrites while AgRP synapses target PVH cell soma [56]. Additionally, there are several accessory proteins that have now been shown to be involved in the regulation of MC4R. AgRP's ability to promote a prolonged orexigenic response has always been of particular interest. Syndecan-3, a cell surface heparan sulfate proteoglycan, has been implicated in facilitating AgRP signaling by localizing AgRP at MC4R neurons in the PVH [57–59]. This is further supported by the fact that AgRP has been shown to be a heparan sulfate binding protein [60]. AgRP and α-MSH are able to regulate an inwardly-rectifying potassium channel (Kir7.1) through MC4R [35]. This occurs in a G protein-independent fashion; however, the mechanism by which MC4R couples to Kir7.1 is unknown. Finally, agonist binding at MC4R has been shown to be modulated by the melanocortin receptor accessory protein 2 (MRAP2) [61–65]. Understanding the role of

syndecans in MC4R signaling, the molecular basis of MC4R's G-protein independent

modulation of Kir7.1, and the mechanism by which MRAP2 regulates MC4R will help

to redefine the current model of melanocortin and GPCR signaling.
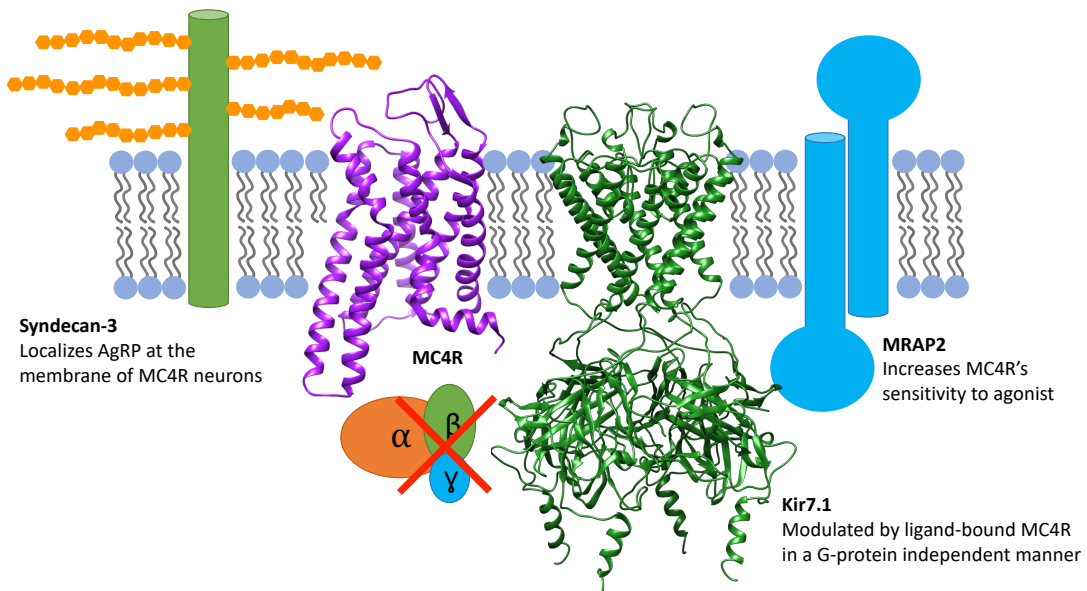
Figure 6 Accessory proteins that modulate MC4R signaling. Syndecan-3, a cell surface proteoglycan, has been implicated in AgRP's prolonged orexigenic effects by localizing AgRP at the membrane of MC4R neurons and protecting AgRP from proteolytic degradation. Kir7.1, an inwardly rectifying potassium channel, has been shown to hyperpolarize or depolarize MC4R neurons in response to AgRP or α-MSH binding to MC4R, respectively. The mechanism by which MC4R couples to Kir7.1 is independent of G-protein signaling. The Kir7.1 model is from the lab of Professor Jared Denton at Vanderbilt University. MRAP2 is an accessory protein that regulates several hypothalamic GPCRs that are important in the regulation of food intake. MRAP2 enhances MC4R signaling by increasing MC4R's sensitivity to α-MSH.

Syndecans

Syndecans are a class of cell-surface heparan sulfate proteoglycans (HSPGs). As its

name suggests, HSPGs are characterized their covalently attached heparan sulfate

glycosaminoglycan chains (GAG). These glycosaminoglycan chains are between 40-300 sugars long, highly heterogenous, and polyanionic due to the presence of sulfate groups and uronic acids [66]. In addition to heparan sulfate chains, syndecan-1 and syndecan-3 also contains chondroitin sulfate chains near the plasma membrane [67]. HSPGS can either be membrane-bound, in secretory-vesicles, or secreted into the extracellular matrix and are known to bind a variety of extracellular ligands such as chemokines, cytokines, and growth factors. Additionally, membrane-bound HSPGs such as syndecans can also act as coreceptors. All four members of the syndecan family are characterized by their attachment to the cell membrane through a single transmembrane core protein with GAG chains covalently linked through threonine and serine residues. Syndecan-3 was first cloned from neonatal rat Schwann cells and then later in humans, where it was found to localize in the brain, adrenal glands, and spleen [68,69]. Syndecans can undergo ectodomain shedding which involves cleavage of a proteolytic site on the extracellular site of the protein. Specifically, syndecan-3 is shed from the cell surface of neurons by matrix metalloproteases [70]. Syndecan-3 has also been implicated in neuronal development as there is high expression of syndecan-3 in the developing nervous system, specifically along axons [71].

There are several lines of evidence that suggest syndecan-3 plays a key role in the regulation of energy balance through the modulation of MC4R signaling. Food deprivation leads to an increase in hypothalamic syndecan-3 levels and transgenic

expression of syndecan-1 in the hypothalamus leads to hyperphagia, severe mature-onset obesity, and diabetes. These mice are also phenotypically similar to agouti lethal yellow, AgRP-overexpression, MC4R null, and POMC null mice [57]. Cell surface syndecan-3 is thought to potentiate AgRP signaling by localizing AgRP at MC4R neurons since hypothalamic AgRP protein levels are significantly reduced in mice lacking syndecan-3 [59]. Consistent with this observation, syndecan-3 null mice are more sensitive to MC4R agonist, MTII [58]. Furthermore, in vitro experiments in HEK293 cells show significant cAMP inhibition by AgRP when MC4R is co-expressed with syndecan-3 [57]. Ectodomain shedding of syndecan-3 by matrix metalloproteases also appears to be important for the regulation of food intake. A pan-selective matrix metalloprotease inhibitor increases food intake in fasted rats. Additionally, the mRNA expression of tissue inhibitor metalloprotease-3 (TIMP-3), which is known to inhibit several metalloproteases, is increased in response to food deprivation [58].

AgRP is known to be a heparan sulfate binding protein and associates with glycosaminoglycan chains through complementary electrostatic interactions [60]. Work by Palomino et al. mapped out regions of AgRP that are relevant to this electrostatic interaction[60]. The introduction of additional lysine residues in AgRP increases overall positive charge as well as increases its affinity to heparan sulfate [36]. In fact, there is a striking positive relationship between AgRP net positive charge and its ability to increase body weight in treated animals [34]. Electrostatic interactions between AgRP

and negatively charged heparan sulfate glycosaminoglycans on syndecan-3 are thought to increase local concentrations of AgRP and protect AgRP from proteolytic degradation. This supports a model where syndecan-3 significantly increase AgRP's half-life, driving AgRP-induced long-term feeding.
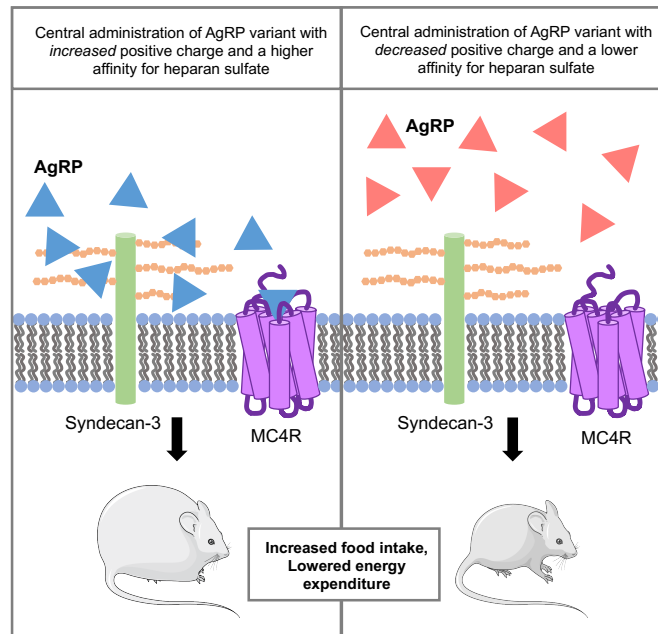
Figure 7 The orexigenic and metabolic effects of AgRP are positively correlated with AgRP's overall positive charge and affinity for heparan sulfate. AgRP has been demonstrated to be heparan sulfate binding protein and heparan sulfate is one of the major glycosaminoglycans that decorate syndecan-3. Additionally, hypothalamic levels of AgRP are significantly reduced in mice lacking syndecan-3.

Ion Channels

G-protein-coupled inwardly rectifying potassium channels (GIRKs), also known as Kir3 channels, are activated by G-proteins, through direct binding of Gβ/γ subunits [72,73]. GIRKs are activated by pertussis toxin-sensitive G-protein complexes, specifically $G_{i/o}$ [73]. When MC4R is expressed in a hypothalamic cell line, it signals in a pertussis toxin-sensitive manner [55]. Additionally, AgRP selectively activates this $G_{i/o}$ signaling pathway. Based on this evidence, it is possible that MC4R signaling can activate GIRKs in vivo.

MC4R also modulates inwardly-rectifying potassium channels that are outside of the Kir3/GIRK family. MC4R couples to Kir7.1, an inwardly-rectifying potassium channel, in a novel G-protein-independent manner [35]. Electrophysiology on MC4R neurons from murine hypothalamic slice preparations showed that treatment with α-MSH depolarized neurons and increased the frequency of action potential firing, while AgRP hyperpolarized these neurons and inhibited action potential firing. The depolarization from α-MSH could not be blocked by GDPβS, an inhibitory GDP analogue or by GTPγS, a nonhydrolyzable GTP analogue, as well as several other inhibitors of G-protein signaling, supporting a G-protein independent mechanism. Current-voltage analysis and a panel of Kir channel blockers were used to pinpoint Kir7.1 as the channel responsible for the α-MSH -induced depolarization. The regulation of Kir7.1 by MC4R ligands was further validated using a thallium flux assay

to measure the flow of Tl$^+$ ions through Kir7.1 in HEK293 cells that are co-expressing MC4R. Prolonged G-protein-coupled signaling through MC4R causes desensitization, however, Tl$^+$ flux through Kir7.1 is hypersensitized by pre-treatment with α-MSH. Additionally, these experiments also showed that AgRP's non-ICK segments are essential for AgRP's modulation of Kir7.1 as AgRP (83-132), but not AgRP(87-120), biases the opening of Kir7.1. Interestingly, MC1R also couples to Kir7.1 and mutations in Kir7.1 cause defects in pigmentation in zebrafish [74].

Tissue-specific deletion of Kir7.1 in MC4R neurons in mice lead to late-onset obesity, increased linear growth, glucose intolerance, and resistance to the anorexic effect of administered melanocortin peptides [75]. Unexpectedly, AgRP-induced feeding is still intact in these mice. The exact mechanism by which MC4R regulates Kir7.1 is unclear. There is evidence that co-expression of GPCR's alters Kir7.1 glycosylation in HEK293 cells and that the glycosylation state of Kir7.1 affects its permeation properties [76]. Further studies are needed to determine exactly how MC4R ligands modulate Kir7.1, however, this novel G-protein-independent signaling pathway supports independent actions of AgRP and α-MSH and may help explain AgRP-induced prolonged feeding and MC4R's gene dosage effects.

Melanocortin Receptor Accessory Protein 2 (MRAP2)

The role of the melanocortin accessory protein 1 (MRAP1) as an obligate accessory protein of MC2R was determined in 2005 after the protein was first identified in 2002 from adipocytes [77,78]. Mutations in MRAP1 result in unresponsiveness to ACTH, a phenotype that is also consistent with mutations in MC2R. MRAP1 is required for trafficking, ACTH-binding, and signaling of MC2R [77,79]. Previously, expression of functional MC2R through transfections was notoriously challenging and was only achieved in cell lines that were adrenocortical in origin [80].

MRAP2, a homolog of MRAP1, is expressed in the brain and the adrenal gland and shares 39% amino acid identity to MRAP1 in the N-terminal and transmembrane domains [81]. MRAP1 and MRAP2 can interact with all five melanocortin receptors. The human MRAP2 gene has 4 exons and codes for a 205 residue protein that has a single glycosylation site at residue 9. MRAP1 and MRAP2 are both single-pass transmembrane proteins (type 1) that have dual topology at the cell surface, meaning they can be threaded through the membrane in both orientations [79,82]. This unusual topology was discovered using bimolecular fluorescence complementation experiments and with epitope detection using antibodies raised against the N- or C-terminal ends of MRAP1 or MRAP2. MRAP1 and MRAP2 are the only two proteins that are known to have dual topology in the eukaryotic proteome. They also both form dimers or higher order oligomers at the cell surface [79,81,82].

MRAP2 is an important component for the regulation of energy balance. Whole body and brain-specific deletion of MRAP2 results in severe obesity in mice, with increased body length and increased white adipose tissue size [61]. In this study, MRAP2 was found to enhance MC4R's response to cAMP. In zebrafish, MRAP2a, the larval form of the protein, inhibits MC4R signaling while MRAP2b, which is expressed later on in development, increase sensitivity of MC4R to α-MSH [62]. Obesity-associated mutations in MRAP2 have also been reported in human [61,83,84]. MRAP2 is clearly an important modulator of MC4R signaling. Interestingly, mice with MC4R knockout alone are more obese than mice with deletion of both MC4R and MRAP2 [61]. This is not consistent with MRAP2 only acting through MC4R and suggests that MRAP2 may also promote feeding through a different mechanism.

MRAP2 has now been shown to regulate several GPCRs in the hypothalamus that are important for food intake that are outside of the melanocortin receptor family. MRAP2 promotes feeding through both inhibition of prokineticin receptor-1 and potentiation of growth hormone secretagogue receptor 1a (GHSR1a, ghrelin receptor) [85–87]. Specifically, MRAP2 is important for starvation sensing in AgRP neurons that express GHSR1a [86]. MRAP2 inhibits constitutive activity of GHSR1a, enhances its G-protein dependent signaling, and inhibits recruitment of β-arrestin [87]. MRAP2 also decreases food intake through inhibition of the orexin receptor 1 (OX1R) [88]. MRAP2

copurifies with OX1R and significantly decreases surface expression of the OX1R. MRAP2 unarguably plays a key role in the regulation of energy homeostasis. However, there are several aspects of MRAP2's biology that are still unknown, such as the mechanisms by which MRAP2 regulates GPCRs. This endeavor will be challenging due to MRAP2's promiscuity.
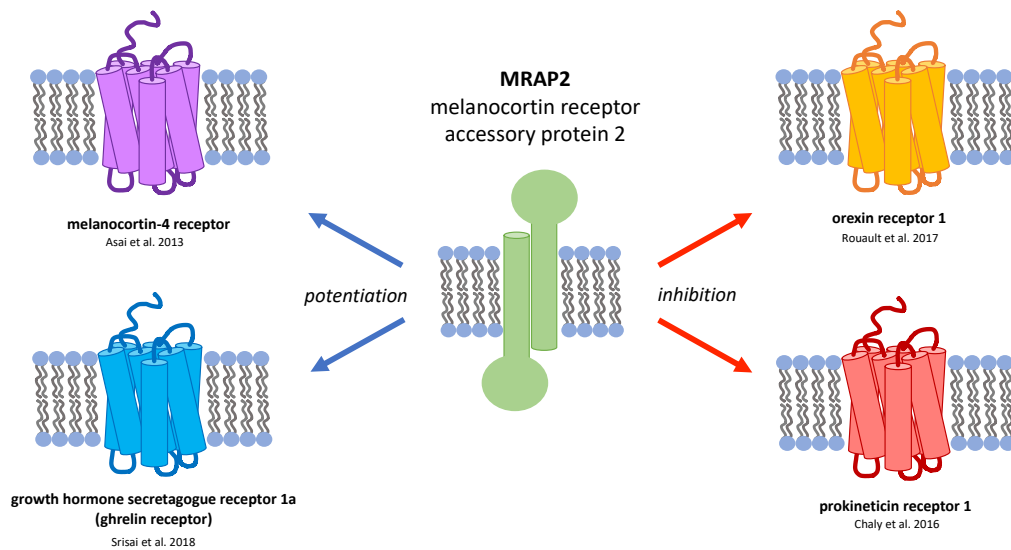
Figure 8 MRAP2 regulates several hypothalamic GPCRs that are important for the regulation of energy homeostasis. MRAP2 promotes feeding in the ARC through potentiation of the ghrelin receptor in ARC AgRP neurons and inhibition of prokineticin receptor 1 signaling. MRAP2 also inhibits feeding in the PVH through enhancement of MC4R signaling and inhibition of orexin receptor 1 trafficking and signaling.

Dissertation Motivation and Specific Aims

In the past decade, the advancements in genetic techniques such as optogenetics and DREADDS (designer receptors exclusively activated by designer drugs) has fueled

several discoveries aimed at untangling the complexities of the melanocortin neural circuit. Using DREADD technology to activate ARC AgRP neurons, there is now direct evidence that AgRP neuropeptide release from these neurons is sufficient for a delayed but prolonged feeding response, while NPY and GABA mediate acute effects [89]. Additionally, through channel rhodopsin-assisted circuit mapping, authors were able to confirm that PVH MC4R neurons are in fact the downstream target for ARC AgRP-driven hunger [90]. There are ARC AgRP efferents to different brain regions that express MC4R such as the lateral hypothalamus and the anterior bed nucleus of the stria terminalis, and while they are sufficient to drive feeding, these projections do not promote food intake through inhibition of MC4R. These experiments that allow for direct stimulation of AgRP and MC4R neurons are critical for understanding how these neurons regulate food intake. AgRP neuron activation likely coincides with AgRP neuropeptide release, however, the mechanistic details after AgRP neuropeptide release remains largely unknown. Chapter 2 of this dissertation aims to elucidate the molecular details of AgRP-induced long-term feeding and how accessory proteins such as syndecan-3 potentiate AgRP's orexigenic effects. We show that AgRP's non-ICK sequence and charge have a clear role in the enhancement of AgRP's orexigenic effects. Additionally, we have gained a great amount of insight into the long-term metabolic effects of AgRP-treated animals and the role accessory proteins play in facilitating AgRP action.

MRAP2 is an important modulator of MC4R signaling and is essential for energy homeostasis across different species, from zebrafish to humans [61,62,84]. Despite MRAP2's emerging role in the regulation of several GPCRs that are critical for food intake, there are very limited structural studies on MRAP2. Based on biochemical experiments, MRAP2 and its homolog MRAP1 form highly unusual anti-parallel dimers at the cell surface [81,82]. It is unclear how MRAP2's oligomerization and dual orientation relate to its ability to modulate MC4R. In order to investigate the mechanism by which MRAP2 regulates MC4R and other GPCRs, we must first understand the molecular details that drive MRAP2's unusual topology and structure. Chapter 3 of this dissertation highlights key differences between MRAP2 and MRAP1 in terms of the structural features that drive dual orientation and oligomerization. Additionally, we show that MRAP2 can oligomerize in a different orientation than previously shown. Uncovering the molecular features that dictate MRAP2's structure and how it relates to MC4R function will undoubtably aid in our understanding of GPCR-accessory protein biology as a whole, as well as improve therapeutic efforts aimed at modulating these receptors.

References

(1) Nakazato, M.; Murakami, N.; Date, Y.; Kojima, M.; Matsuo, H.; Kangawa, K.; Matsukura, S. A Role for Ghrelin in the Central Regulation of Feeding. *Nature* **2001**, *409* (6817), 194–198.

(2) Kamegai, J.; Tamura, H.; Shimizu, T.; Ishii, S.; Sugihara, H.; Wakabayashi, I. Chronic Central Infusion of Ghrelin Increases Hypothalamic Neuropeptide Y and Agouti-Related Protein MRNA Levels and Body Weight in Rats. *Diabetes* **2001**, *50* (11), 2438–2443.

(3) Chen, H. Y.; Trumbauer, M. E.; Chen, A. S.; Weingarth, D. T.; Adams, J. R.; Frazier, E. G.; Shen, Z.; Marsh, D. J.; Feighner, S. D.; Guan, X.-M.; Ye, Z.; Nargund, R. P.; Smith, R. G.; Van der Ploeg, L. H. T.; Howard, A. D.; MacNeil, D. J.; Qian, S. Orexigenic Action of Peripheral Ghrelin Is Mediated by Neuropeptide Y and Agouti-Related Protein. *Endocrinology* **2004**, *145* (6), 2607–2612.

(4) Wang, Q.; Liu, C.; Uchida, A.; Chuang, J.-C.; Walker, A.; Liu, T.; Osborne-Lawrence, S.; Mason, B. L.; Mosher, C.; Berglund, E. D.; Elmquist, J. K.; Zigman, J. M. Arcuate AgRP Neurons Mediate Orexigenic and Glucoregulatory Actions of Ghrelin. *Mol Metab* **2013**, *3* (1), 64–72.

(5) Mizuno, T. M.; Mobbs, C. V. Hypothalamic Agouti-Related Protein Messenger Ribonucleic Acid Is Inhibited by Leptin and Stimulated by Fasting. *Endocrinology* **1999**, *140* (2), 814–817.

(6) Mizuno, T. M.; Kleopoulos, S. P.; Bergen, H. T.; Roberts, J. L.; Priest, C. A.; Mobbs, C. V. Hypothalamic Pro-Opiomelanocortin MRNA Is Reduced By Fasting in Ob/Ob and Db/Db Mice, but Is Stimulated by Leptin. *Diabetes* **1998**, *47* (2), 294–297.

(7) Gantz, I.; Miwa, H.; Konda, Y.; Shimoto, Y.; Tashiro, T.; Watson, S. J.; DelValle, J.; Yamada, T. Molecular Cloning, Expression, and Gene Localization of a Fourth Melanocortin Receptor. *J. Biol. Chem.* **1993**, *268* (20), 15174–15179.

(8) Mountjoy, K. G.; Mortrud, M. T.; Low, M. J.; Simerly, R. B.; Cone, R. D. Localization of the Melanocortin-4 Receptor (MC4-R) in Neuroendocrine and Autonomic Control Circuits in the Brain. *Mol Endocrinol* **1994**, *8* (10), 1298–1308.

(9) Kishi, T.; Aschkenasi, C. J.; Lee, C. E.; Mountjoy, K. G.; Saper, C. B.; Elmquist, J. K. Expression of Melanocortin 4 Receptor MRNA in the Central Nervous System of the Rat. *J. Comp. Neurol.* **2003**, *457* (3), 213–235.

(10) Gautron, L.; Lee, C.; Funahashi, H.; Friedman, J.; Lee, S.; Elmquist, J. Melanocortin-4 Receptor Expression in a Vago-Vagal Circuitry Involved in Postprandial Functions. *J Comp Neurol* **2010**, *518* (1), 6–24.

(11) Panaro, B. L.; Tough, I. R.; Engelstoft, M. S.; Matthews, R. T.; Digby, G. J.; Møller, C. L.; Svendsen, B.; Gribble, F.; Reimann, F.; Holst, J. J.; Holst, B.; Schwartz, T. W.; Cox, H. M.; Cone, R. D. The Melanocortin-4 Receptor Is Expressed in Enteroendocrine L Cells and Regulates the Release of Peptide YY and Glucagon-like Peptide 1 In Vivo. *Cell Metabolism* **2014**, *20* (6), 1018–1029.

(12) Stäubert, C.; Tarnow, P.; Brumm, H.; Pitra, C.; Gudermann, T.; Grüters, A.; Schöneberg, T.; Biebermann, H.; Römpler, H. Evolutionary Aspects in Evaluating Mutations in the Melanocortin 4 Receptor. *Endocrinology* **2007**, *148* (10), 4642–4648.

(13) Pogozheva, I. D.; Chai, B.-X.; Lomize, A. L.; Fong, T. M.; Weinberg, D. H.; Nargund, R. P.; Mulholland, M. W.; Gantz, I.; Mosberg, H. I. Interactions of Human Melanocortin 4 Receptor with Nonpeptide and Peptide Agonists,. *Biochemistry* **2005**, *44* (34), 11329–11341.

(14) Jing, Y.; Gimenez, L. E.; Hernandez, C. C.; Wu, Y.; Wein, A. H.; Han, G. W.; McClary, K.; Mittal, S. R.; Burdsall, K.; Stauch, B.; Wu, L.; Stevens, S. N.; Peisley, A.; Williams, S. Y.; Chen, V.; Millhauser, G. L.; Zhao, S.; Cone, R. D.; Stevens, R. C. Determination of the Melanocortin-4 Receptor Structure Identifies Ca2+ as a Cofactor for Ligand Binding. *Science* **2020**.

(15) Zhou, A.; Bloomquist, B. T.; Mains, R. E. The Prohormone Convertases PC1 and PC2 Mediate Distinct Endoproteolytic Cleavages in a Strict Temporal Order during Proopiomelanocortin Biosynthetic Processing. *J. Biol. Chem.* **1993**, *268* (3), 1763–1769.

(16) Pritchard, L. E.; Turnbull, A. V.; White, A. Pro-Opiomelanocortin Processing in the Hypothalamus: Impact on Melanocortin Signalling and Obesity. *Journal of Endocrinology* **2002**, *172* (3), 411–421.

(17) Vergoni, A. V.; Poggioli, R.; Bertolini, A. Corticotropin Inhibits Food Intake in Rats. *Neuropeptides* **1986**, *7* (2), 153–158.

(18) Yaswen, L.; Diehl, N.; Brennan, M. B.; Hochgeschwender, U. Obesity in the Mouse Model of Pro-Opiomelanocortin Deficiency Responds to Peripheral Melanocortin. *Nature Medicine* **1999**, *5* (9), 1066–1070.

(19) Krude, H.; Biebermann, H.; Luck, W.; Horn, R.; Brabant, G.; Grüters, A. Severe Early-Onset Obesity, Adrenal Insufficiency and Red Hair Pigmentation Caused by POMC Mutations in Humans. *Nature Genetics* **1998**, *19* (2), 155–157.

(20) Kühnen, P.; Clément, K.; Wiegand, S.; Blankenstein, O.; Gottesdiener, K.; Martini, L. L.; Mai, K.; Blume-Peytavi, U.; Grüters, A.; Krude, H. Proopiomelanocortin Deficiency Treated with a Melanocortin-4 Receptor Agonist. *New England Journal of Medicine* **2016**, *375* (3), 240–246.

(21) Clément, K.; Biebermann, H.; Farooqi, I. S.; Ploeg, L.; Wolters, B.; Poitou, C.; Puder, L.; Fiedorek, F.; Gottesdiener, K.; Kleinau, G.; Heyder, N.; Scheerer, P.; Blume-Peytavi, U.; Jahnke, I.; Sharma, S.; Mokrosinski, J.; Wiegand, S.; Müller, A.; Weiß, K.; Mai, K.; Spranger, J.; Grüters, A.; Blankenstein, O.; Krude, H.; Kühnen, P. MC4R Agonism Promotes Durable Weight Loss in Patients with Leptin Receptor Deficiency. *Nature Medicine* **2018**, *24* (5), 551–555.

(22) Lu, D.; Willard, D.; Patel, I. R.; Kadwell, S.; Overton, L.; Kost, T.; Luther, M.; Chen, W.; Woychik, R. P.; Wilkison, W. O.; Cone, R. D. Agouti Protein Is an Antagonist of the Melanocyte-Stimulating-Hormone Receptor. *Nature* **1994**, *371* (6500), 799–802.

(23) Yen, T. T.; Gill, A. M.; Frigeri, L. G.; Barsh, G. S.; Wolff, G. L. Obesity, Diabetes, and Neoplasia in Yellow A(vy)/- Mice: Ectopic Expression of the Agouti Gene. *The FASEB Journal* **1994**, *8* (8), 479–488.

(24) Miller, M. W.; Duhl, D. M.; Vrieling, H.; Cordes, S. P.; Ollmann, M. M.; Winkes, B. M.; Barsh, G. S. Cloning of the Mouse Agouti Gene Predicts a Secreted Protein Ubiquitously Expressed in Mice Carrying the Lethal Yellow Mutation. *Genes Dev.* **1993**, *7* (3), 454–467.

(25) Shutter, J. R.; Graham, M.; Kinsey, A. C.; Scully, S.; Lüthy, R.; Stark, K. L. Hypothalamic Expression of ART, a Novel Gene Related to Agouti, Is up-Regulated in Obese and Diabetic Mutant Mice. *Genes Dev.* **1997**, *11* (5), 593–602.

(26) Graham, M.; Shutter, J. R.; Sarmiento, U.; Sarosi, L.; Stark, K. L. Overexpression of Agrt Leads to Obesity in Transgenic Mice. *Nature Genetics* **1997**, *17* (3), 273.

(27) Cone, R. D. Studies on the Physiological Functions of the Melanocortin System. *Endocrine Reviews* **2006**, *27* (7), 736–749.

(28) Haskell-Luevano, C.; Chen, P.; Li, C.; Chang, K.; Smith, M. S.; Cameron, J. L.; Cone, R. D. Characterization of the Neuroanatomical Distribution of Agouti-Related Protein Immunoreactivity in the Rhesus Monkey and the Rat. *Endocrinology* **1999**, *140* (3), 1408–1415.

(29) Ollmann, M. M.; Wilson, B. D.; Yang, Y.-K.; Kerns, J. A.; Chen, Y.; Gantz, I.; Barsh, G. S. Antagonism of Central Melanocortin Receptors in Vitro and in Vivo by Agouti-Related Protein. *Science* **1997**, *278* (5335), 135–138.

(30) Hagan, M. M.; Benoit, S. C.; Rushing, P. A.; Pritchard, L. M.; Woods, S. C.; Seeley, R. J. Immediate and Prolonged Patterns of Agouti-Related Peptide-(83–132)-Induced c-Fos Activation in Hypothalamic and Extrahypothalamic Sites. *Endocrinology* **2001**, *142* (3), 1050–1056.

(31) Joppa, M. A.; Gogas, K. R.; Foster, A. C.; Markison, S. Central Infusion of the Melanocortin Receptor Antagonist Agouti-Related Peptide (AgRP(83-132)) Prevents Cachexia-Related Symptoms Induced by Radiation and Colon-26 Tumors in Mice. *Peptides* **2007**, *28* (3), 636–642.

(32) Creemers, J. W. M.; Pritchard, L. E.; Gyte, A.; Le Rouzic, P.; Meulemans, S.; Wardlaw, S. L.; Zhu, X.; Steiner, D. F.; Davies, N.; Armstrong, D.; Lawrence, C. B.; Luckman, S. M.; Schmitz, C. A.; Davies, R. A.; Brennand, J. C.; White, A. Agouti-Related Protein Is Posttranslationally Cleaved by Proprotein Convertase 1 to Generate Agouti-Related Protein (AGRP)83–132: Interaction between AGRP83–132 and Melanocortin Receptors Cannot Be Influenced by Syndecan-3. *Endocrinology* **2006**, *147* (4), 1621–1631.

(33) Jackson, P. J.; McNulty, J. C.; Yang, Y.-K.; Thompson, D. A.; Chai, B.; Gantz, I.; Barsh, G. S.; Millhauser, G. L. Design, Pharmacology, and NMR Structure of a Minimized Cystine Knot with Agouti-Related Protein Activity†. *Biochemistry* **2002**, *41* (24), 7565–7572.

(34) Madonna, M. E.; Schurdak, J.; Yang, Y.; Benoit, S.; Millhauser, G. L. Agouti-Related Protein Segments Outside of the Receptor Binding Core Are Required for Enhanced Short- and Long-Term Feeding Stimulation. *ACS Chem. Biol.* **2012**, *7* (2), 395–402.

(35) Ghamari-Langroudi, M.; Digby, G. J.; Sebag, J. A.; Millhauser, G. L.; Palomino, R.; Matthews, R.; Gillyard, T.; Panaro, B. L.; Tough, I. R.; Cox, H. M.; Denton, J. S.; Cone, R. D. G-Protein-Independent Coupling of MC4R to Kir7.1 in Hypothalamic Neurons. *Nature* **2015**.

(36) Chen, J.; Chen, V.; Kawamura, T.; Hoang, I.; Yang, Y.; Wong, A. T.; McBride, R.; Repunte-Canonigo, V.; Millhauser, G. L.; Sanna, P. P. Charge Characteristics of

Agouti-Related Protein Implicate Potent Involvement of Heparan Sulfate Proteoglycans in Metabolic Function. *iScience* **2019**, *22*, 557–570.

(37) Huszar, D.; Lynch, C. A.; Fairchild-Huntress, V.; Dunmore, J. H.; Fang, Q.; Berkemeier, L. R.; Gu, W.; Kesterson, R. A.; Boston, B. A.; Cone, R. D.; Smith, F. J.; Campfield, L. A.; Burn, P.; Lee, F. Targeted Disruption of the Melanocortin-4 Receptor Results in Obesity in Mice. *Cell* **1997**, *88* (1), 131–141.

(38) Marie, L. S.; Miura, G. I.; Marsh, D. J.; Yagaloff, K.; Palmiter, R. D. A Metabolic Defect Promotes Obesity in Mice Lacking Melanocortin-4 Receptors. *PNAS* **2000**, *97* (22), 12339–12344.

(39) Butler, A. A.; Marks, D. L.; Fan, W.; Kuhn, C. M.; Bartolome, M.; Cone, R. D. Melanocortin-4 Receptor Is Required for Acute Homeostatic Responses to Increased Dietary Fat. *Nature Neuroscience* **2001**, *4* (6), 605–611.

(40) Yeo, G. S. H.; Farooqi, I. S.; Aminian, S.; Halsall, D. J.; Stanhope, R. G.; O'Rahilly, S. A Frameshift Mutation in MC4R Associated with Dominantly Inherited Human Obesity. *Nature Genetics* **1998**, *20* (2), 111–112.

(41) Vaisse, C.; Clement, K.; Guy-Grand, B.; Froguel, P. A Frameshift Mutation in Human MC4R Is Associated with a Dominant Form of Obesity. *Nature Genetics* **1998**, *20* (2), 113–114.

(42) Hinney, A.; Schmidt, A.; Nottebom, K.; Heibült, O.; Becker, I.; Ziegler, A.; Gerber, G.; Sina, M.; Görg, T.; Mayer, H.; Siegfried, W.; Fichter, M.; Remschmidt, H.; Hebebrand, J. Several Mutations in the Melanocortin-4 Receptor Gene Including a Nonsense and a Frameshift Mutation Associated with Dominantly Inherited Obesity in Humans. *J Clin Endocrinol Metab* **1999**, *84* (4), 1483–1486.

(43) Vaisse, C.; Clement, K.; Durand, E.; Hercberg, S.; Guy-Grand, B.; Froguel, P. Melanocortin-4 Receptor Mutations Are a Frequent and Heterogeneous Cause of Morbid Obesity. *J Clin Invest* **2000**, *106* (2), 253–262.

(44) Farooqi, I. S.; Yeo, G. S. H.; Keogh, J. M.; Aminian, S.; Jebb, S. A.; Butler, G.; Cheetham, T.; O'Rahilly, S. Dominant and Recessive Inheritance of Morbid Obesity Associated with Melanocortin 4 Receptor Deficiency. *J Clin Invest* **2000**, *106* (2), 271–279.

(45) Farooqi, I. S.; Keogh, J. M.; Yeo, G. S. H.; Lank, E. J.; Cheetham, T.; O'Rahilly, S. Clinical Spectrum of Obesity and Mutations in the Melanocortin 4 Receptor Gene. *New England Journal of Medicine* **2003**, *348* (12), 1085–1095.

(46) Xu, P.; Grueter, B. A.; Britt, J. K.; McDaniel, L.; Huntington, P. J.; Hodge, R.; Tran, S.; Mason, B. L.; Lee, C.; Vong, L.; Lowell, B. B.; Malenka, R. C.; Lutter, M.; Pieper, A. A. Double Deletion of Melanocortin 4 Receptors and SAPAP3 Corrects Compulsive Behavior and Obesity in Mice. *PNAS* **2013**, *110* (26), 10759–10764.

(47) Tao, Y.-X. The Melanocortin-4 Receptor: Physiology, Pharmacology, and Pathophysiology. *Endocr Rev* **2010**, *31* (4), 506–543.

(48) Srinivasan, S.; Lubrano-Berthelier, C.; Govaerts, C.; Picard, F.; Santiago, P.; Conklin, B. R.; Vaisse, C. Constitutive Activity of the Melanocortin-4 Receptor Is Maintained by Its N-Terminal Domain and Plays a Role in Energy Homeostasis in Humans. *J Clin Invest* **2004**, *114* (8), 1158–1164.

(49) Ersoy, B. A.; Pardo, L.; Zhang, S.; Thompson, D. A.; Millhauser, G.; Govaerts, C.; Vaisse, C. Mechanism of N-Terminal Modulation of Activity at the Melanocortin-4 Receptor GPCR. *Nat Chem Biol* **2012**, *8* (8), 725–730.

(50) Hinney, A.; Hohmann, S.; Geller, F.; Vogel, C.; Hess, C.; Wermter, A.-K.; Brokamp, B.; Goldschmidt, H.; Siegfried, W.; Remschmidt, H.; Schäfer, H.; Gudermann, T.; Hebebrand, J. Melanocortin-4 Receptor Gene: Case-Control Study and Transmission Disequilibrium Test Confirm That Functionally Relevant Mutations Are Compatible with a Major Gene Effect for Extreme Obesity. *J Clin Endocrinol Metab* **2003**, *88* (9), 4258–4267.

(51) Mountjoy, K. G.; Kong, P. L.; Taylor, J. A.; Willard, D. H.; Wilkison, W. O. Melanocortin Receptor-Mediated Mobilization of Intracellular Free Calcium in HEK293 Cells. *Physiological Genomics* **2001**, *5* (1), 11–19.

(52) Newman, E. A.; Chai, B.-X.; Zhang, W.; Li, J.-Y.; Ammori, J. B.; Mulholland, M. W. Activation of the Melanocortin-4 Receptor Mobilizes Intracellular Free Calcium in Immortalized Hypothalamic Neurons. *J. Surg. Res.* **2006**, *132* (2), 201–207.

(53) Li, Y.-Q.; Shrestha, Y.; Pandey, M.; Chen, M.; Kablan, A.; Gavrilova, O.; Offermanns, S.; Weinstein, L. S. $G_{q/11}\alpha$ and $G_s\alpha$ Mediate Distinct Physiological Responses to Central Melanocortins. *J Clin Invest* **2016**, *126* (1), 40–49.

(54) Breit, A.; Wolff, K.; Kalwa, H.; Jarry, H.; Büch, T.; Gudermann, T. The Natural Inverse Agonist Agouti-Related Protein Induces Arrestin-Mediated Endocytosis of Melanocortin-3 and -4 Receptors. *J. Biol. Chem.* **2006**, *281* (49), 37447–37456.

(55) Büch, T. R. H.; Heling, D.; Damm, E.; Gudermann, T.; Breit, A. Pertussis Toxin-Sensitive Signaling of Melanocortin-4 Receptors in Hypothalamic GT1-7 Cells Defines Agouti-Related Protein as a Biased Agonist. *J. Biol. Chem.* **2009**, *284* (39), 26411–26420.

(56) Atasoy, D.; Betley, J. N.; Li, W.-P.; Su, H. H.; Sertel, S. M.; Scheffer, L. K.; Simpson, J. H.; Fetter, R. D.; Sternson, S. M. A Genetically Specified Connectomics Approach Applied to Long-Range Feeding Regulatory Circuits. *Nat Neurosci* **2014**, *17* (12), 1830–1839.

(57) Reizes, O.; Lincecum, J.; Wang, Z.; Goldberger, O.; Huang, L.; Kaksonen, M.; Ahima, R.; Hinkes, M. T.; Barsh, G. S.; Rauvala, H.; Bernfield, M. Transgenic Expression of Syndecan-1 Uncovers a Physiological Control of Feeding Behavior by Syndecan-3. *Cell* **2001**, *106* (1), 105–116.

(58) Reizes, O.; Benoit, S. C.; Strader, A. D.; Clegg, D. J.; Akunuru, S.; Seeley, R. J. Syndecan-3 Modulates Food Intake by Interacting with the Melanocortin/AgRP Pathway. *Annals of the New York Academy of Sciences* **2003**, *994* (1), 66–73.

(59) Zheng, Q.; Zhu, J.; Shanabrough, M.; Borok, E.; Benoit, S. C.; Horvath, T. L.; Clegg, D. J.; Reizes, O. Enhanced Anorexigenic Signaling in Lean Obesity Resistant Syndecan-3 Null Mice. *Neuroscience* **2010**, *171* (4), 1032–1040.

(60) Palomino, R.; Lee, H.-W.; Millhauser, G. L. The Agouti-Related Peptide Binds Heparan Sulfate Through Segments Critical For Its Orexigenic Effects. *J. Biol. Chem.* **2017**, jbc.M116.772822.

(61) Asai, M.; Ramachandrappa, S.; Joachim, M.; Shen, Y.; Zhang, R.; Nuthalapati, N.; Ramanathan, V.; Strochlic, D. E.; Ferket, P.; Linhart, K.; Ho, C.; Novoselova, T. V.; Garg, S.; Ridderstråle, M.; Marcus, C.; Hirschhorn, J. N.; Keogh, J. M.; O'Rahilly, S.; Chan, L. F.; Clark, A. J.; Farooqi, I. S.; Majzoub, J. A. Loss of Function of the Melanocortin 2 Receptor Accessory Protein 2 Is Associated with Mammalian Obesity. *Science* **2013**, *341* (6143), 275–278.

(62) Sebag, J. A.; Zhang, C.; Hinkle, P. M.; Bradshaw, A. M.; Cone, R. D. Developmental Control of the Melanocortin-4 Receptor by MRAP2 Proteins in Zebrafish. *Science* **2013**, *341* (6143), 278–281.

(63) Schonnop, L.; Kleinau, G.; Herrfurth, N.; Volckmar, A.-L.; Cetindag, C.; Müller, A.; Peters, T.; Herpertz, S.; Antel, J.; Hebebrand, J.; Biebermann, H.; Hinney, A. Decreased Melanocortin-4 Receptor Function Conferred by an Infrequent Variant at the Human Melanocortin Receptor Accessory Protein 2 Gene. *Obesity* **2016**, *24* (9), 1976–1982.

(64) Bruschetta, G.; Kim, J. D.; Diano, S.; Chan, L. F. Overexpression of Melanocortin 2 Receptor Accessory Protein 2 (MRAP2) in Adult Paraventricular MC4R Neurons Regulates Energy Intake and Expenditure. *Molecular Metabolism* **2018**.

(65) Liang, J.; Li, L.; Jin, X.; Xu, B.; Pi, L.; Liu, S.; Zhu, W.; Zhang, C.; Luan, B.; Gong, L.; Zhang, C. Pharmacological Effect of Human Melanocortin-2 Receptor Accessory Protein 2 Variants on Hypothalamic Melanocortin Receptors. *Endocrine* **2018**, *61* (1), 94–104.

(66) Sarrazin, S.; Lamanna, W. C.; Esko, J. D. Heparan Sulfate Proteoglycans. *Cold Spring Harb Perspect Biol* **2011**, *3* (7).

(67) Bernfield, M.; Götte, M.; Park, P. W.; Reizes, O.; Fitzgerald, M. L.; Lincecum, J.; Zako, M. Functions of Cell Surface Heparan Sulfate Proteoglycans. *Annual Review of Biochemistry* **1999**, *68* (1), 729–777.

(68) Carey, D. J.; Evans, D. M.; Stahl, R. C.; Asundi, V. K.; Conner, K. J.; Garbes, P.; Cizmeci-Smith, G. Molecular Cloning and Characterization of N-Syndecan, a Novel Transmembrane Heparan Sulfate Proteoglycan. *J Cell Biol* **1992**, *117* (1), 191–201.

(69) Berndt, C.; Casaroli-Marano, R. P.; Vilaró, S.; Reina, M. Cloning and Characterization of Human Syndecan-3*. *Journal of Cellular Biochemistry* **2001**, *82* (2), 246–259.

(70) Asundi, V. K.; Erdman, R.; Stahl, R. C.; Carey, D. J. Matrix metalloproteinase-dependent shedding of syndecan-3, a transmembrane heparan sulfate proteoglycan, in Schwann cells. *Journal of Neuroscience Research - Wiley Online Library* **2003**

(71) Hsueh, Y.-P.; Sheng, M. Regulated Expression and Subcellular Localization of Syndecan Heparan Sulfate Proteoglycans and the Syndecan-Binding Protein CASK/LIN-2 during Rat Brain Development. *J. Neurosci.* **1999**, *19* (17), 7415–7425.

(72) Lei, Q.; Jones, M. B.; Talley, E. M.; Schrier, A. D.; McIntire, W. E.; Garrison, J. C.; Bayliss, D. A. Activation and Inhibition of G Protein-Coupled Inwardly Rectifying Potassium (Kir3) Channels by G Protein By Subunits. *PNAS* **2000**, *97* (17), 9771–9776.

(73) Dascal, N. Signalling Via the G Protein-Activated K+ Channels. *Cellular Signalling* **1997**, *9* (8), 551–573.

(74) Iwashita, M.; Watanabe, M.; Ishii, M.; Chen, T.; Johnson, S. L.; Kurachi, Y.; Okada, N.; Kondo, S. Pigment Pattern in Jaguar/Obelix Zebrafish Is Caused by a Kir7.1 Mutation: Implications for the Regulation of Melanosome Movement. *PLOS Genet* **2006**, *2* (11), e197.

(75) Anderson, E. J. P.; Ghamari-Langroudi, M.; Cakir, I.; Litt, M. J.; Chen, V.; Reggiardo, R. E.; Millhauser, G. L.; Cone, R. D. Late Onset Obesity in Mice with Targeted Deletion of Potassium Inward Rectifier Kir7.1 from Cells Expressing the Melanocortin-4 Receptor. *Journal of Neuroendocrinology* **2019**, *31* (1), e12670.

(76) Carrington, S.; Hernandez, C.; Swale, D.; Aluko, O. A.; Denton, J. S.; Cone, R. G Protein–Coupled Receptors Differentially Regulate Glycosylation and Activity of the Inwardly Rectifying Potassium Channel Kir7.1. *J. Biol. Chem.* **2018**, jbc.RA118.003238.

(77) Metherell, L. A.; Chapple, J. P.; Cooray, S.; David, A.; Becker, C.; Rüschendorf, F.; Naville, D.; Begeot, M.; Khoo, B.; Nürnberg, P.; Huebner, A.; Cheetham, M. E.; Clark, A. J. L. Mutations in MRAP , Encoding a New Interacting Partner of the ACTH Receptor, Cause Familial Glucocorticoid Deficiency Type 2. *Nature Genetics* **2005**, *37* (2), 166–170.

(78) Xu, A.; Choi, K.-L.; Wang, Y.; Permana, P. A.; Yi Xu, L.; Bogardus, C.; Cooper, G. J. S. Identification of Novel Putative Membrane Proteins Selectively Expressed during Adipose Conversion of 3T3-L1 Cells. *Biochemical and Biophysical Research Communications* **2002**, *293* (4), 1161–1167.

(79) Sebag, J. A.; Hinkle, P. M. Melanocortin-2 Receptor Accessory Protein MRAP Forms Antiparallel Homodimers. *Proc Natl Acad Sci U S A* **2007**, *104* (51), 20244–20249.

(80) Yang, Y.-K.; Ollmann, M. M.; Wilson, B. D.; Dickinson, C.; Yamada, T.; Barsh, G. S.; Gantz, I. Effects of Recombinant Agouti-Signaling Protein on Melanocortin Action. *Mol Endocrinol* **1997**, *11* (3), 274–280.

(81) Chan, L. F.; Webb, T. R.; Chung, T.-T.; Meimaridou, E.; Cooray, S. N.; Guasti, L.; Chapple, J. P.; Egertová, M.; Elphick, M. R.; Cheetham, M. E.; Metherell, L. A.; Clark, A. J. L. MRAP and MRAP2 Are Bidirectional Regulators of the Melanocortin Receptor Family. *PNAS* **2009**, *106* (15), 6146–6151.

(82) Sebag, J. A.; Hinkle, P. M. Regulation of G Protein–Coupled Receptor Signaling: Specific Dominant-Negative Effects of Melanocortin 2 Receptor Accessory Protein 2. *Sci Signal* **2010**, *3* (116), ra28.

(83) Geets, E.; Zegers, D.; Beckers, S.; Verrijken, A.; Massa, G.; Van Hoorenbeeck, K.; Verhulst, S.; Van Gaal, L.; Van Hul, W. Copy Number Variation (CNV) Analysis and Mutation Analysis of the 6q14.1–6q16.3 Genes SIM1 and MRAP2 in Prader Willi like Patients. *Molecular Genetics and Metabolism* **2016**, *117* (3), 383–388.

(84) Baron, M.; Maillet, J.; Huyvaert, M.; Dechaume, A.; Boutry, R.; Loiselle, H.; Durand, E.; Toussaint, B.; Vaillant, E.; Philippe, J.; Thomas, J.; Ghulam, A.; Franc, S.; Charpentier, G.; Borys, J.-M.; Lévy-Marchal, C.; Tauber, M.; Scharfmann, R.; Weill, J.; Aubert, C.; Kerr-Conte, J.; Pattou, F.; Roussel, R.; Balkau, B.; Marre, M.; Boissel, M.; Derhourhi, M.; Gaget, S.; Canouil, M.; Froguel, P.; Bonnefond, A. Loss-of-Function Mutations in MRAP2 Are Pathogenic in Hyperphagic Obesity with Hyperglycemia and Hypertension. *Nature Medicine* **2019**, *25* (11), 1733–1738.

(85) Chaly, A. L.; Srisai, D.; Gardner, E. E.; Sebag, J. A. The Melanocortin Receptor Accessory Protein 2 Promotes Food Intake through Inhibition of the Prokineticin Receptor-1. *eLife Sciences* **2016**, *5*, e12397.

(86) Srisai, D.; Yin, T. C.; Lee, A. A.; Rouault, A. A. J.; Pearson, N. A.; Grobe, J. L.; Sebag, J. A. MRAP2 Regulates Ghrelin Receptor Signaling and Hunger Sensing. *Nature Communications* **2017**, *8* (1), 713.

(87) Rouault, A. A. J.; Rosselli-Murai, L. K.; Hernandez, C. C.; Gimenez, L. E.; Tall, G. G.; Sebag, J. A. The GPCR Accessory Protein MRAP2 Regulates Both Biased Signaling and Constitutive Activity of the Ghrelin Receptor GHSR1a. *Sci. Signal.* **2020**, *13* (613).

(88) Rouault, A. A. J.; Lee, A. A.; Sebag, J. A. Regions of MRAP2 Required for the Inhibition of Orexin and Prokineticin Receptor Signaling. *Biochimica et Biophysica Acta (BBA) - Molecular Cell Research* **2017**, *1864* (12), 2322–2329.

(89) Krashes, M. J.; Shah, B. P.; Koda, S.; Lowell, B. B. Rapid versus Delayed Stimulation of Feeding by the Endogenously Released AgRP Neuron Mediators, GABA, NPY and AgRP. *Cell Metab* **2013**, *18* (4).

(90) Garfield, A. S.; Li, C.; Madara, J. C.; Shah, B. P.; Webber, E.; Steger, J. S.; Campbell, J. N.; Gavrilova, O.; Lee, C. E.; Olson, D. P.; Elmquist, J. K.; Tannous, B. A.; Krashes, M. J.; Lowell, B. B. A Neural Basis for Melanocortin-4 Receptor-Regulated Appetite. *Nat Neurosci* **2015**, *18* (6), 863–871.

Chapter 2

Charge Characteristics of Agouti-Related Protein Implicate Potent Involvement of Heparan Sulfate Proteoglycans in Metabolic Function

Jihuan Chen†, Valerie Chen†, Tomoya Kawamura, Ivy Hoang, Yang Yang, Ashley Tess Wong, Ryan McBride, Vez Repunte-Canonigo, Glenn L. Millhauser & Pietro Paolo Sanna*

† Authors contributed equally
*Corresponding author: psanna@scripps.edu

Summary

The endogenous melanocortin peptide agouti-related protein (AgRP) plays a well-known role in foraging, but its contribution to metabolic regulation is less understood. Mature AgRP(83-132) has distinct residues for melanocortin receptor binding and heparan sulfate interactions. Here, we show that AgRP increases ad libitum feeding and operant responding for food in mice, decreases oxygen consumption, and lowers body temperature and activity, indicating lower energy expenditure. AgRP increased the respiratory exchange ratio, indicating a reduction of fat oxidation and a shift toward carbohydrates as the primary fuel source. The duration and intensity of AgRP's effects depended on the density of its positively charged amino acids, suggesting that its orexigenic and metabolic effects depend on its affinity for heparan sulfate. These findings may have major clinical implications by unveiling the critical involvement of interactions between AgRP and heparan sulfate to the central regulation of energy expenditure, fat utilization, and possibly their contribution to metabolic disease.

Introduction

There is a pressing need to identify the underlying mechanisms of metabolic disease. The central melanocortin system regulates feeding, body weight, and energy expenditure. However, the contribution of the central melanocortin peptide agouti-related protein (AgRP) and its interaction with heparan sulfate to metabolic regulation has not been characterized. Here, we found that AgRP increases both ad libitum food

38

intake and motivation for food in an operant paradigm and reduces energy expenditure and fat oxidation, which has been linked to a higher risk for metabolic disease. Both orexigenic and metabolic actions of AgRP depended on the density of AgRP positive charges, which determines its affinity for heparan sulfate independently of the binding of AgRP to central melanocortin receptors. These results support a role for heparan sulfate in the regulation of energy homeostasis by the melanocortin system.

The central melanocortin system includes neurons in the arcuate nucleus (ARC) of the hypothalamus that coexpress agouti-related protein (AgRP) and neuropeptide Y (NPY) and the neurotransmitter γ-aminobutyric acid (GABA) and neurons that coexpress proopiomelanocortin (POMC) and cocaine- and amphetamine-regulated transcript (CART) [1]. Evidence from mutant mice and human mutations indicates that the central melanocortin system plays a key role in coordinating nutrient intake, energy metabolism, fat accumulation, and body weight [2–6]. However, the contribution of AgRP to metabolic regulation is not well understood because of its coexpression with GABA and NPY, which is also a key regulator of appetite and energy balance [7,8].

Neuropeptide Y/AgRP-coexpressing neurons promote feeding and weight gain, whereas POMC neurons attenuate feeding and promote weight loss [9]. Both NPY/AgRP and POMC/CART neurons express receptors for the adipocyte-derived hormone leptin

and insulin that, together with other hormones (e.g., the gut peptides ghrelin and peptide YY, among others) and nutrients, such as glucose, fatty acids, and peptides, allow them to sense peripheral energy status and needs [1]. Circulating leptin and insulin interact with neurons in the ARC through special properties of the blood-brain barrier in this region of the hypothalamus, resulting in the inhibition of NPY/AgRP neurons and activation of POMC/CART neurons, leading to a reduction of food intake [9].

Numerous studies support a central role for NPY/AgRP neurons in regulating energy expenditure, food intake, and body weight. NPY/AgRP neurons mediate insulin's central effects on hepatic glucose production [10–12]. Fat accumulation and obesity comprise the primary phenotype of lower central melanocortin-3 receptor (MC3R) and MC4R loss-of-function [2–6]. Insulin receptor signaling in NPY/AgRP neurons in the ARC inhibits hepatic glucose production via vagus nerves that are associated with food intake [10–12]. Additionally, NPY/AgRP neurons control insulin sensitivity by regulating brown adipose tissue (BAT) [13]. The deletion of suppressor of cytokine signaling 3 (SOCS3) in NPY/AgRP or POMC/CART neurons enhanced insulin signaling and improved whole-body glucose metabolism in diet-induced obese mice [9]. The deletion of activating transcription factor 4 (ATF4) in NPY/AgRP neurons resulted in a lean phenotype with an increase in energy expenditure and resistance to high fat diet (HFD)-induced obesity [14].

The melanocortin system includes five G protein-coupled receptors (GPCRs) that contribute to diverse physiological processes [15–17]. Agonists of MCRs derive from POMC through proteolytic cleavage to produce adrenocorticotropic hormone (ACTH) and various melanocyte-stimulating hormone (MSH) variants, such as α-MSH, β-MSH, and γ-MSH. MC1R is involved in skin and hair pigmentation by regulating the production of melanin [15–17]. MC2R is mainly expressed in the adrenal cortex where it serves as an ACTH receptor, inducing glucocorticoid production [18]. MC3Rs and MC4Rs are expressed in the brain and involved in the regulation of energy homeostasis and metabolism [15–17]. α-MSH is released by POMC/CART neurons and acts as the endogenous agonist of central MC3Rs and MC4Rs. Central MC4Rs and peripheral MC1Rs exhibit elevated basal activity in the absence of agonists, and their activity is regulated by two pivotal endogenous peptides that act as inverse agonists: AgRP in the central nervous system (CNS) and agouti-signaling protein (ASP; the main product of the agouti gene in the skin) [15–17].

AgRP is a key modulator of central MC3Rs and MC4Rs [19]. Full-length AgRP is a 132-residue pro-protein that is posttranslationally processed by pro-protein convertase 1/3 into its mature form, AgRP(83-132) [20]. AgRP(83-132) contains five disulfide bonds, three of which form an inhibitor cystine knot (ICK) motif (Figure 1), which is sufficient for MC3/4R antagonism, whereas positively charged residues in the N-terminal segment and C-terminal loop allow AgRP to bind heparan sulfate independently of its

receator affinity and signaling ability through a reduction of cyclic adenosine monophosphate (cAMP) [21–23].
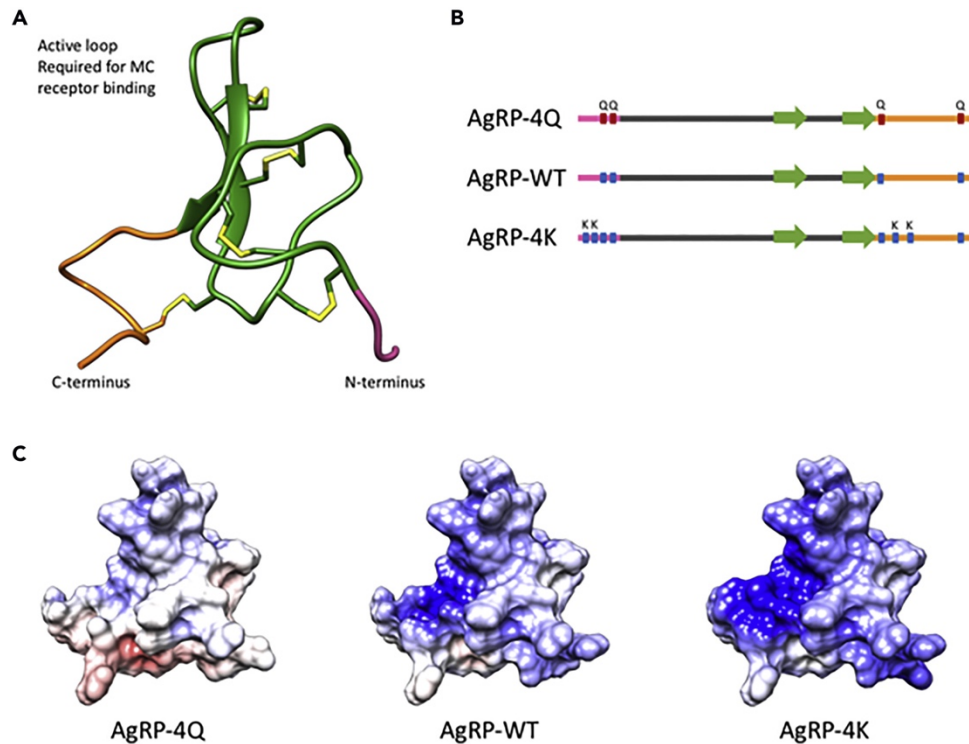
Figure 1 Structure and Electrostatic Potential Maps for AgRP and Charge-Modified AgRP Variants. A, Nuclear magnetic resonance structure (Protein DataBank: 1HYK) of mature AgRP-WT(83-132) depicting the inhibitor cystine knot (ICK) core (green) and non-ICK N-terminal segment (pink) and C-terminal loop (orange). Disulfide-bonds are in yellow. The ICK core that contains the active loop is sufficient for MC3/4R binding and antagonism. However, the N-terminal segment and C-terminal loop that flank the ICK core are highly conserved and required for AgRP-induced long-term feeding. B, Schematic diagram of the location of lysine mutations in AgRP-4K and glutamine mutations in AgRP-4Q. All charge mutations are located outside of the ICK core. C, Electrostatic potential surface maps for AgRP-4Q, AgRP-WT, and AgRP-4K, calculated by Adaptive Poisson-Boltzmann Solver (APBS). AgRP-4K adds positive charges to an existing positively charged patch that is present in AgRP-WT.

Heparan sulfate proteoglycans were originally considered structural elements of the extracellular matrix, but they have subsequently emerged as key modulators of biological processes [24,25]. Sulfate groups provide docking sites for numerous positively charged peptide ligands, including AgRP, that are involved in diverse biological processes [24,25].

The contribution of AgRP and its interaction with heparan sulfate to metabolic regulation has not been previously characterized. The present study investigated the effects of AgRP peptides, including AgRP(83-132) (i.e., the mature form of AgRP) and two charge-modified AgRP variants that differed in their affinity for heparan sulfate, on food intake and energy metabolism. We found that the intracerebroventricular (ICV) administration of AgRP in addition to ad libitum feeding in the home cage increased operant responding for food in a manner that depended on the density of AgRP positive charges, which determined its affinity for heparan sulfate. Similarly, we found that AgRP decreased energy expenditure and shifted fuel utilization from fatty acids toward carbohydrates, which also required heparan sulfate binding. Lower fatty acid oxidation at rest promotes an increase in fat storage and is associated with a higher risk of type 2 diabetes and metabolic syndrome [26–28]. All of the AgRP variants reduced body temperature and activity, suggesting lower energy expenditure. However, the effects of the variant that had a lower density of positive charges had faster onsets and were less protracted.

Overall, the present results indicate that the orexigenic effects of AgRP are accompanied by complex metabolic changes that are characterized by lower energy expenditure, a reduction of fat oxidation, and a shift in substrate utilization toward carbohydrate oxidation. Although the AgRP variants that were tested did not differ in receptor affinity or in vitro potency, their in vivo potency and duration of action significantly depended on positively charged amino acids that mediate heparan sulfate binding.

Results

Binding of AgRP and Charge-Modified AgRP Variants to Heparan Sulfate Glycan Arrays

As shown in Figure 2, the mature form of AgRP (AgRP[83-132]), henceforth referred to as wild-type AgRP (AgRP-WT), binds broadly to different heparan-sulfate-derived oligosaccharides in glycan arrays. AgRP binding affinity was correlated with the state of sulfation and length of the heparan sulfate oligosaccharides. AgRP binding appeared to be favored by 6S and NS sulfation but not by 3S sulfation. We next compared the binding of AgRP-WT and two charge-modified AgRP variants, including AgRP-4Q (in which positive charges were eliminated by replacing Arg and Lys residues with Gln) and AgRP-4K (in which additional positively charged amino acids were included by mutating Gly123 and Ala125 and the two Ser residues in the N-terminal segment to Lys) [23]. These modifications have been shown to not affect MC3R or MC4R

44

binding [23]. As shown in Figure 3, these two charge-modified AgRP variants resulted in alterations of the affinity for heparan sulfate in a glycan array using immobilized hexasaccharide that was representative of a highly sulfated heparan sulfate. AgRP-4Q exhibited negligible binding to sulfated hexasaccharide, whereas AgRP-4K exhibited approximately 50-times greater binding than AgRP-WT (Figure 3).

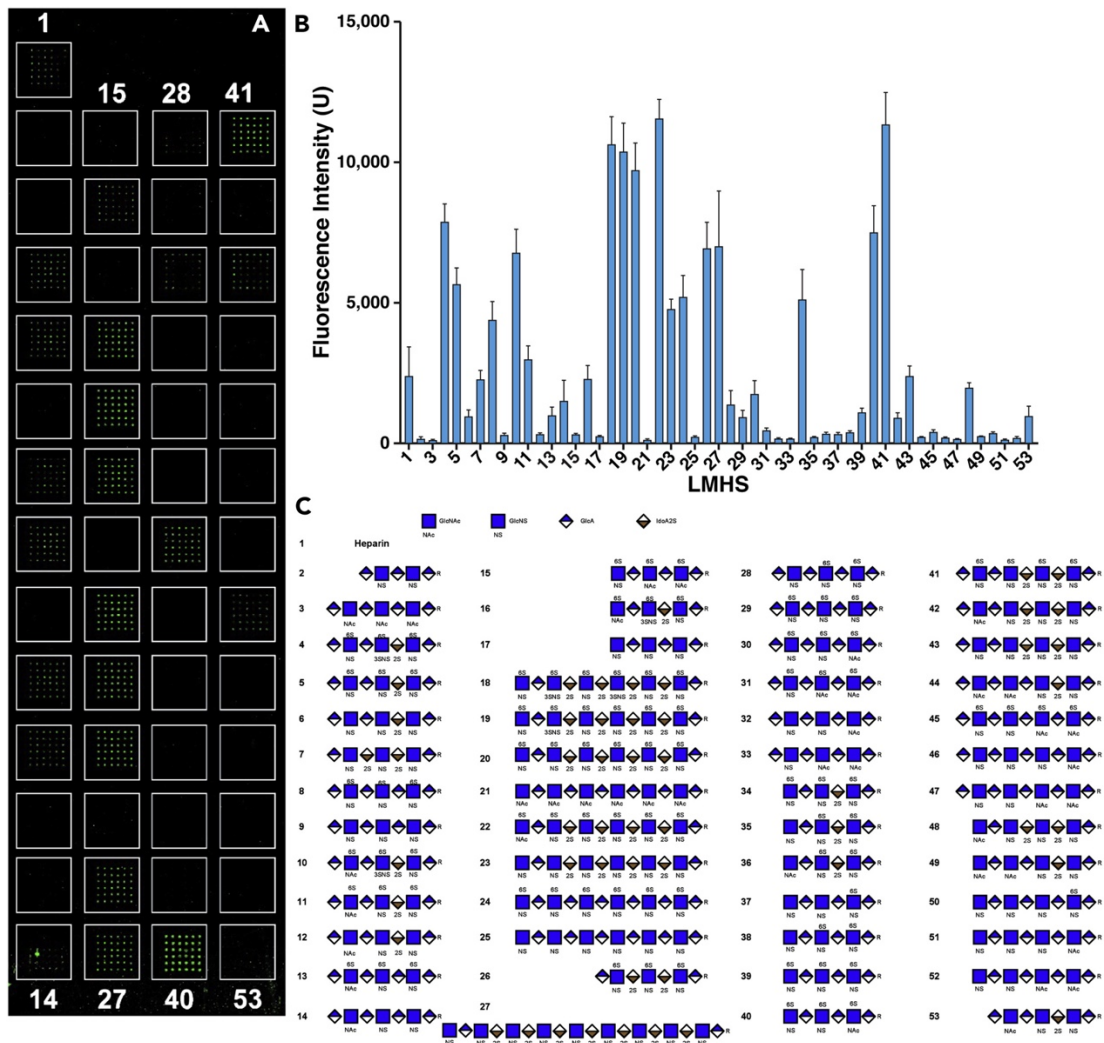**Figure 2 Glycan Array Analysis of AgRP Binding to Heparan Sulfate Oligosaccharides.** A, Fluorescent image of the glass slide glycan arrays showing fluorescence signals (green dots) of AgRP binding to 52 immobilized heparan sulfate oligosaccharides (low-molecular-weight heparan sulfate, LMHS). B, Bar graph showing the relative fluorescence intensity of AgRP binding to the heparan sulfate oligosaccharides arrays.

Heparan sulfate oligosaccharides 22 and 41 show the highest intensity. C, The structures of the different heparan sulfate oligosaccharides on the slide microarray in A. Data are represented as mean ± SEM.
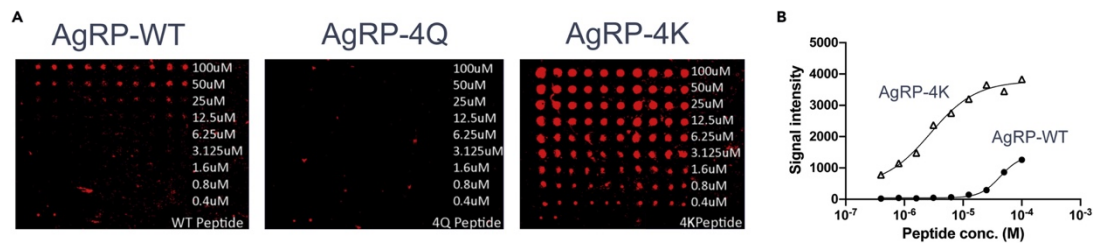
Figure 3 Binding of AgRP and Charge-Modified AgRP Variants to a Heparan Sulfate Hexasaccharide Glycan Array. A, AgRP(83-132) (AgRP-WT) and AgRP-4K, in which Gly123 and Ala125 and the two Ser residues in the N-terminal segment were replaced with Lys, showed concentration-dependent binding to a glycan array of the heparan sulfate hexasaccharide GlcNS6S-GlcA-GlcNS6S-IdoA2S-GlcNS6S-GlcA-NH2 (Array 34 in Figure 2 is the hexasaccharide used in this figure). The printed concentration of hexasaccharides was from 100 μM and serially diluted by a dilution factor of 2 down to a minimum concentration of 0.4 μM. Each concentration had 10 replicates. AgRP-4Q, in which Arg and Lys residues were replaced with Gln, showed negligible binding to the heparan sulfate hexasaccharide glycan array. B, Semiquantitative determination of binding of AgRP variants to heparan sulfate hexasaccharide glycan array. The signal intensity (arbitrary units) was determined by ImageJ software. The AgRP-4K binding curve showed a dramatic leftward shift that was indicative of approximately 50-times greater binding affinity for the heparan sulfate hexasaccharide glycan array than AgRP-WT. Data are represented as mean ± SEM.

Effects of Charge-Modified AgRP Variants on ad libitum Food Intake and Body Weight

We first tested the effects of AgRP-WT and AgRP variants with a decrease or an increase in positive charges (AgRP-4Q and AgRP-4K, respectively) on ad libitum food intake in mice in their home cages (Figure 4). Each AgRP variant was injected ICV into the lateral ventricle. Food consumption and body weight were measured daily. As

shown in Figure 4, the ICV administration of AgRP-WT and AgRP-4K but not AgRP-4Q

significantly increased food intake and body weight. AgRP-4K exerted a more

pronounced and long-lasting effect than AgRP-WT.
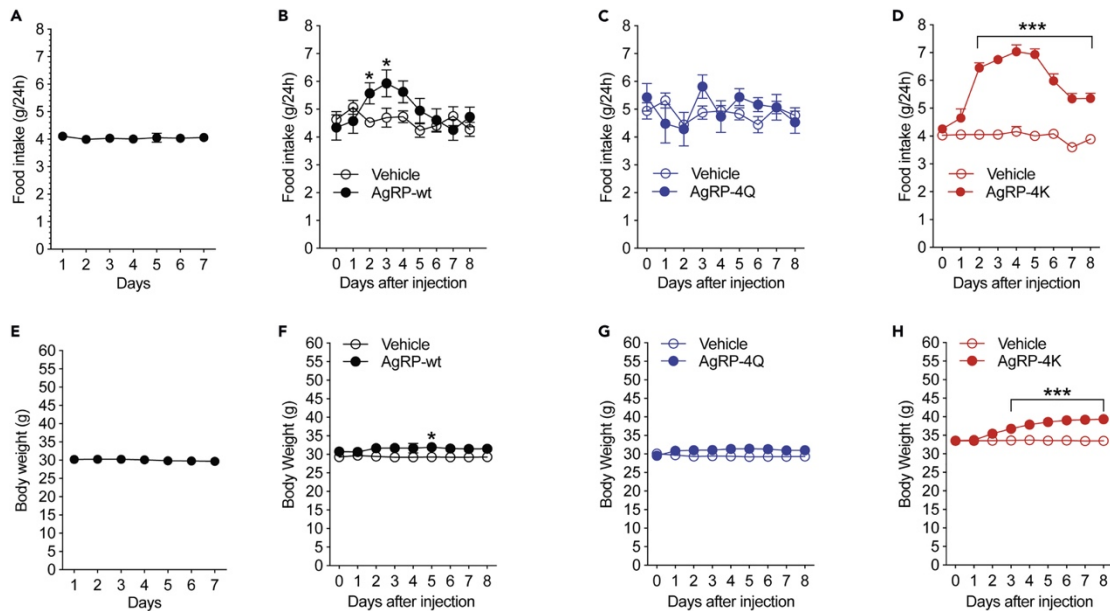
Figure 4 Effects of AgRP and Charge-Modified AgRP Variants on Ad Libitum Food Intake and Body Weight. Baseline levels of A, food intake and E, body weight were recorded daily for seven days, and then the AgRP peptides were injected ICV in the lateral ventricle (1 nmol in 1 μL of saline). B, The mature wild-type form of AgRP (AgRP-WT) significantly increased the amount of food that was consumed. The two-way repeated-measures ANOVA revealed a significant main effect of days ($F_{8,152}$ = 3.65, p = 0.0006) and a significant AgRP variant × days interaction ($F_{8,152}$ = 3.736, p = 0.0005) n = 10–11/group. The post hoc analysis showed that the increases in food consumption were statistically significant on the second and third days of AgRP administration. *p < 0.05, compared with mice that were injected with vehicle; ***p < 0.001, compared with vehicle group (post hoc test). n = 10–11/group. C, The mutant form with lower positive charges (AgRP-4Q) did not significantly alter ad libitum food consumption. D, The mutant form with higher positive charges (AgRP-4K) caused a significant and long-lasting increase in food intake, which peaked on the second day of injection. The two-way repeated-measures ANOVA revealed significant main effects of AgRP ($F_{1,25}$ = 143.2, p < 0.0001) and time course ($F_{8,200}$ = 25.65, p < 0.0001) and a significant AgRP × time course interaction ($F_{8,200}$ = 20.85, p < 0.0001).

F, AgRP-WT caused a transient significant increase in body weight on day 5 post-injection. G, AgRP-4Q did not affect body weight. H, AgRP-4K caused a significant increase in body weight that started on day 3 post-injection, which lasted through the testing period. The two-way repeated-measures ANOVA revealed significant main effects of AgRP ($F_{1,25} = 9.403$, $p < 0.01$) and time course ($F_{8,200} = 127.5$, $p < 0.0001$) and a significant AgRP × time course interaction ($F_{8,200} = 125.2$, $p < 0.0001$). ***$p < 0.001$, compared with vehicle group (post hoc test). n = 13–14/group. Data are represented as mean ± SEM.

Effects of Charge-Modified AgRP Variants on Operant Responding for Food

We then tested the effects of AgRP variants in an operant food self-administration paradigm. The mice were trained in an operant chamber to obtain food pellets by pressing a lever on the wall. During the training phase, an FR1 schedule was used, whereby one active lever press resulted in the delivery of one food pellet. After the acquisition of stable lever-pressing behavior, the mice were gradually switched to an FR5 schedule and then remained at this FR throughout the remainder of the experimental period. AgRP-4Q, the variant with a decrease in positive charges, significantly and rapidly increased food responding on the first day of the injection, but the effect subsided within a few hours (Figure 5A). AgRP-4K, the variant with an increase in positive charges, induced a delayed increase in responding for food, starting approximately 10 h after the injection. However, the AgRP-4K-induced increase in responding for food was quite protracted and statistically significant for five days (Figure 5B). Altogether, these results indicated that the positive charge and affinity of AgRP for heparan sulfate were associated with an increase in food intake and motivation for food.
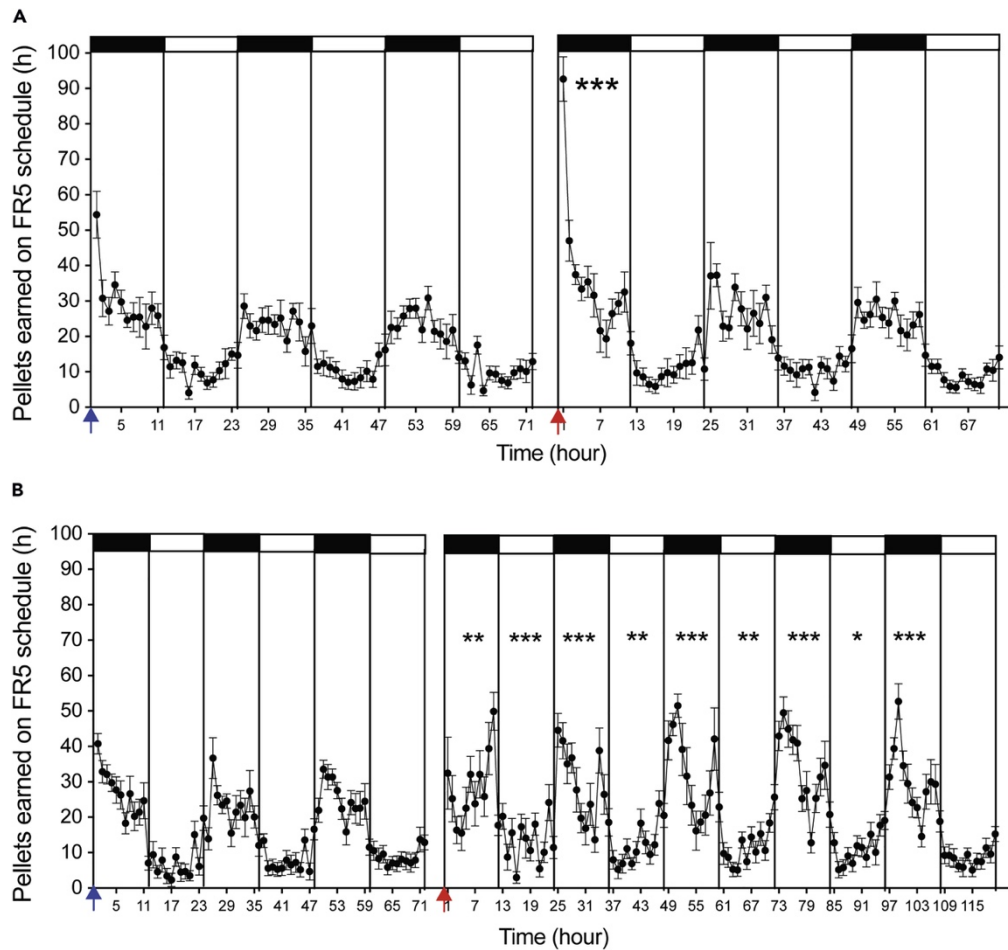
Figure 5 Effects of AgRP and Charge-Modified AgRP Variants on Operant Food Self-Administration. A, AgRP-4Q significantly increased food self-administration during the dark phase on the first day of injection. This feeding-promoting effect of AgRP-4Q subsided rapidly in the following periods. The two-way repeated-measures ANOVA revealed significant main effects of AgRP variant ($F_{1,16}$ = 7.452, p = 0.015) and time ($F_{7,112}$ = 183.4, p < 0.0001) and a significant AgRP variant × time interaction ($F_{7,112}$ = 2.577, p = 0.017). ***p < 0.001, relative to the level before AgRP injection. B, AgRP-4K induced a longer-lasting increase in food self-administration compared with AgRP-4Q. Data are represented as mean ± SEM.

Effects of Charge-Modified AgRP Variants on Energy Expenditure and Fuel Source

49

We next investigated the effects of AgRP variants on energy expenditure and fuel source using CLAMS chambers. One hour before being placed in the CLAMS chamber, the mice received an injection of AgRP-WT, AgRP-4Q, or AgRP-4K. Body temperature, VO2, and carbon dioxide production (VCO2) were recorded continuously for five days. The respiratory exchange ratio (RER; i.e., the ratio of VCO2 to VO2) was calculated to estimate the fuel source that was utilized for energy production, based on the difference in the number of oxygen molecules that are required for the oxidation of glucose vs. fatty acids.

All three AgRP variants reduced body temperature, suggesting a decrease in energy expenditure (Figure 6A). The reductions of body temperature that were induced by AgRP-WT and AgRP-4K had later onsets and were more protracted than the reduction that was induced by AgRP-4Q (Figure 6A). AgRP-WT also significantly reduced VO2 for a protracted time (Figure 6B, left). AgRP-4K, but not AgRP-4Q, showed a similar protracted trend toward a VO2 reduction, but this reduction did not reach statistical significance (Figure 6B, right).
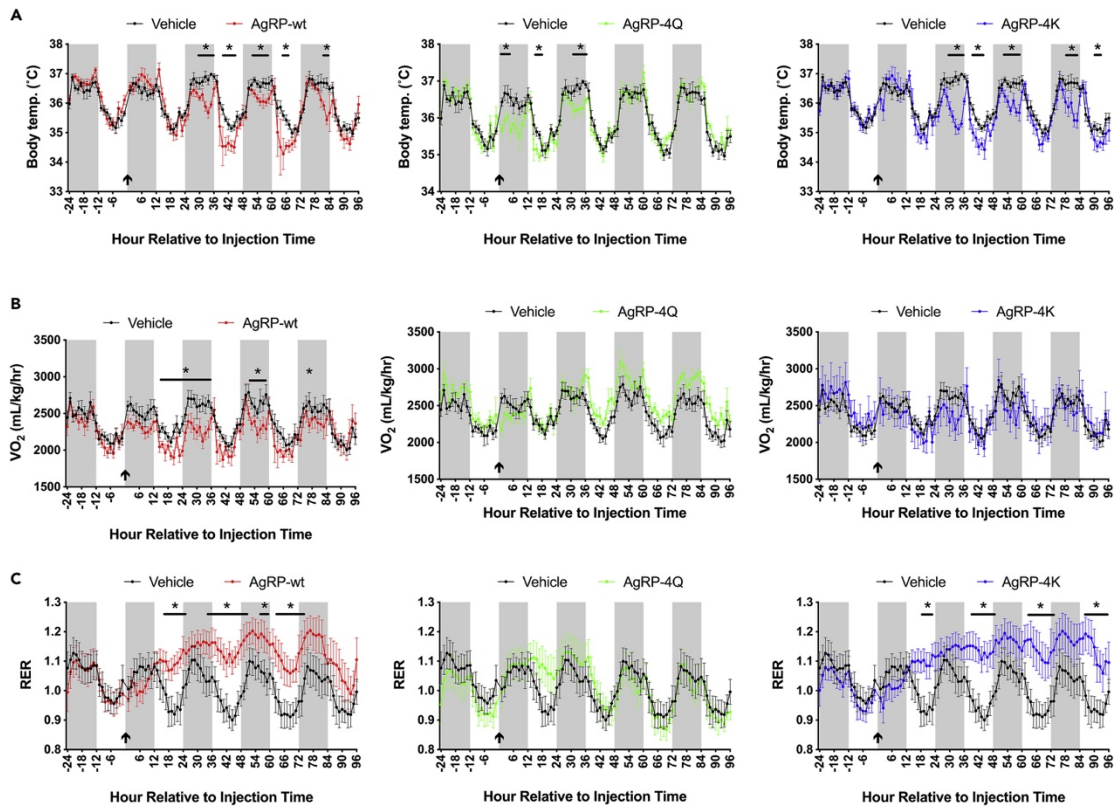
Figure 6 Effects of AgRP and Charge-Modified AgRP Variants on Energy Expenditure and Fuel Source Energy expenditure was assessed by body temperature and VO2 in the CLAMS. A, All three variants of AgRP—AgRP-WT (left), AgRP-4Q (middle), and AgRP-4K (right)—significantly decreased body temperature, suggesting that AgRP reduces energy expenditure. The effect of AgRP-4Q (center) had a faster onset and was less protracted than the effects of AgRP-WT (left) and AgRP-4K (right). Two-way repeated-measures ANOVA revealed significant AgRP variant × hours interactions for all three variants (AgRP-WT: $F_{99,990} = 2.225$, $p < 0.0001$; AgRP-4Q: $F_{99,856} = 1.754$, $p < 0.0001$; AgRP-4K: $F_{99,891} = 2.828$, $p < 0.0001$). B, VO2 was significantly decreased by AgRP-WT, indicating that AgRP reduced energy expenditure. C, Effects of AgRP on the respiratory exchange rate (RER) in the CLAMS. AgRP-WT (left) and AgRP-4K (right) but not AgRP-4Q (middle) significantly increased the RER specifically during the light phase (AgRP-WT: $F_{4.577,45.77} = 10.73$, $p < 0.0001$; AgRP-4K: $F_{6.708,60.37} = 24.91$, $p < 0.0001$; AgRP-4Q: $F_{3.734,37.20} = 11.38$, $p < 0.05$), indicating that AgRP reduced fat oxidation and increased carbohydrate utilization as the predominant fuel source. *p < 0.05, compared with vehicle group (post hoc test). Data are represented as mean ± SEM.

AgRP-WT and AgRP-4K, but not AgRP-4Q, significantly increased the RER at rest (during the light, inactive phase), indicating a reduction of fat oxidation and a shift in fuel utilization toward carbohydrates at rest (Figure 6C). AgRP-4K also caused a significant short-term elevation of VCO2 (not shown). Collectively, these results indicate that AgRP decreases energy expenditure, reduces fat oxidation, and increases carbohydrate oxidation. AgRP-WT significantly decreased energy expenditure, measured by VO2.

All three AgRP variants reduced body temperature, regardless of their positive charges. However, reductions of body temperature that were induced by AgRP-WT and AgRP-4K (i.e., the more positively charged AgRP variants with affinity for heparan sulfate) had a more delayed onset, were more protracted, and were associated with a decrease in fat oxidation and an increase in carbohydrate oxidation.

Effects of Charge-Modified AgRP Variants on Activity, Feeding, and Drinking in CLAMS Chambers

Activity was assessed by the triple-axis detection of animal motion using the infrared photocell technology of the CLAMS. All three variants of AgRP significantly decreased total activity, ambulation, and rearing during the dark cycle (Figure 7). The AgRP-4Q-induced reduction of activity had a faster onset and a shorter duration than the AgRP variants that had greater positive charges, suggesting that heparan sulfate binding

contributes to the duration of the AgRP-induced downregulation of activity. Access to food and water can be simultaneously monitored automatically in the CLAMS. AgRP-WT and AgRP-4K but not AgRP-4Q significantly increased both food and water intake (Figures 8 and 9). These results indicate that the AgRP variants decreased activity, regardless of their positive charges. However, the reductions of activity that were induced by the more positively charged AgRP variants (AgRP-WT and AgRP-4K) had a more delayed onset, were more protracted, and were associated with increases in food and water intake.
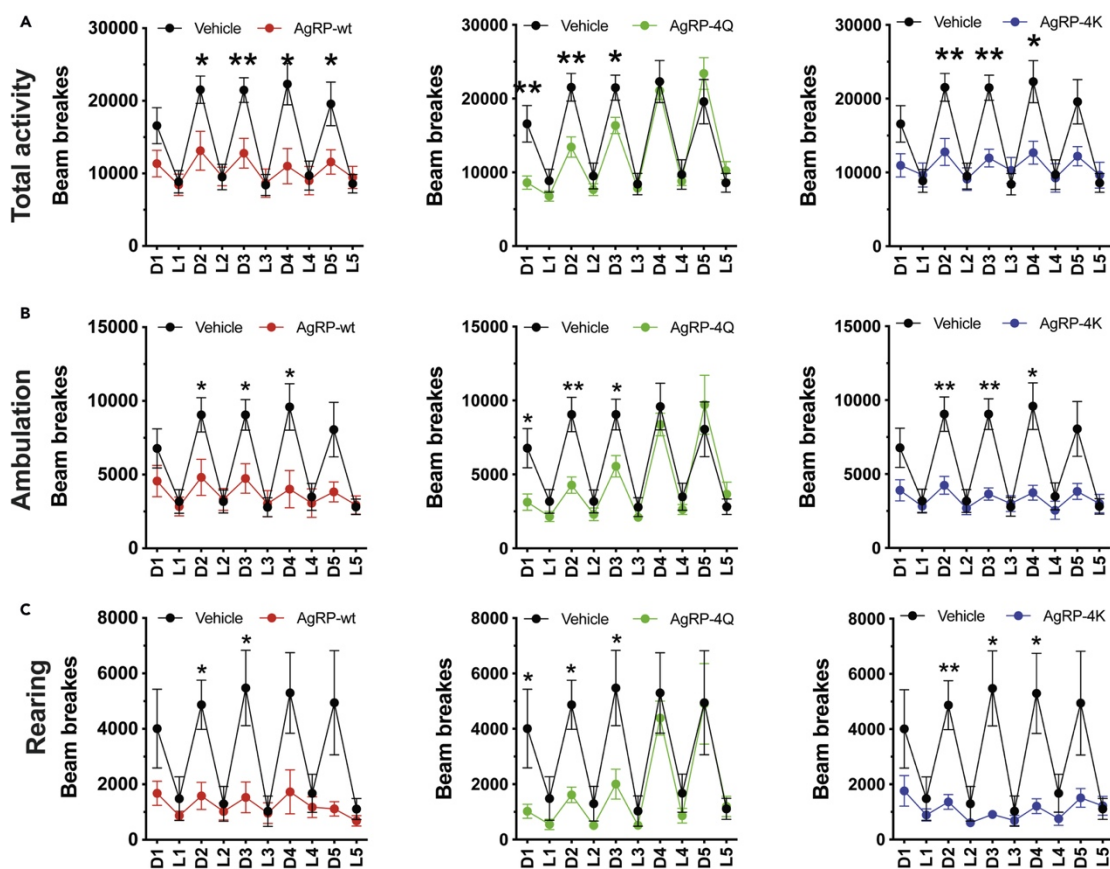
Figure 7 Effects of AgRP and Charge-Modified AgRP Variants on Activity. AgRP significantly decreased activity in mice, including total activity, ambulation, and rearing (vertical activity) in the CLAMS. The effect of AgRP-4Q (center) had a faster onset and was less protracted than the effects of AgRP-WT (left) and AgRP-4K (right). A, All three variants of AgRP—AgRP-WT (left), AgRP-4Q (middle), and AgRP-4K (right)—reduced total activity, particularly during the dark phase. Total activity during the light phase was unaffected. The two-way repeated-measures ANOVA revealed a significant AgRP variant × hours interaction for all three variants (AgRP-WT: $F_{9,90} = 6.535$, $p < 0.0001$; AgRP-4Q: $F_{9,81} = 2.824$, $p = 0.0001$; AgRP-4K: $F_{9,90} = 8.464$, $p < 0.0001$). B, Ambulation. The two-way repeated-measures ANOVA revealed a significant AgRP variant × hours interaction for all three variants (AgRP-WT: $F_{9,90} = 4.824$, $p < 0.0001$; AgRP-4Q: $F_{9,81} = 2.844$, $p = 0.0058$; AgRP-4K: $F_{9,90} = 6.222$, $p < 0.0001$). C, Rearing. The two-way repeated-measures ANOVA revealed a significant AgRP variant × hours interaction for two of the variants (AgRP-WT: $F_{9,90} = 3.226$, $p = 0.0020$; AgRP-4K: $F_{9,90} = 3.767$, $p = 0.0005$). *$p < 0.05$, **$p < 0.01$, ***$p < 0.001$, significant difference between AgRP and vehicle groups. The data are presented in the form of a 12 h/12 h light/dark cycle. D, dark phase; L, light phase. *$p < 0.05$, **$p <$

0.01, compared with vehicle group (post hoc test). Data are represented as mean ± SEM.
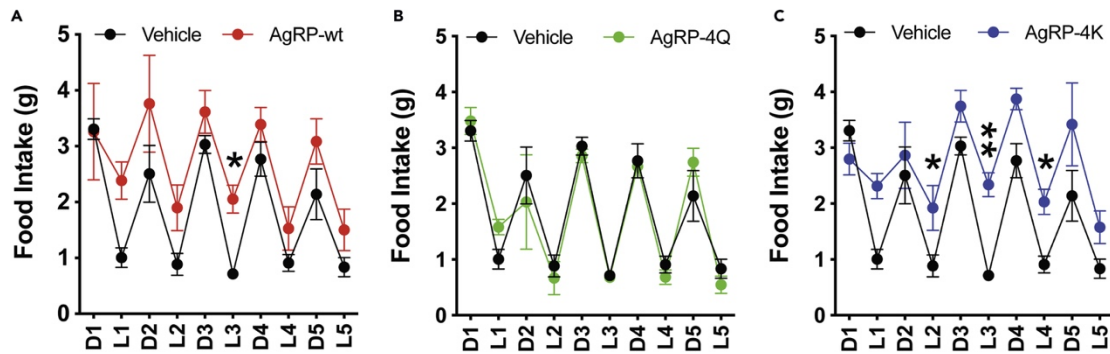
Figure 8 Effects of AgRP and Charge-Modified AgRP Variants on Food Intake in the CLAMS. Mice received AgRP-WT, AgRP-4Q, and AgRP-4K injections in the lateral ventricles, and food intake was monitored in the CLAMS for the following five days. A, AgRP-WT and C, AgRP-4K but not B, AgRP-4Q increased food intake compared with the vehicle-treated group. All of the CLAMS experiments were performed under a 12 h/12 h light/dark cycle. D, dark phase; L, light phase. $*p < 0.05$, $**p < 0.01$, compared with vehicle group (post hoc test). Data are represented as mean ± SEM.
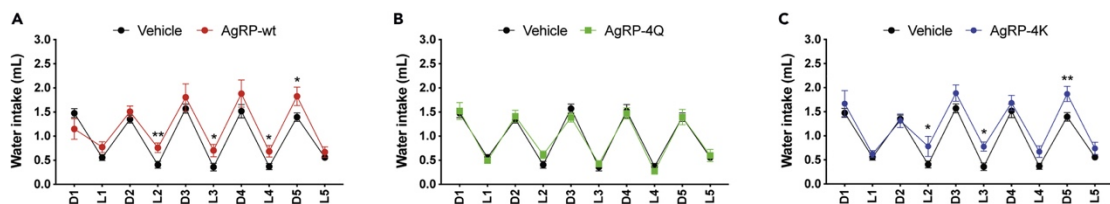
Figure 9 Effects of AgRP and Charge-Modified AgRP Variants on Water Intake in the CLAMS. A, AgRP-WT and C, AgRP-4K but not B, AgRP-4Q increased water intake. The two-way repeated-measures ANOVA revealed significant main effects of AgRP-WT ($F_{1,18} = 4.499$, $p = 0.048$) and AgRP-4K ($F_{1,18} = 6.265$, $p = 0.022$). D, dark phase; L, light phase. $*p < 0.05$, $**p < 0.01$, compared with vehicle group (post hoc test). Data are represented as mean ± SEM.

Discussion

Neurons in the ARC of the hypothalamus that express the peptides AgRP and NPY and the neurotransmitter GABA promote feeding and weight gain and repress energy expenditure, whereas neurons that express POMC and CART inhibit food intake [9]. The specific contributions of these peptides and their classic neurotransmitter systems to feeding have only recently begun to be elucidated, but their respective functions in metabolic control are less characterized [29].

Interactions between AgRP and its central receptors are believed to be facilitated by heparan sulfate proteoglycan binding, which has been proposed to act as a co-receptor and storage mechanism for heparan sulfate binding peptides such as AgRP [24,25,30]. Consistent with this view, the genetic ablation of heparanase, which selectively cleaves heparan sulfate chains, increases fat mass [31]. Conversely, heparanase-overexpressing transgenic mice have lower body fat, despite an increase in food intake, and exhibit a greater utilization of fat as the main fuel source [31]. The activation of NPY/AgRP neurons in the ARC by designer receptor exclusively activated by designer drugs (DREADDs) technology or optogenetics increases both ad libitum food intake and the motivation to work for food reinforcement in mice [32,33]. However, AgRP neurons were found not to be required for feeding responses that are induced by palatable food that recruits hedonic neural circuits [34].

The present study investigated the effects of AgRP and its interaction with heparan

sulfate on food intake and metabolism using AgRP(83-132), the mature form of AgRP

(AgRP-WT), and two charge-modified AgRP variants (AgRP-4K and AgRP-4Q) with

either a higher or lower density of positively charged amino acids outside the ICK

motif, resulting in either higher or lower affinity for heparan sulfate, respectively.

Because the ICK motif mediates the AgRP interaction with MC3/4R, AgRP-WT, AgRP-

4Q, and AgRP-4K all have identical receptor affinities and potency in vitro [23].

We found that the ICV administration of AgRP enhanced both ad libitum food intake

in the home cage and the motivation for food in an operant paradigm, which were

correlated with the density of positive charges of the AgRP variants. The AgRP-induced

increase in ad libitum food intake was abolished in AgRP-4Q (i.e., the AgRP variant

that had the least positive charges that also exhibited deficient heparan sulfate

binding) and more pronounced and protracted with AgRP-4K (i.e., the most positively

charged AgRP variant that also exhibited the greatest affinity for heparan sulfate).

However, a rapid but transient increase in operant responding for food was observed

in mice that were treated with AgRP-4Q. The increase in operant responding for food

was delayed in mice that were treated with AgRP-4K, but the increase was protracted

and lasted for approximately four days. These results indicate that in addition to ad

libitum food intake, AgRP increases the motivation for food, and both of these effects

depended on its affinity for heparan sulfate. AgRP-WT and AgRP-4K also increased

water intake, which was correlated with the increase in feeding and thus may reflect a general increase in consummatory behavior that was induced by the AgRP variants that exhibited higher positive charges and thus higher heparan sulfate binding affinity. All of the AgRP variants that were tested herein reduced body temperature, suggesting a decrease in energy expenditure. The effect on body temperature of AgRP-4Q, the variant with a lower density of positive charges, had a faster onset and was less protracted. AgRP-WT decreased oxygen consumption (VO2), indicating lower energy expenditure. A similar, although nonsignificant, trend toward a decrease in VO2 was observed with AgRP-4K, the variant with higher positive charges, but not AgRP-4Q, the variant with lower positive charges.

AgRP-WT and AgRP-4K, but not AgRP-4Q, induced a protracted and significant increase in the RER at rest (during the light phase), indicating a reduction of fat oxidation and a shift toward carbohydrates as the predominant fuel source [35–38]. In humans, overnight fasting is associated with high rates of fat oxidation (low RER), which is blunted in individuals with a family history of type 2 diabetes, reminiscent of the present results in AgRP-WT- and AgRP-4K-treated mice [28]. Reduced fatty acid oxidation at rest promotes increased fat storage, whereas exercise training can promote higher rates of fatty acid oxidation at rest as well as during acute exercise [26,39]. A high RER at rest (reduced fat oxidation and greater carbohydrate oxidation) in moderately overweight men has been linked to greater metabolic syndrome risk

compared with a low RER (greater fat oxidation at rest) [27]. The increase in the RER in

AgRP-WT- and AgRP-4K-treated mice appears to be consistent with findings of higher

fat oxidation in mice with perinatal deletions of NPY/AgRP neurons and mice with the

transgenic overexpression of heparanase, which selectively cleaves heparan sulfate

chains [31,40].

The present results showed that AgRP increased both ad libitum food intake and

operant responding for food, and these orexigenic effects of AgRP were accompanied

by metabolic changes that were characterized by lower energy expenditure and a

reduction of fat utilization as the fuel source. These actions generally depended on

the density of positively charged amino acids, indicating that the affinity of AgRP for

heparan sulfate is a key determinant of both the orexigenic and metabolic effects of

AgRP. The delayed and protracted kinetics of most actions of AgRP-WT and AgRP-4K,

which can interact with heparan sulfate unlike AgRP-4Q, are consistent with a role for

heparan sulfate proteoglycans in the extracellular matrix in controlling the diffusion

of heparan/heparin-binding peptides that act as storage mechanisms [24,25,30]. This

function of heparan sulfate proteoglycans in the extracellular matrix results in the

establishment of gradients of signaling peptides during development and has been

proposed to act as a repository of growth factors that possibly results in their

sequestration or localization in the proximity of receptors and prolongation of their

action [24,25,30].

The differential effects of AgRP on feeding and various aspects of metabolic regulation that were observed in the present study may reflect complex anatomical relationships between NPY/AgRP neurons in the ARC and their energy-relevant connections [41,42]. Populations of NPY/AgRP neurons with segregated axonal projections that differentially innervate target brain regions have been observed with cell-type-specific neuron manipulations [41,42]. A low rate of ARC neuron collateralization has been reported in rats and mice [41–43]. The optogenetic activation of NPY/AgRP neurons has shown that different projections of NPY/AgRP neurons are involved in the long-term regulation of feeding behavior through POMC/CART neurons and the acute control of appetite through an interconnected forebrain circuit that includes the paraventricular nucleus of the hypothalamus, anterior bed nucleus of the stria terminalis, and lateral hypothalamus, among other regions that are involved in feeding behavior [41,42]. The regulation of different NPY/AgRP neuronal populations appears to be specific. For example, the responsiveness to ghrelin and food deprivation characterizes both intrahypothalamic and extrahypothalamic NPY/AgRP neuronal projection subpopulations. The leptin receptor is expressed in NPY/AgRP neurons that project outside of the hypothalamus but not in neurons that project within the hypothalamus [41,42]. These considerations suggest that distinct NPY/AgRP neuronal projections may subserve the regulation of energy metabolism and food intake and that the duration and intensity of AgRP's actions on food intake and

metabolism are differentially affected by the positive charges of AgRP and its affinity for heparan sulfate.

Conclusions

The present results indicate that the orexigenic effects of AgRP are accompanied by complex metabolic changes that are characterized by lower energy expenditure, a reduction of fat oxidation, and a shift in substrate utilization toward carbohydrate oxidation. To investigate the effects of AgRP and its interaction with heparan sulfate on food intake and metabolism, we used the mature form of AgRP and two additional charge-modified AgRP variants with either a higher or a lower density of positively charged amino acids outside the receptor-binding motif, resulting in either an increase or a decrease in binding to heparan sulfate, respectively. The AgRP variants that were tested had identical MC3/4R receptor affinity and in vitro potency, but we observed significant differences between their orexigenic and metabolic responses in vivo. The in vivo potency and duration of action of AgRP largely depended on positively charged amino acids that mediate heparan sulfate binding independently of MC3/4R receptor binding. Overall, the present results support a role for AgRP and its interaction with heparan sulfate in the regulation of energy expenditure and metabolic balance between carbohydrate and lipid utilization.

Limitations of the Study

Despite convincing evidence that heparan sulfate proteoglycans are key modulators of the actions of AgRP, we cannot exclude the potential contribution of other complementary mechanisms for AgRP positive charges in potentiating and prolonging its orexigenic and metabolic effects. For instance, AgRP positive charge density may have effects at the receptor level, such as the stabilization of alternative active states of MC3Rs and MC4Rs, and may act as a biased agonist at MC4Rs on the regulation of Kir7.1 potassium channels or on the recruitment of β-arrestins [44,45]. Future studies will also investigate whether AgRP is also bound by other glycosaminoglycans, such as chondroitin sulfate.

Experimental Procedures

Peptide Synthesis, Purification, and Folding

The AgRP peptide sequences were previously described in Madonna et al., 2012. The peptide was produced on a CEM Liberty1 microwave peptide synthesizer using standard Fmoc (fluorenylmethyloxycarbonyl chloride) chemistry. Amino acids were purchased from AAPPTec and assembled on H-Rink amide ChemMatrix resin. Fmoc protecting groups were removed using 20% piperidine and 0.1 M hydroxybenzotriazole (HOBt) in dimethylformamide (DMF). Each amino acid was double coupled using four molar equivalents of Fmoc-amino acid, five molar equivalents of diisopropylcarbodiimide (DIC), and 10 molar equivalents of HOBt in DMF. Cleavage of the peptide from resin was performed in a trifluoroacetic acid

(TFA)/triisopropylsilane (TIS)/1,2-ethanedithiol (EDT)/phenol (90:4:4:2) mixture for 90 min. The resin was filtered, and the filtrate was added to 90 mL of cold dry diethyl ether. The precipitate was collected by centrifugation, and the diethyl ether was discarded. Oxidative folding was achieved in folding buffer (2.0 M GuHCl/0.1 M Tris, 3 mM GSH, 400 µM GSSG [pH 8–8.5]) at a peptide concentration of 0.1 mg/mL and stirred for 24 h. Folding was monitored by reverse-phase HPLC, which revealed one major species that was used in subsequent experiments. The folded products were purified on a C18 reverse-phase HPLC column and identified as fully oxidized peptides and confirmed with the correct molecular weight by electrospray ionization-mass spectrometry.

Glycan Array Fabrication

Amine(-NH2)-linked heparan sulfate glycan compounds (Glycan Therapeutics) were immobilized on NHS-activated surface-coated slides (Nexterion Slide-H, Applied Microarrays) using a robotic microarray printer (Microgrid II, Digilab) that was equipped with StealthSMP4B microarray pins (Telechem) to couple heparan sulfate glycan compounds by covalent binding via (-NH2) reactive chemistry. Custom printing was performed by the robotic pin deposition of 0.6 nL of (-NH2)-conjugated heparan sulfate glycan compounds in print buffer (150 mM phosphate [pH 8.5], which contained 0.01% Tween 20) onto NexterionSlide H glass slides (Applied Microarrays). Slide printing with the heparan sulfate glycan compounds was kept at 80% relative

humidity for 1 h, followed by desiccation overnight. Printed slide microarrays were placed in a sealed slide box and stored at −20°C. Before use, unreacted NHS groups on the printed slides were immersed in blocking buffer (50 mM ethanolamine in 50 mM borate buffer [pH 9.2]) for 1 h. The slides were then rinsed with water and dried before the binding assays.

Heparan Sulfate-AgRP Binding Assay

The printed slides were pre-wetted with Tris-Metal-Salts (TMS) buffer (25 mM Tris, 2.7 mM KCl, 2 mM $CaCl_2$, 2 mM $MgCl_2$, and 137 mM NaCl [pH 7.4], containing 0.05% Triton X-100). Peptides of AgRP(83-132) and AgRP charge variants were then diluted to 50 μg/mL in TMS buffer and directly applied to the pre-wetted arrays. After incubation at room temperature for 1 h, the AgRP solution or its variants were removed, and the arrays were washed with TMS buffer three successive times. A pre-complexed antibody mixture of Rb anti-human AgRP (10 μg/mL, Novus Biologicals) and anti-Rb IgG-Alexa 488 (5 μg/mL, Life Technologies) was subsequently added to the arrays and incubated for an additional 1 h at room temperature. The slides were washed by successive rinses with TMS, TMS without Triton X-100, and deionized H_2O. The washed arrays were dried by centrifugation and immediately scanned for green fluorescence using an InnoScan confocal microarray scanner (Innopsys, Carbonne, France). Images were analyzed using Mapix software and processed with ImageJ software.

Animals

Male C57BL/6 mice, 20–24 weeks old, were single-housed in a climate-controlled vivarium on a 12 h/12 h light/dark cycle (lights on 6:00 AM to 6:00 PM) and fed a standard diet (58 kcal% carbohydrate, 17 kcal% fat, and 25 kcal% protein; LM-485; Teklad Diets, Madison, WI, USA). Daily food consumption was measured by weighing the pellets in the home cage every day at the same time while the mice's body weights were recorded. All of the procedures adhered to the National Institutes of Health Guide for the Care and Use of Laboratory Animals (eighth edition) and were approved by the Institutional Animal Care and Use Committee of The Scripps Research Institute.

Ad Libitum Food Intake and Operant Responding for Food

Daily ad libitum food consumption was measured manually by weighing the standard laboratory chow (Teklad LM-485, catalog no. 7012, Teklad Diets, Madison, WI, USA) that was placed in the home cage. Body weights at the corresponding times were also monitored daily. For operant responding for food, the mice were trained to lever-press for food pellets in operant chambers (Med Associates, St. Albans, VT, USA) as described previously with minor modifications. For three days before training, 20 food pellets (14 mg, Bio-Serv, 64.5 kcal% carbohydrate, 10.1 kcal% fat, and 25.4 kcal% protein; total energy, 3.35 kcal/g) were placed in the home cage to prevent potential effects of neophobia on operant performance. The mice were trained 1 h/day under

a fixed-ratio 1 (FR1) schedule, in which each active lever-press resulted in the delivery of one pellet, accompanied by illumination of the cue light above the lever that signaled a 5-s timeout period. Water was available from a sipper in the front side of the wall opposite the levers and food receptacle. After the mice developed stable responding for food (≥20 rewards received per session and ≥75% total responses at the active lever over three consecutive sessions), the response requirement was gradually increased from FR1 to FR5 until stable responding was reached for two consecutive sessions.

Comprehensive Lab Animal Monitoring System

The comprehensive lab animal monitoring system (CLAMS; Columbus Instruments) is an open-circuit indirect calorimeter that allows simultaneous multiple parameter scoring, including measurements of gas concentrations and flow, core body temperature, activity, feeding, drinking, etc. Oxygen consumption (VO2) is a measure of the volume of oxygen that is used to convert energy substrate into adenosine triphosphate. Energy expenditure can thus be assessed by measuring core body temperature and VO2. The mice were acclimated to the CLAMS chambers for 72 h before they received an injection of AgRP and then were recorded for five days after the injection. Food and water were provided in the chamber ad libitum throughout the experiments. The RER (i.e., the ratio of VO2 to CO2 production) can be used to estimate the fuel source. An RER = 0.7 indicates that fatty acids are the predominant

fuel source for oxidative metabolism. An RER = 0.85 suggests a mix of fat and carbohydrates. An RER ≥1.00 indicates that carbohydrates are the primary fuel source [35–38].

Intracranial Cannula Implantation and ICV Microinjection Procedure

Intracranial stereotaxic surgery was performed as described previously [46]. Briefly, the mice were immobilized in a stereotaxic frame in the flat-skull position (Kopf Instruments), and a cannula (26 gauge, Plastics One, Roanoke, VA, USA) was implanted in the lateral ventricle (anterior/posterior, −0.22 mm; medial/lateral, 1.0 mm; dorsal/ventral, −1.5 mm). The mice were allowed to recover from surgery for 7–10 days. On the test day, a stainless-steel injector (33 gauge, extended 1 mm below the tip of the cannula; Plastics One, Roanoke, VA, USA) was inserted into the cannula, and the AgRP solution (1 nmole in 1 μL of saline) was delivered slowly at a rate of 0.5 μL/min through the injector by a syringe pump (KD Scientific). The injector remained in place for 2 min to allow for diffusion and then was withdrawn slowly to avoid backflow of the fluid.

Data Analysis

Two-way repeated-measures analysis of variance (ANOVA) was used to assess the main effects of AgRP treatment. Significant differences between the AgRP group and vehicle control group were assessed using Fisher's Least Significant Difference post

hoc test. Values of $p < 0.05$ were considered statistically significant. All of the behavioral data are expressed as means ± SEM and were analyzed using GraphPad Prism 8.0 software.

Acknowledgments

Author Contributions

Conceptualization: P.P.S. and G.L.M. Methodology and investigation: J.C., V.C., T.K., Y.Y., I.H., A.W., R.M.B., V.R.C., and P.P.S. Data analysis: J.C., V.C., T.K., I.H., R.M.B., and V.R.C. Manuscript writing: J.C., V.C., T.K., P.P.S., and G.L.M. Review and editing: J.C., V.C., T.K., Y.Y., I.H., A.W., R.M.B., J.C.P., V.R.C., G.L.M., and P.P.S. Funding acquisition: P.P.S. and G.L.M.

References

(1) van der Klaauw, A. A. Neuropeptides in Obesity and Metabolic Disease. *Clin. Chem.* **2018**, *64* (1), 173–182.

(2) Butler, A. A.; Kesterson, R. A.; Khong, K.; Cullen, M. J.; Pelleymounter, M. A.; Dekoning, J.; Baetscher, M.; Cone, R. D. A Unique Metabolic Syndrome Causes Obesity in the Melanocortin-3 Receptor-Deficient Mouse. *Endocrinology* **2000**, *141* (9), 3518–3521.

(3) Chen, A. S.; Marsh, D. J.; Trumbauer, M. E.; Frazier, E. G.; Guan, X. M.; Yu, H.; Rosenblum, C. I.; Vongs, A.; Feng, Y.; Cao, L.; Metzger, J. M.; Strack, A. M.; Camacho, R. E.; Mellin, T. N.; Nunes, C. N.; Min, W.; Fisher, J.; Gopal-Truter, S.; MacIntyre, D. E.; Chen, H. Y.; Van der Ploeg, L. H. Inactivation of the Mouse Melanocortin-3 Receptor Results in Increased Fat Mass and Reduced Lean Body Mass. *Nat. Genet.* **2000**, *26* (1), 97–102.

(4) Ehtesham, S.; Qasim, A.; Meyre, D. Loss-of-Function Mutations in the Melanocortin-3 Receptor Gene Confer Risk for Human Obesity: A Systematic Review and Meta-Analysis. *Obes Rev* **2019**, *20* (8), 1085–1092.

(5) Lede, V.; Franke, C.; Meusel, A.; Teupser, D.; Ricken, A.; Thiery, J.; Schiller, J.; Huster, D.; Schöneberg, T.; Schulz, A. Severe Atherosclerosis and Hypercholesterolemia in Mice Lacking Both the Melanocortin Type 4 Receptor and Low Density Lipoprotein Receptor. *PLoS ONE* **2016**, *11* (12), e0167888.

(6) Nuutinen, S.; Ailanen, L.; Savontaus, E.; Rinne, P. Melanocortin Overexpression Limits Diet-Induced Inflammation and Atherosclerosis in LDLR-/- Mice. *J. Endocrinol.* **2018**, *236* (3), 111–123.

(7) Krashes, M. J.; Shah, B. P.; Koda, S.; Lowell, B. B. Rapid versus Delayed Stimulation of Feeding by the Endogenously Released AgRP Neuron Mediators, GABA, NPY and AgRP. *Cell Metab* **2013**, *18* (4).

(8) Loh, K.; Herzog, H.; Shi, Y.-C. Regulation of Energy Homeostasis by the NPY System. *Trends Endocrinol. Metab.* **2015**, *26* (3), 125–135.

(9) Dodd, G. T.; Tiganis, T. Insulin Action in the Brain: Roles in Energy and Glucose Homeostasis. *J. Neuroendocrinol.* **2017**, *29* (10).

(10) Könner, A. C.; Janoschek, R.; Plum, L.; Jordan, S. D.; Rother, E.; Ma, X.; Xu, C.; Enriori, P.; Hampel, B.; Barsh, G. S.; Kahn, C. R.; Cowley, M. A.; Ashcroft, F. M.; Brüning, J. C. Insulin Action in AgRP-Expressing Neurons Is Required for Suppression of Hepatic Glucose Production. *Cell Metab.* **2007**, *5* (6), 438–449.

(11) Obici, S.; Zhang, B. B.; Karkanias, G.; Rossetti, L. Hypothalamic Insulin Signaling Is Required for Inhibition of Glucose Production. *Nat. Med.* **2002**, *8* (12), 1376–1382.

(12) Pocai, A.; Lam, T. K. T.; Gutierrez-Juarez, R.; Obici, S.; Schwartz, G. J.; Bryan, J.; Aguilar-Bryan, L.; Rossetti, L. Hypothalamic K(ATP) Channels Control Hepatic Glucose Production. *Nature* **2005**, *434* (7036), 1026–1031.

(13) Steculorum, S. M.; Ruud, J.; Karakasilioti, I.; Backes, H.; Engström Ruud, L.; Timper, K.; Hess, M. E.; Tsaousidou, E.; Mauer, J.; Vogt, M. C.; Paeger, L.; Bremser, S.; Klein, A. C.; Morgan, D. A.; Frommolt, P.; Brinkkötter, P. T.; Hammerschmidt, P.; Benzing, T.; Rahmouni, K.; Wunderlich, F. T.; Kloppenburg, P.; Brüning, J. C. AgRP Neurons Control Systemic Insulin Sensitivity via Myostatin Expression in Brown Adipose Tissue. *Cell* **2016**, *165* (1), 125–138.

(14) Deng, J.; Yuan, F.; Guo, Y.; Xiao, Y.; Niu, Y.; Deng, Y.; Han, X.; Guan, Y.; Chen, S.; Guo, F. Deletion of ATF4 in AgRP Neurons Promotes Fat Loss Mainly via Increasing Energy Expenditure. *Diabetes* **2017**, *66* (3), 640–650.

(15) Goodfellow, V. S.; Saunders, J. The Melanocortin System and Its Role in Obesity and Cachexia. *Curr Top Med Chem* **2003**, *3* (8), 855–883.

(16) Kalra, S. P.; Dube, M. G.; Pu, S.; Xu, B.; Horvath, T. L.; Kalra, P. S. Interacting Appetite-Regulating Pathways in the Hypothalamic Regulation of Body Weight. *Endocr. Rev.* **1999**, *20* (1), 68–100.

(17) Williams, G.; Bing, C.; Cai, X. J.; Harrold, J. A.; King, P. J.; Liu, X. H. The Hypothalamus and the Control of Energy Homeostasis: Different Circuits, Different Purposes. *Physiol. Behav.* **2001**, *74* (4–5), 683–701.

(18) Schiöth, H. B.; Chhajlani, V.; Muceniece, R.; Klusa, V.; Wikberg, J. E. Major Pharmacological Distinction of the ACTH Receptor from Other Melanocortin Receptors. *Life Sci.* **1996**, *59* (10), 797–801.

(19) Cone, R. D.; Cowley, M. A.; Butler, A. A.; Fan, W.; Marks, D. L.; Low, M. J. The Arcuate Nucleus as a Conduit for Diverse Signals Relevant to Energy Homeostasis. *Int. J. Obes. Relat. Metab. Disord.* **2001**, *25 Suppl 5*, S63-67.

(20) Creemers, J. W. M.; Pritchard, L. E.; Gyte, A.; Le Rouzic, P.; Meulemans, S.; Wardlaw, S. L.; Zhu, X.; Steiner, D. F.; Davies, N.; Armstrong, D.; Lawrence, C. B.; Luckman, S. M.; Schmitz, C. A.; Davies, R. A.; Brennand, J. C.; White, A. Agouti-Related Protein Is Posttranslationally Cleaved by Proprotein Convertase 1 to

Generate Agouti-Related Protein (AGRP)83–132: Interaction between AGRP83–132 and Melanocortin Receptors Cannot Be Influenced by Syndecan-3. *Endocrinology* **2006**, *147* (4), 1621–1631.

(21) McNulty, J. C.; Thompson, D. A.; Bolin, K. A.; Wilken, J.; Barsh, G. S.; Millhauser, G. L. High-Resolution NMR Structure of the Chemically-Synthesized Melanocortin Receptor Binding Domain AGRP(87-132) of the Agouti-Related Protein. *Biochemistry* **2001**, *40* (51), 15520–15527.

(22) Palomino, R.; Lee, H.-W.; Millhauser, G. L. The Agouti-Related Peptide Binds Heparan Sulfate Through Segments Critical For Its Orexigenic Effects. *J. Biol. Chem.* **2017**, jbc.M116.772822.

(23) Madonna, M. E.; Schurdak, J.; Yang, Y.; Benoit, S.; Millhauser, G. L. Agouti-Related Protein Segments Outside of the Receptor Binding Core Are Required for Enhanced Short- and Long-Term Feeding Stimulation. *ACS Chem. Biol.* **2012**, *7* (2), 395–402.

(24) Kim, S.-H.; Turnbull, J.; Guimond, S. Extracellular Matrix and Cell Signalling: The Dynamic Cooperation of Integrin, Proteoglycan and Growth Factor Receptor. *J. Endocrinol.* **2011**, *209* (2), 139–151.

(25) Sarrazin, S.; Lamanna, W. C.; Esko, J. D. Heparan Sulfate Proteoglycans. *Cold Spring Harb Perspect Biol* **2011**, *3* (7).

(26) Must, A.; Spadano, J.; Coakley, E. H.; Field, A. E.; Colditz, G.; Dietz, W. H. The Disease Burden Associated with Overweight and Obesity. *JAMA* **1999**, *282* (16), 1523–1529.

(27) Rosenkilde, M.; Nordby, P.; Nielsen, L. B.; Stallknecht, B. M.; Helge, J. W. Fat Oxidation at Rest Predicts Peak Fat Oxidation during Exercise and Metabolic Phenotype in Overweight Men. *Int J Obes (Lond)* **2010**, *34* (5), 871–877.

(28) Ukropcova, B.; Sereda, O.; de Jonge, L.; Bogacka, I.; Nguyen, T.; Xie, H.; Bray, G. A.; Smith, S. R. Family History of Diabetes Links Impaired Substrate Switching and Reduced Mitochondrial Content in Skeletal Muscle. *Diabetes* **2007**, *56* (3), 720–727.

(29) Andermann, M. L.; Lowell, B. B. Toward a Wiring Diagram Understanding of Appetite Control. *Neuron* **2017**, *95* (4), 757–778.

(30) Reizes, O.; Lincecum, J.; Wang, Z.; Goldberger, O.; Huang, L.; Kaksonen, M.; Ahima, R.; Hinkes, M. T.; Barsh, G. S.; Rauvala, H.; Bernfield, M. Transgenic Expression of Syndecan-1 Uncovers a Physiological Control of Feeding Behavior by Syndecan-3. *Cell* **2001**, *106* (1), 105–116.

(31) Karlsson-Lindahl, L.; Schmidt, L.; Haage, D.; Hansson, C.; Taube, M.; Egecioglu, E.; Egeciouglu, E.; Tan, Y.; Admyre, T.; Jansson, J.-O.; Vlodavsky, I.; Li, J.-P.; Lindahl, U.; Dickson, S. L. Heparanase Affects Food Intake and Regulates Energy Balance in Mice. *PLoS ONE* **2012**, *7* (3), e34313.

(32) Aponte, Y.; Atasoy, D.; Sternson, S. M. AGRP Neurons Are Sufficient to Orchestrate Feeding Behavior Rapidly and without Training. *Nat. Neurosci.* **2011**, *14* (3), 351–355.

(33) Krashes, M. J.; Koda, S.; Ye, C.; Rogan, S. C.; Adams, A. C.; Cusher, D. S.; Maratos-Flier, E.; Roth, B. L.; Lowell, B. B. Rapid, Reversible Activation of AgRP Neurons Drives Feeding Behavior in Mice. *J. Clin. Invest.* **2011**, *121* (4), 1424–1428.

(34) Denis, R. G. P.; Joly-Amado, A.; Webber, E.; Langlet, F.; Schaeffer, M.; Padilla, S. L.; Cansell, C.; Dehouck, B.; Castel, J.; Delbès, A.-S.; Martinez, S.; Lacombe, A.; Rouch, C.; Kassis, N.; Fehrentz, J.-A.; Martinez, J.; Verdié, P.; Hnasko, T. S.; Palmiter, R. D.; Krashes, M. J.; Güler, A. D.; Magnan, C.; Luquet, S. Palatability Can Drive Feeding Independent of AgRP Neurons. *Cell Metab.* **2015**, *22* (4), 646–657.

(35) Lusk, G. ANIMAL CALORIMETRY Twenty-Fourth Paper. ANALYSIS OF THE OXIDATION OF MIXTURES OF CARBOHYDRATE AND FAT. *J. Biol. Chem.* **1924**, *59* (1), 41–42.

(36) Marvyn, P. M.; Bradley, R. M.; Mardian, E. B.; Marks, K. A.; Duncan, R. E. Data on Oxygen Consumption Rate, Respiratory Exchange Ratio, and Movement in C57BL/6J Female Mice on the Third Day of Consuming a High-Fat Diet. *Data Brief* **2016**, *7*, 472–475.

(37) Schmidt-Nielsen, K. *Animal Physiology: Adaptation and Environment*; Cambridge University Press, 1997.

(38) Speakman, J. R. Measuring Energy Metabolism in the Mouse - Theoretical, Practical, and Analytical Considerations. *Front Physiol* **2013**, *4*, 34.

(39) van Loon, L. J.; Jeukendrup, A. E.; Saris, W. H.; Wagenmakers, A. J. Effect of Training Status on Fuel Selection during Submaximal Exercise with Glucose Ingestion. *J. Appl. Physiol.* **1999**, *87* (4), 1413–1420.

(40) Cansell, C.; Denis, R. G. P.; Joly-Amado, A.; Castel, J.; Luquet, S. Arcuate AgRP Neurons and the Regulation of Energy Balance. *Front Endocrinol (Lausanne)* **2012**, *3*, 169.

(41) Betley, J. N.; Cao, Z. F. H.; Ritola, K. D.; Sternson, S. M. Parallel, Redundant Circuit Organization for Homeostatic Control of Feeding Behavior. *Cell* **2013**, *155* (6), 1337–1350.

(42) Sternson, S. M.; Atasoy, D. Agouti-Related Protein Neuron Circuits That Regulate Appetite. *Neuroendocrinology* **2014**, *100* (2–3), 95–102.

(43) Chronwall, B. M. Anatomy and Physiology of the Neuroendocrine Arcuate Nucleus. *Peptides* **1985**, *6 Suppl 2*, 1–11.

(44) Ghamari-Langroudi, M.; Digby, G. J.; Sebag, J. A.; Millhauser, G. L.; Palomino, R.; Matthews, R.; Gillyard, T.; Panaro, B. L.; Tough, I. R.; Cox, H. M.; Denton, J. S.; Cone, R. D. G-Protein-Independent Coupling of MC4R to Kir7.1 in Hypothalamic Neurons. *Nature* **2015**

(45) Breit, A.; Wolff, K.; Kalwa, H.; Jarry, H.; Büch, T.; Gudermann, T. The Natural Inverse Agonist Agouti-Related Protein Induces Arrestin-Mediated Endocytosis of Melanocortin-3 and -4 Receptors. *J. Biol. Chem.* **2006**, *281* (49), 37447–37456.

(46) Chen, J.; Repunte-Canonigo, V.; Kawamura, T.; Lefebvre, C.; Shin, W.; Howell, L. L.; Hemby, S. E.; Harvey, B. K.; Califano, A.; Morales, M.; Koob, G. F.; Sanna, P. P. Hypothalamic Proteoglycan Syndecan-3 Is a Novel Cocaine Addiction Resilience Factor. *Nat Commun* **2013**, *4*, 1955.

Chapter 3

Membrane Orientation and Oligomerization of the Melanocortin Receptor Accessory Protein 2

Valerie Chen, Antonio E. Bruno, Laura L. Britt, Ciria C. Hernandez, Luis E. Gimenez, Alys Peisley, Roger D. Cone & Glenn L. Millhauser*

*Corresponding author: glennm@ucsc.edu

Summary

The melanocortin receptor accessory protein 2 (MRAP2) plays a pivotal role in the regulation of several G-protein coupled receptors (GPCR) that are essential for energy balance and food intake. MRAP2 loss-of-function results in obesity in mammals. MRAP2 and its homolog MRAP1 have an unusual membrane topology and are the only known eukaryotic proteins that thread into the membrane in both orientations. In this study, we demonstrate that the conserved polybasic motif that dictates the membrane topology and dimerization of MRAP1 does not control the membrane orientation and dimerization of MRAP2. We also show that MRAP2 dimerizes through its transmembrane domain and can form higher order oligomers that arrange MRAP2 monomers in a parallel orientation. Investigating the molecular details of MRAP2 structure is essential for understanding the mechanism by which it regulates GPCRs and will aid in elucidating the pathways involved in metabolic dysfunction.

Introduction

The melanocortin receptor accessory protein 2 (MRAP2) regulates several G-protein coupled receptors (GPCRs) that play a critical role in the regulation of energy homeostasis, and heterozygous MRAP2 variants have been identified in obese humans[1–4]. MRAP2 modulates the signaling of the melanocortin-4 receptor (MC4R), one of the five GPCRs in the melanocortin receptor family[1,5]. MC4R and MRAP2 are

75

expressed in the paraventricular nucleus of the hypothalamus (PVH), a critical region for the control of food intake. MC4R is essential for energy homeostasis and heterozygous mutations in MC4R are the most common monogenic cause of human obesity[6,7]. In zebrafish, MRAP2 allows for developmental control of MC4R signaling[5]. Zebrafish MRAP2a, which is restricted to larval development suppresses MC4R signaling while MRAP2b, which is expressed in adult zebrafish, increases MC4R's sensitivity to its agonist α-melanocyte-stimulating hormone. Furthermore, MRAP2 enhances signaling through MC4R *in vitro* and overexpression of MRAP2 in MC4R-containing PVH neurons leads to a reduction in food intake and increased energy expenditure in female mice[1,8]. Targeted deletion of MRAP2 in mice results in an obese phenotype, however, mice lacking only MC4R are more obese than mice lacking both MRAP2 and MC4R[1]. This suggests that there are other mechanisms by which MRAP2 also promotes feeding. It is now understood that MRAP2's regulation over GPCRs is not limited to the melanocortin receptor family. MRAP2 has been shown to promote feeding through inhibition of the prokineticin receptor-1 as well as to decrease food intake through inhibition of the orexin receptor[9,10]. Additionally, MRAP2 regulates hunger sensing by potentiating ghrelin signaling through its interaction with the growth hormone secretagogue receptor 1a (GHSR1a) in the arcuate nucleus of the hypothalamus (ARC)[11,12].

MRAP2, as well as its well-studied homolog MRAP1, are single-pass transmembrane proteins that can insert into the membrane in both orientations – N-terminal domain out or in (Figure 1A, 1B) [13–15]. Like MRAP1, MRAP2 can homodimerize and form anti-parallel dimers[16,17]. MRAP2 and MRAP1 are the only two proteins in the eukaryotic proteome that are currently known to exhibit this unusual membrane orientation. The orientation of most membrane proteins is predicted by the "positive inside rule," where the charged amino acids flanking the transmembrane domain determine the overall orientation such that the more positive region faces the cytosol [18,19]. Based on this rule, MRAP1 is predicted to insert into the membrane in both orientations, which agrees with experimental data. Using the same line of logic, MRAP2 is predicted to have its N-terminal domain in the cytosol. Nevertheless, recent findings show that MRAP2 has dual topology. It is evident that the "positive inside rule" is not sufficient for explaining MRAP2's membrane orientation.

A

GPCR   MRAP2

B

```
hMRAP2    1  MSAQRLISNRTSQQSASNSDYTWEYEYYETGPVSFEGLKAHKYSIVIGFWVGLAVFVIFY
hMRAP1    1  MANG------T-NASAPYYSYEMYLDYLDIIPVDEKKLKAHKHSIVIAFWVSLAAFVVLL
                                                    transmembrane

hMRAP2   61  FFVLTLLTKLGAPHQDNAESSEKRFRMNSFVSDFGRPLEPDKVFSRQGNEESRSLFHCYL
hMRAP1   54  FLILLYMSWSASPQMRNSPKHHQTCPWSH---------------------------GL

hMRAP2  121  NEVERLDRAKACHQTTALDSDVQLQEAIR-SSGQPEEPLNRLMKFDIPNF-VNTDQNYFG
hMRAP1   85  NLHLCTQKCLPCHREPLATSQAQASSVEPGSRTGPDQPLRQESSSTPLGGFQTHPTLLW

hMRAP2  179  EDDPL--------ISEPPIVLETKPLSQTSHKDLD
hMRAP1  145  PLTLNGGPLVRSKPSEPPPGDRTSQLQS-------
```

C

```
              38        44
              L K A H K Y S
       N9

N-  [  NTD  ][ ][ TM ][         CTD         ]  -C

              ↑
        Dimerization/orientation
          motif from MRAP1
```
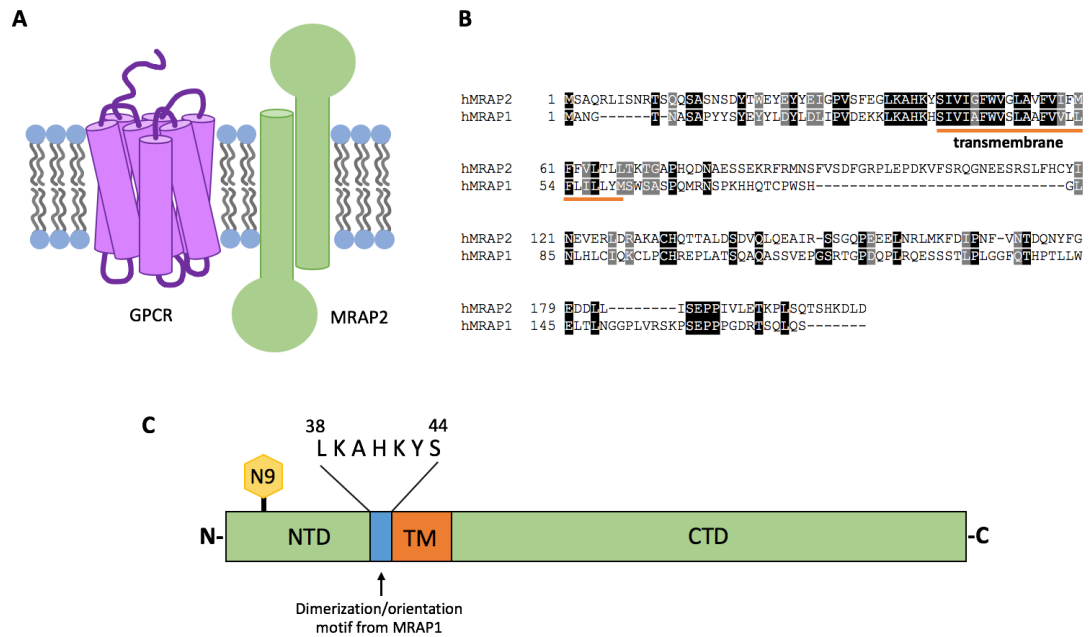
Figure 1 MRAP2 is an oligomeric, single-pass transmembrane protein that is critical for the modulation of GPCRs that are essential for energy homeostasis. A, Schematic depicting MRAP2's dual topology. B, Protein alignment of human MRAP2 and human MRAP1. The transmembrane domain is underlined in orange. MRAP2 and MRAP1 are most conserved in their N-terminal and transmembrane domains. C, Schematic of MRAP2 protein. MRAP2 is glycosylated at residue 9, shown in yellow. The N-terminal domain (NTD) and C-terminal domain (CTD) are in green. The transmembrane (TM) domain is in orange. The conserved, polybasic motif required for the dual topology and dimerization of MRAP1 is in blue.

Despite the important role MRAP2 plays in the modulation of energy homeostasis, the sequence features within MRAP2 that dictate membrane orientation and dimerization are unknown. MRAP1's membrane orientation and oligomeric state are dependent on a short polybasic segment adjacent to the transmembrane domain [13,14]. While this motif is conserved in MRAP2, we show that this sequence does not dictate MRAP2's membrane orientation or dimerization in cell culture. Additionally, using

truncation mutations, we identify the transmembrane domain of MRAP2 as the minimal dimerization domain. Finally, we show that contrary to the assumption that MRAP2 can only form anti-parallel dimers, MRAP2 can form parallel dimers as well as higher order oligomers. Our results not only highlight important differences between MRAP1 and MRAP2 but also offer new insight into MRAP2 structure. Understanding the molecular details that determine MRAP2's oligomeric state and membrane orientation will aid in elucidating the mechanism by which MRAP2 regulates GPCRs that are essential for metabolic processes.

Results

The conserved polybasic motif (38-44) that is required for dual topology and dimerization of MRAP1 is not required for dual topology and dimerization of MRAP2.

The dual topology and oligomeric state of MRAP1 is dictated by a short polybasic segment in the N-terminal domain that is directly adjacent to the transmembrane domain (Figure 1C). Sebag and Hinkle showed that mouse MRAP1 lacking residues 31 to 37 (MRAP1 Δ31-37) has a fixed membrane orientation such that the N-terminus of MRAP1 is extracellular and the C-terminus is cytosolic.[13] This polybasic motif that determines the membrane orientation of MRAP1 is conserved in MRAP2. In order to investigate whether this sequence is required for dual topology of MRAP2, immunocytochemistry and microscopy were used to detect cell surface MRAP2 from

intact, non-permeabilized cells that are transiently transfected with either N-terminally FLAG epitope-tagged or C-terminally FLAG epitope-tagged MRAP2 in human embryonic kidney 293T (HEK293T) cells (Figure 2A). Both the N-terminal domain and the C-terminal domain of wild-type MRAP2 were detected extracellularly. Unexpectedly, both the N-terminal domain and the C-terminal domain of MRAP2 lacking the polybasic motif (MRAP2 Δ38-44) were also detected on the cell surface. Immunocytochemistry and flow cytometry were used to measure the cell surface N-terminal domain to C-terminal domain ratio of wild-type MRAP2 Δ38-44 (Figure 2B). As expected, we find that wild-type MRAP2 has a cell surface N-terminal domain to C-terminal domain ratio of approximately 1. As a control, RAMP3, a single-pass transmembrane protein that was previously shown to favor a conformation with an extracellular N-terminus[13,20] does in fact have an N-terminal domain to C-terminal domain ratio of approximately 2. We confirm that while deletion of the polybasic motif in MRAP2 does result in a modest preference for an extracellular N-terminal domain, MRAP2 Δ38-44 still has dual topology. Additionally, the presence of an immunoreactive "doublet band" for MRAP2 Δ38-44 indicates that the N-terminal asparagine residue exists in both glycosylated and unglycosylated forms (Figure 2C). This further indicates dual topology of MRAP2 Δ38-44 since the N-terminus must be in the ER lumen for glycosylation to occur. These results show that the conserved polybasic segment that is required for the dual topology of MRAP1 is not required for the dual topology of MRAP2.

MRAP1 Δ31-37 cannot form dimers, likely due to the fact that it has a fixed membrane orientation.[13] To determine whether MRAP2 Δ38-44 can form dimers or higher order oligomers, HEK293T cells were co-transfected with both FLAG- and HA-epitope tagged versions of either wild-type MRAP2 or MRAP2 Δ38-44. Co-immunoprecipitation, followed by western blotting showed that both wild-type MRAP2 and MRAP2 Δ38-44 form dimers or higher order oligomers (Figure 2D). The same experiment was performed in Chinese hamster ovary (CHO) cells and yielded the same results (Figure 3). Densitometry analysis was used to measure the amount of FLAG-tagged material that was co-purified with HA-tagged protein (Figure 2E). From this analysis, MRAP2 Δ38-44 has a lower propensity for forming dimers than wild-type MRAP2. Overall, these results indicate that the conserved polybasic motif that is required for dual topology and dimerization in MRAP1 is not required for either dual topology or dimerization of MRAP2.
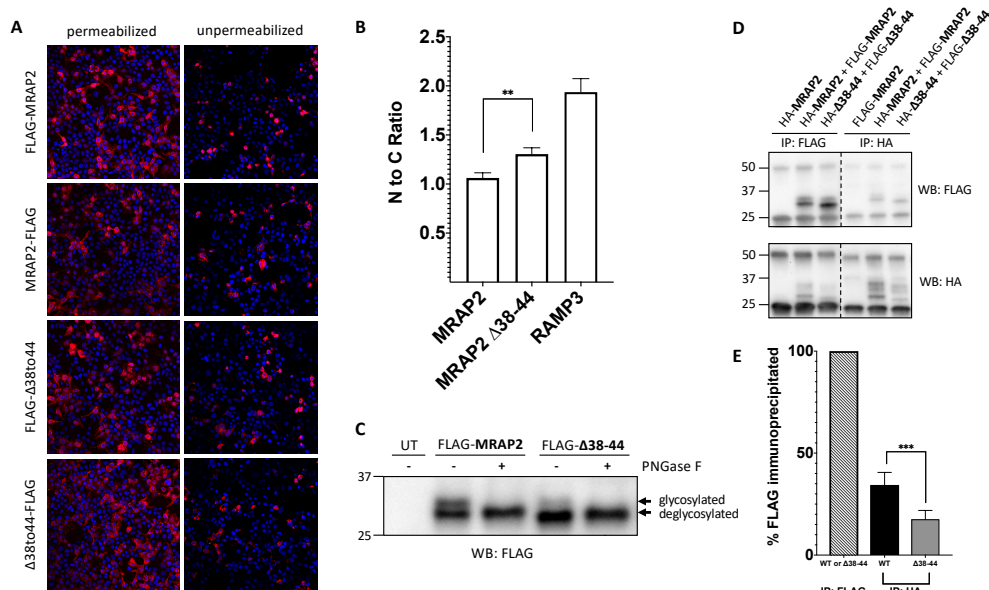
Figure 2 The conserved motif required for dual topology and dimerization of MRAP1 is not required for dual topology and dimerization of MRAP2. A, Both the N-terminus and C-terminus of MRAP2 WT and Δ38-44 are detected from intact, unpermeabilized HEK293 cells, as seen by immunofluorescence. B, Flow cytometry was used to determine the N-terminal to C-terminal fluorescence ratio for MRAP2 WT, Δ38-44, and RAMP3 from intact cells expressing N-terminally tagged constructs and C-terminally tagged constructs. Expression levels for each construct were normalized using parallel experiments with permeabilized cells. Analysis was performed using three independent experiments. C, Immunoblot showing two protein species for FLAG-MRAP2 and FLAG-Δ38-44. Treatment with PNGase F results in a single, deglycosylated protein species. D, Immunoblot showing co-immunoprecipitation of HA- and FLAG-tagged MRAP2 and HA- and FLAG-tagged Δ38-44. E, Densitometry analysis was used to measure the relative amounts of protein immunoprecipitated. The amount of FLAG-MRAP2 and FLAG-Δ38-44 immunoprecipitated was set to 100%. The data show that MRAP2 Δ38-44 has a lower propensity for forming higher order oligomers than WT MRAP2. Analysis was performed using six independent experiments. Error bars are SEM. ***$p < 0.001$, **$p < 0.01$
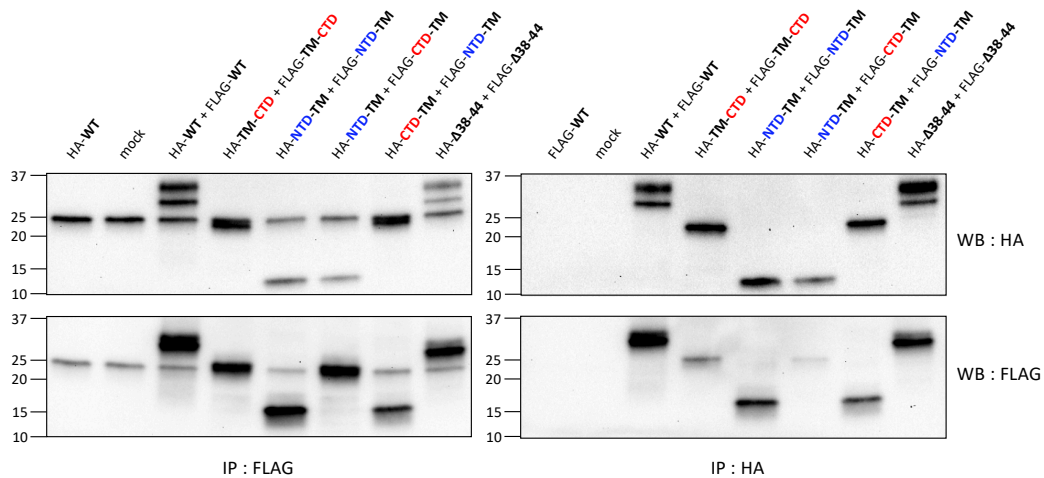
Figure 3 Co-immunoprecipitation of MRAP2 HA- and FLAG-tagged constructs from CHO cells. CHO cells are co-transfected with HA- and FLAG-tagged MRAP2 constructs. Co-immunoprecipitations from cell lysates followed by immunoblotting show that neither the N-terminal domain, nor the C-terminal domain, nor residues 38 to 44 are required for MRAP2 dimerization.

MRAP2 dimerizes through its transmembrane domain

MRAP2 is known to form dimers or higher order oligomers but the dimerization domain has not been identified. In order to identify the dimerization domain, constructs were created that either truncate the C-terminal domain (NTD-TM) or N-terminal domain (TM-CTD). HEK293T cells were co-transfected with both FLAG- and HA-epitope tagged constructs in the following combinations: TM-CTD + TM-CTD, NTD-TM + NTD-TM, or NTD-TM + TM-CTD. Co-immunoprecipitation, followed by western blotting show that neither the N-terminal domain nor the C-terminal domain are required for dimerization (Figure 4A). Specifically, TM-CTD can be co-immunoprecipitated with itself and with NTD-TM (Figure 4A, lanes 3, 5 and 6) and

NTD-TM can be co-immunoprecipitated with itself (Figure 4A, lane 4). The experiment

was also performed in CHO cells and yielded the same results (Figure 3). Based on

these results MRAP2 dimerizes through its transmembrane domain. An alternative

but unlikely hypothesis is that either the N-terminal domain or the C-terminal domain

is sufficient for dimerization.

The GxxxG motif is common in transmembrane helix interactions[21,22]. We then

investigated whether the glycine residues within the transmembrane domain of

MRAP2 are required for dimerization. HEK293T cells were co-transfected with both

HA- and FLAG-tagged MRAP2 WT or MRAP2 G48L+G52L. Co-immunoprecipitations

from cell lysates followed by immunoblotting show that the glycine residues within

the transmembrane domain are not required for MRAP2 dimerization (Figure 4C).
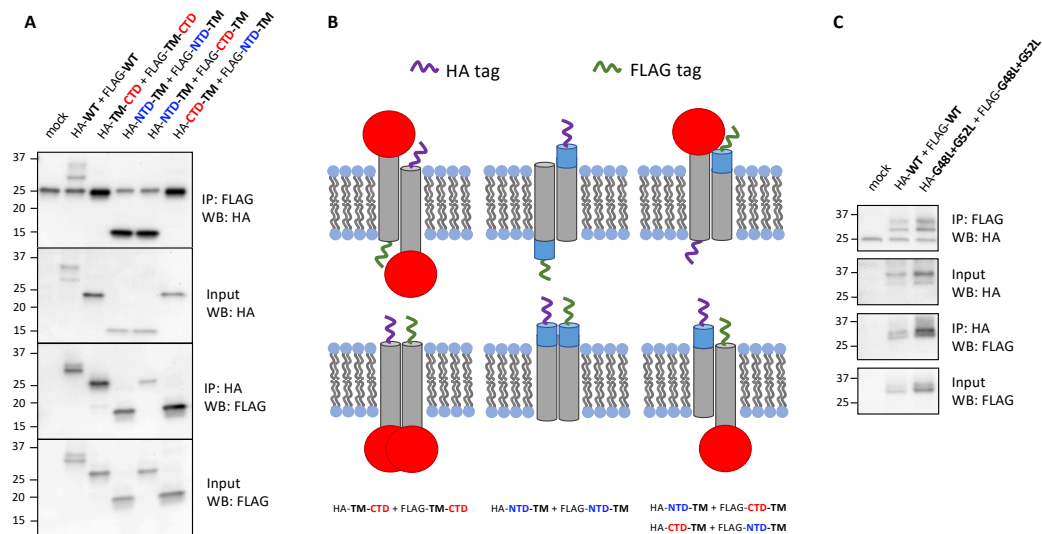
Figure 4 MRAP2 dimerizes through its transmembrane domain. A, HEK293 cells are co-transfected with HA- and FLAG-tagged MRAP2 constructs that possess either N-terminal domain truncations (TM-CTD) for C-terminal domain truncations (NTD-TM). Co-immunoprecipitations from cell lysates followed by immunoblotting show that neither the N-terminal domain nor C-terminal domain are required for dimerization of MRAP2. B, Schematic depicting the co-immunoprecipitated HA- and FLAG-tagged MRAP2 dimers. C, HEK293 cells are co-transfected with HA- and FLAG-tagged MRAP2 WT or MRAP2 G48L+G52L. Co-immunoprecipitations from cell lysates followed by immunoblotting show that the glycine residues within the transmembrane domain are not required for MRAP2 dimerization.

MRAP2 can form parallel dimers and higher order oligomers

Based on bimolecular fluorescence complementation experiments by Sebag and Hinkle, MRAP2, like MRAP1, forms anti-parallel dimers[16]. While previous experiments show that MRAP1 forms exclusively anti-parallel dimers and does not form parallel dimers, it is unclear as to whether this holds true for MRAP2. To determine whether MRAP2 forms parallel dimers, a NanoBiT protein-protein interaction assay was performed. The NanoBiT system is composed of a large BiT (LgBiT) and small BiT

(SmBiT) that have very little to no luciferase activity on their own. However, when LgBiT and SmBiT are in close proximity within the cell, the functional luciferase will then generate a luminescent signal at even low protein expression levels, driven by weak HSV-TK promoter. The low intrinsic affinity between the isolated SmBiT and LgBiT lessens the likelihood of spurious dimerization driven by these segments. The following combinations of DNA were transfected into HEK293T cells: MRAP2-LgBiT + SmBiT-PRKACA, LgBiT-MRAP2 + SmBiT-PRKACA, MRAP2-LgBiT + MRAP2-SmBiT, and LgBiT-MRAP2 + MRAP2-SmBiT. PRKACA is a non-interacting cytosolic protein that is used as a negative control. Surprisingly, when MRAP2-LgBiT and MRAP2-SmBiT are transfected together, we see a NanoBiT luminescence signal that is significantly higher than the negative control (Figure 5A). These results show that the C-terminal domains are of MRAP2 are in close proximity to each other in live cells (Figure 5B). Unexpectedly, when LgBiT-MRAP2 and MRAP2-SmBiT are transfected together, there is less NanoBiT signal than the negative control. The absence of a significant NanoBiT signal from the anti-parallel orientation may be due to the length of the linker between MRAP2 and LgBiT. Once MRAP2 multimers are positioned in the membrane, the linker may not be long enough to favorably allow for a LgBiT and SmBiT interaction. These results indicate that the C-terminal domains of MRAP2 are in close-proximity in the cell but does not exclude anti-parallel MRAP2 dimers.
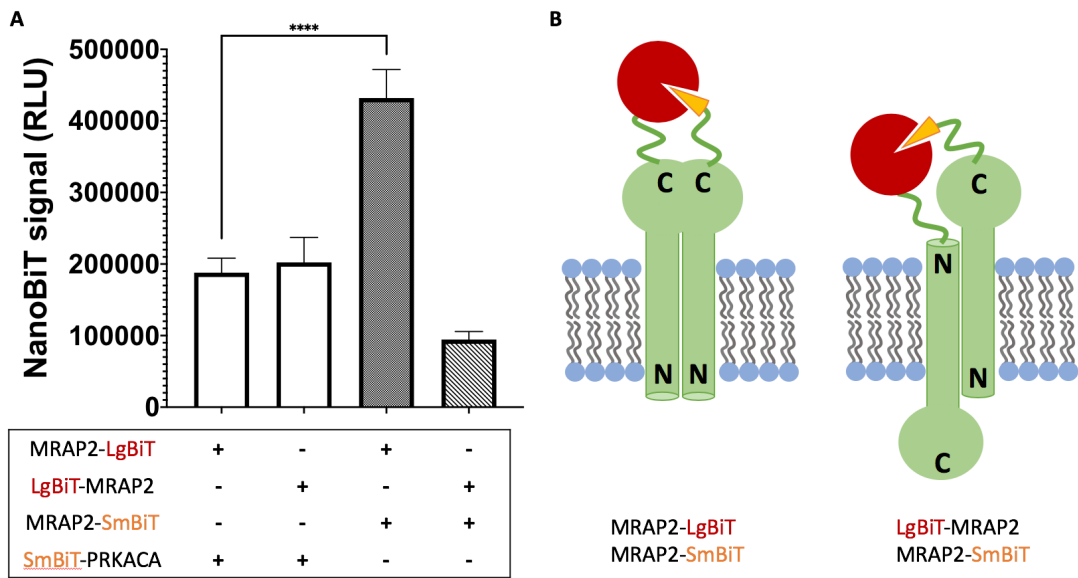
Figure 5 MRAP2 forms parallel dimers or higher order oligomers. A, NanoBiT signal from live cells co-expressing MRAP2-SmBiT with MRAP-LgBiT or MRAP2-SmBiT with LgBiT-MRAP2. SmBiT-PRKACA is a cytosolic control construct with SmBiT fused to cAMP-dependent protein kinase catalytic subunit alpha. Bars include data from 8 or 9 experiments. B, Schematic showing reconstituted NanoLuc luciferase from MRAP2 parallel dimers (left) and anti-parallel dimers (right) Error bars are SEM. ****$p < 0.0001$

To determine whether MRAP2 forms higher order oligomers, whole-cell cross-linking and blue native polyacrylamide gel electrophoresis were employed. Whole-cells expressing FLAG-MRAP2 were cross-linked with a membrane-permeable, lysine-reactive cross-linker and the resulting whole cell lysates were analyzed by SDS-PAGE and western blotting (Figure 6A). The presence of higher molecular weight bands with the apparent molecular weights of cross-linked dimeric and trimeric MRAP2 suggests that MRAP2 forms higher order oligomers that can be cross-linked in whole cells. MRAP2 containing lysates from non-cross-linked cells were also separated on a

polyacrylamide gel under native conditions with varying concentrations of *n*-dodecyl-ß-maltoside detergent (Figure 6B). Consistent with the cross-linking results, non-cross-linked MRAP2 forms higher molecular weight structures. These structures are most likely dimers, tetramers, and octamers based on the molecular weights of the bands. In summary, these results indicate that MRAP2 forms parallel dimers and higher order oligomers such that the C-terminal domains of MRAP2 proteins are in close proximity in the membrane (Figure 6C).
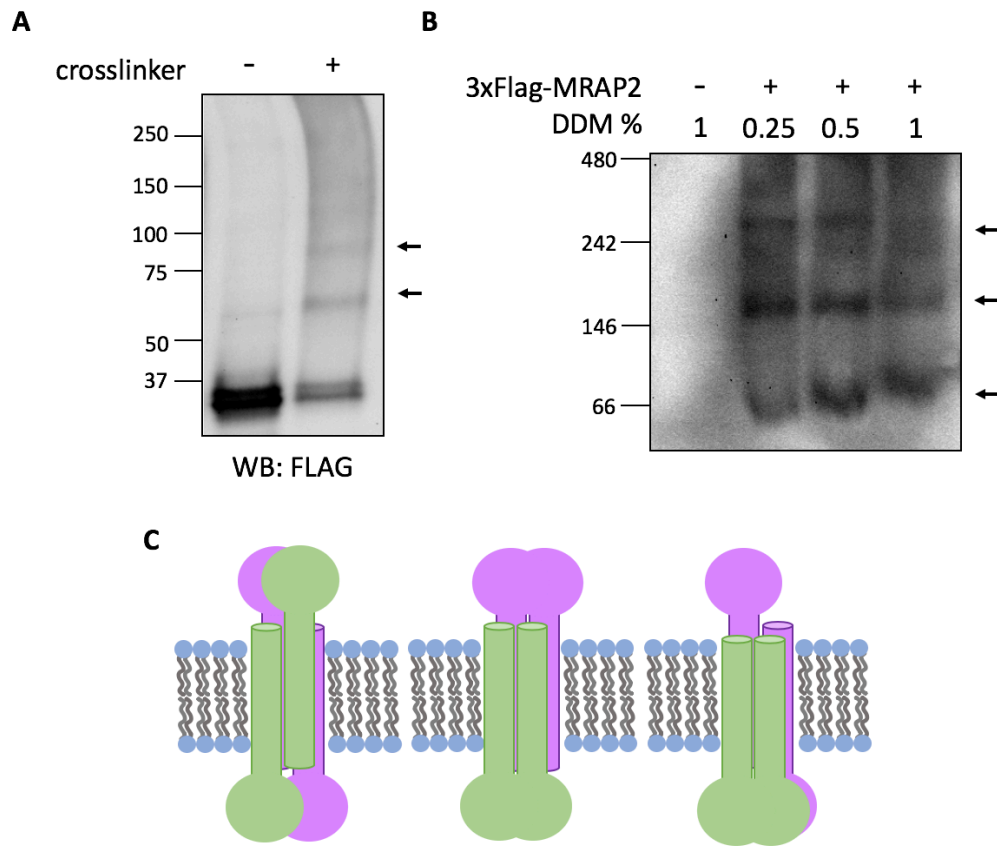
Figure 6 MRAP2 forms higher order oligomers. A, HEK293T cells transfected with FLAG-MRAP2 were incubated with an irreversible cross-linker (DSG or DSS). Proteins in cell lysate were separated by SDS-PAGE and immunoblotted. B, HEK293T cells expressing FLAG-MRAP2 were solubilized with varying concentrations of *n*-dodecyl-ß-maltoside (DDM) and analyzed by blue native PAGE and immunoblotted. The band around 66 kDa is the approximately the molecular weight of a FLAG-MRAP2 dimer. C, Schematic showing possible MRAP2 higher order oligomers.

Discussion

The N-terminal and transmembrane domains of MRAP2 and MRAP1 are highly conserved and the N-terminal domain of MRAP1 is essential for its dual topology and homodimerization. However, we show that the mechanism that regulates MRAP2

dimerization is distinct from that of MRAP1. Deletion of the conserved polybasic motif

that dictates MRAP1's membrane orientation from MRAP2 does not abolish dual

membrane orientation nor dimerization of MRAP2. The "positive-inside" rule that

predicts the orientation of transmembrane domains is based on approximately 15

residues on either side of the transmembrane domain and establishes that the more

positively-charged side will end up on the cytosolic side of the plasma membrane [18,19].

In fact, single point mutations in dual topology membrane proteins from bacteria that

have a near zero charge bias can shift the orientations of these proteins[25]. Previous

experiments that investigated MRAP1's membrane topology are consistent with both

the positive-inside rule and algorithms that predict transmembrane helices and

membrane topology such as TMHMM[26] (Figure 7). Around half of MRAP1 is

glycosylated, supporting the fact that MRAP1 can be inserted into the membrane in

both N_{exo}/C_{cyto} and N_{cyto}/C_{exo} orientations. MRAP1's dual topology has also been

validated by bimolecular fluorescence complementation experiments and the

presence of both N- and C-terminal antibody epitopes on the cell surface [15]. Based on

the positive-inside rule and computational predictions, MRAP2 is predicted to favor a

N_{cyto}/C_{exo} orientation. However, this study, along with previous studies[16] support

MRAP2 having dual topology, contrary to the predicted N_{cyto}/C_{exo} orientation.

MRAP2's dual topology defies the positive-inside rule. Our study reveals that the

molecular features that dictate MRAP1 and MRAP2 orientations are distinctly

different. These differences between MRAP1 and MRAP2 highlight the importance of

identifying the mechanism behind MRAP2's dual topology and this will be the subject
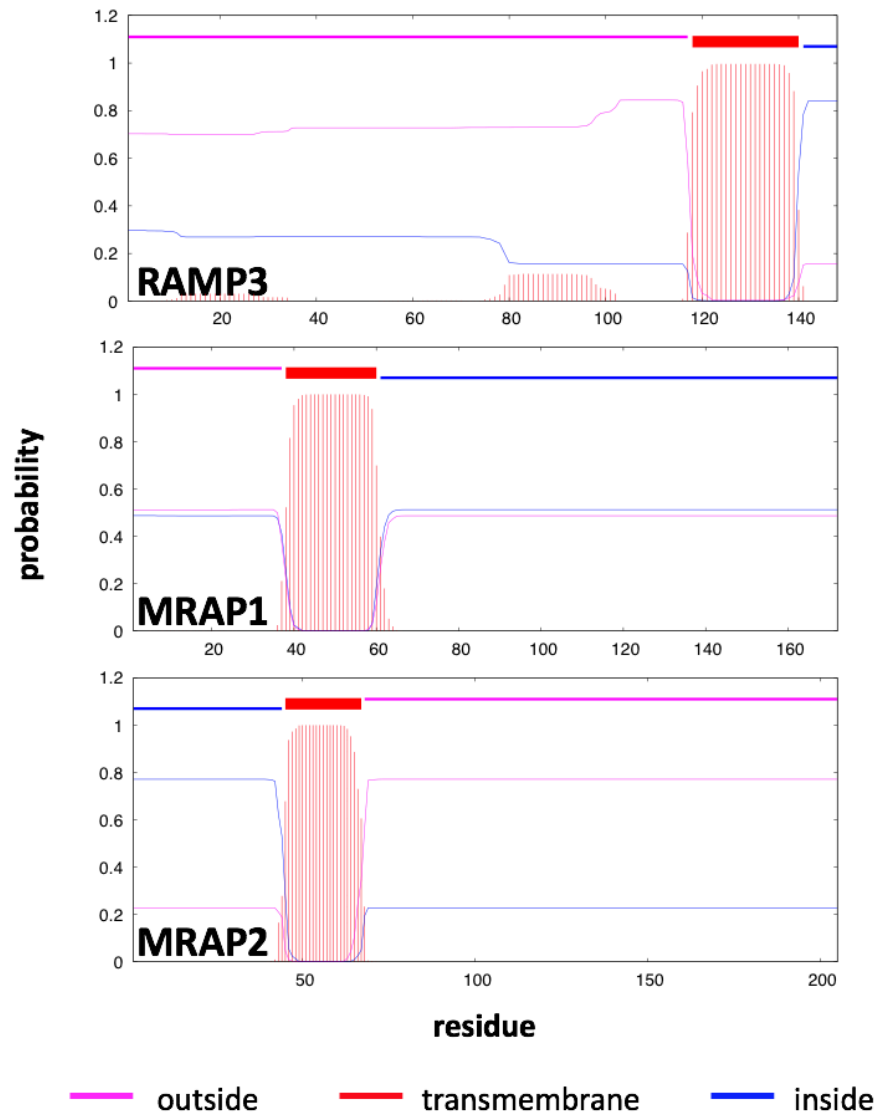
of future studies.

Figure 7 MRAP2 is predicted to favor an N$_{cyto}$/C$_{exo}$ orientation. The transmembrane helix and topology for RAMP3, MRAP1, and MRAP2 were predicted using TMHMM2.0.

MRAP2 has been shown to co-immunoprecipitate with several GPCRs including all five melanocortin receptors, the orexin receptor 1 (OX1R), the prokineticin receptor 1 (PKR1), and the growth hormone secretagogue receptor 1a (GHSR1a)[9–12,17]. The C-terminal domain of MRAP2 is highly conserved and is necessary for modulation of OX1R, PKR1, and GHSR1a[10,12]. While there is sufficient evidence pointing towards the C-terminus of MRAP2 as being the most important domain for the regulation of GPCRs, until this point, the regions of MRAP2 that are essential for its homodimerization have not been identified. In this study, we show that MRAP2 dimerizes through its transmembrane domain. Interestingly, the transmembrane domain of MRAP2 does not appear to be necessary for OX1R and PKR1 inhibition, but has been shown to be play a role in potentiating GHSR1a signaling[10,12]. An obesity-linked mutation within the transmembrane of MRAP2 has also been reported[4]. Additionally, the transmembrane domain of MRAP1 is essential for MC2R trafficking[13,14]. RAMP1 dimers are inhibited by the presence of the calcitonin receptor-like receptor (CRLR) and RAMP1 forms heterodimers with CRLR at a 1:1 ratio, suggesting that RAMP1 interacts with this receptor as a monomer[27]. A series of MRAP-MC2R or MRAP-MRAP-MC2R fusion proteins were used by Malik et al. to show that MRAP1 dimers were required for MC2R activity[28]. It will be interesting to see if MRAP2 dimerization is required for function in the same manner as MRAP1 or if MRAP2 binds to GPCRs as a monomer like RAMP1. Since MRAP2 is somewhat promiscuous and appears to interact with several GPCRs, it is possible that the oligomeric state of

functional MRAP2 is GPCR-specific. Further experimentation is needed to determine whether MRAP2 dimerization is necessary for its modulation of GPCRs, as well as to identify motifs or residues within the transmembrane domain that facilitate dimerization. Transmembrane helix-packing motifs that consist of small residues occurring every four or seven residues have been identified[21,22,29]. EmrE, a small bacterial multidrug transporter, forms antiparallel dimers through conserved glycine residues[30]. However, we find that the glycine residues within MRAP2's transmembrane domain are not required for dimerization.

Bimolecular fluorescence complementation experiments that incorporate yellow fluorescent protein (YFP) fragments on the N- and C-terminal ends of MRAP1 show that MRAP1 forms exclusively anti-parallel dimers since YFP can only be reconstituted when fragments are on opposite ends and there is no YFP complementation when fragments are place on the same ends of MRAP1[13,14,16]. Similar experiments have been performed for MRAP2 supporting anti-parallel MRAP2 dimers. However, there have been no experiments ruling out a parallel orientation for MRAP2 dimers. Surprisingly, we find that the C-terminal domains of MRAP2 are in close proximity in live cells. This suggests that MRAP2 forms parallel dimers or oligomerizes in such a way that brings the C-terminal domains in close proximity. It is important to note that the absence of data supporting an anti-parallel MRAP2 dimer in our experiments does not eliminate the possibility that MRAP2 can form anti-parallel dimers, rather, it is possible that the

linkers used in our NanoBiT experiments prevent an N- to C-terminal interaction from occurring.

We also present evidence for higher-order MRAP2 oligomers that may also explain the presence of parallel MRAP2 dimers. At this juncture, it is not clear whether these higher order oligomers are required for function and it is possible that the oligomeric state of MRAP2 is dependent on the local environment that it exists in. MRAP2 has been shown to form dimers that are resistant to reducing and denaturing conditions from mouse tissue immunoblots[17]. Similarly, the proteolipid protein (PLP), an abundant CNS myelin protein important for the stabilization of myelin membranes, also forms SDS-resistant dimers in the ER[31]. PLP forms higher order oligomers only after reaching the cell surface. An attractive hypothesis is that MRAP2 facilitates the trafficking of GPCRs to the cell surface and once at the cell surface, the changes in MRAP2's oligomeric state could act as a molecular switch to tune its regulation over GPCRs.

Currently, there is very little information regarding MRAP2 structure and it is not uncommon for single-pass transmembrane proteins to have intrinsically disordered domains making them difficult to study using classic biophysical techniques [32]. These disordered regions often have functional importance since this flexibility allows them to interact with multiple protein partners. While the transmembrane domain of

MRAP2 is most likely a transmembrane helix, there is very little predicted secondary structure in the N- and C-terminal domains. Since MRAP2 has been shown to interact with several receptors, it is possible that in the presence of these receptors, MRAP2 adopts a more rigid conformation allowing high resolution structures to become more obtainable.

MRAP2 and MRAP1 are the only known eukaryotic proteins that adopt a highly unique dual topology in the membrane. While the N-termini and transmembrane domains of these homologs are highly conserved, we show key differences between MRAP2 and MRAP1 membrane orientation and oligomerization. We provide evidence for the transmembrane domain as being the minimal dimerization domain and identify a new parallel orientation for MRAP2 oligomers. Elucidating the molecular framework behind MRAP2 structure will give insight into the mechanisms by which other single-pass transmembrane proteins and accessory proteins modulate their receptors. Furthermore, given the essential role of MRAP2 in the modulation of GPCRs that are critical for the maintenance of energy homeostasis, understanding the structure of MRAP2 will aid in unraveling the complex neural circuitry responsible for the central regulation of energy balance.

Experimental Procedures

Expression Constructs.

3xFlag-tagged wild-type MRAP2 constructs are in pSF vectors and 3xHA-tagged RAMP3 expression constructs are in pcDNA3.1 vectors. Wild-type expression constructs were kindly provided by Dr. Roger Cone (University of Michigan, Life Science Institute, Ann Arbor, MI). Mutations in MRAP2 constructs were generated using PCR primer-based site-directed mutagenesis, using primers generated manually and by www.primerdesigner.com[23]. NanoBit vectors were purchased from Promega (Madison, WI). MRAP2 was cloned into NanoBiT vectors by directional cloning with the following restriction sites : SacI and XhoI for C-terminal LgBiT and SmBiT, SacI and NheI for N-terminal LgBiT and SmBiT. All constructs were verified by DNA sequencing.

Cell culture and transfections.

HEK293T cells (ATCC CRL-3216, Lot # 62729596) were cultured in Dulbecco's Modified Eagles Medium (DMEM) and CHO cells were cultured in F-12 medium. Both cell lines were cultured in media supplemented with 10% fetal bovine serum and GlutaMAX from Life Technologies (Carlsbad, CA) at 37 °C in 5% CO_2. Cells were transfected with Lipofectamine 2000 DNA transfection reagent from Invitrogen (Carlsbad, CA) 18-24 hours after plating. All experiments were performed 24 hours post-transfection.

Co-immunoprecipitation and western blot.

HEK293T cells were co-transfected with N-terminally HA-tagged and N-terminally Flag-tagged MRAP2 wild-type or mutant constructs using Lipofectamine 2000 following manufacturer's instructions. After 24 hours post-transfection, cells were washed with ice-cold phosphate buffered saline (PBS, pH 7.4) and lysed with 0.2% *n*-dodecyl-ß-maltoside (DDM) in PBS with EDTA and HALT protease inhibitors (Pierce Biotechnology, Rockford, IL) added. The lysed cells were incubated on ice for 30 minutes and the lysate was clarified at 17,000 x g at 4°C for 25 minutes. Protein concentrations were determined using a BCA protein quantitation kit (Pierce Biotechnology, Rockford, IL) according to the manufacturer's instructions. Samples treated with PNGase F (New England Biolabs, Ipswich, MA) were treated according to the manufacturer's instructions under denaturing reaction conditions. For immunoprecipitations, lysates were incubated with either anti-FLAG M2 agarose beads (Sigma-Aldrich, St. Louis, MO) or anti-HA HA-7 agarose beads (Sigma-Aldrich, St. Louis, MO) overnight at 4°C with end-over-end mixing. The same volume of lysate was used for anti-Flag and anti-HA pull-downs. The beads were washed four times with 0.1% % DDM in PBS. The protein from the beads were either eluted with Laemmli buffer with DTT and boiled for 5 mins or eluted with Laemmli buffer without DTT and reduced with DTT for 30 minutes at 37 °C after separating the beads from the sample. The eluted proteins or whole cell lysates were separated by SDS-polyacrylamide gel electrophoresis on a 4-20% gradient gel (Bio-Rad Laboratories, Hercules, CA) and transferred to polyvinylidene fluoride (PVDF) membranes. The membranes were

blocked overnight at 4°C with 5% bovine serum albumin (BSA) in tris-buffered saline with 0.1% Tween-20 (TBST). Either mouse M2 Flag or mouse HA-7 primary antibodies (Sigma-Aldrich, St. Louis, MO) were used at a 1:1000 dilution in 2.5% BSA in TBST for 1 hour at room temperature. The blots were washed (4X, 3 min) with TBST. A secondary goat anti-mouse HRP (horse radish peroxidase)-conjugated antibody (Abcam, Cambridge, United Kingdom) was used at a 1:10,000 dilution for 1 hour at room temperature. The blots were washed (4X, 3 min) with TBST before adding the ECL western blotting substrate (Pierce Biotechnology, Rockford, IL). The blots were imaged using a ChemiDoc™ XRS+ System and analyzed using Image Lab™ Software (Bio-Rad Laboratories, Hercules, CA).

Immunostaining and confocal microscopy

HEK293T cells were plated in 8-well chamber slides (ibidi GmbH, Martinsreid, Planegg, Germany) previously coated with poly-D-lysine. Cells were transfected with either N-terminally Flag-tagged MRAP2 or MRAP2 Δ38-44 and C-terminally Flag-tagged MRAP2 or MRAP2 Δ38-44. After 24 hours post-transfection, transfected cells were washed twice with ice-cold PBS and fixed with 2% formaldehyde in PBS for 10 minutes at room temperature. Cells were washed with PBS (3X, 5 min) and permeabilized samples were incubated with 0.5% saponin in PBS for 10 minutes. Unpermeabilized cells were incubated with PBS for 10 minutes. Cells were washed with PBS (3X, 5 min). Cells were then blocked with 1% BSA in PBS for unpermeabilized cells or 1% BSA, 0.1% saponin

in PBS for permeabilized cells for 30 minutes. Blocked cells were then incubated with a mouse M2 Flag antibody (Sigma-Aldrich, St. Louis, MO) at a 1:600 dilution in 1% BSA in PBS for 1 hour. Cells were washed again with PBS (3X, 5 min) and incubated with a goat anti-mouse Alexa 568 antibody (highly cross adsorbed) (Invitrogen, Carlsbad, CA) at a 1:1000 dilution in 1% BSA in PBS for 1 hr in the dark. Cell were washed with PBS (3X, 5 min), stained with Hoechst 33342 (5 ug/mL) (Invitrogen, Carlsbad, CA) for 1 min, washed with PBS again (3X, 5 min) and slides were mounted with Fluoromount-G mounting medium (SouthernBiotech, Birmingham, AL). Images were acquired on a Leica SP5 confocal microscope and analyzed by Fiji ImageJ.

Immunostaining and flow cytometry.

HEK293T cells were transfected with either N-terminally Flag-tagged MRAP2 or MRAP2 Δ38-44, C-terminally Flag-tagged MRAP2 or MRAP2 Δ38-44, N-terminally HA-tagged RAMP3, or C-terminally HA-tagged RAMP3. After 24 hours post-transfection, transfected cells were washed twice with ice-cold PBS and fixed with 2% formaldehyde in PBS for 15 minutes at room temperature. Fixed cells were then washed twice with PBS and split into two separate samples. Each of the samples was further washed with either FACS buffer without Triton X-100 (PBS pH 7.4 with 1% BSA, 1 mM EDTA, 0.05% sodium azide) for non-permeabilized samples or FACS buffer with Triton X-100 (PBS pH 7.4 with 1% BSA, 1 mM EDTA, 0.05% sodium azide, 0.1% Triton X-100) for permeabilized samples. Unpermeabilized cells were resuspended in FACS

buffer and permeabilized cells were resuspended in FACS buffer with Triton X-100. Alexa Fluor 488 conjugated anti-HA (Cell Signaling Technologies #2350, Danvers, MA) or anti-FLAG (Cell Signaling Technologies #15008, Danvers, MA) antibodies were added at a 1:50 dilution and cell were incubated with the fluorescent antibodies for 1 hour in the dark at 4°C. Stained cells were then washed with FACS buffer three times and resuspended in FACS buffer before flow analysis. Cells were analyzed on a BD LSRII and 10,000 cells were counted and analyzed for each sample. FlowJo was used for data processing. The median fluorescence intensity (MFI) value for the unpermeabilized cells was divided by the MFI of the permeabilized samples to normalize for differences in protein expression levels.

NanoBiT protein-protein interaction assay.

HEK293T cells were plated in an opaque, white 96-well plate. Cells were transfected with Lipofectamine 2000 according to manufacturer's instructions. After 24 hours post-transfection, media is removed and replaced with Opti-MEM (Life Technologies, Carlsbad, CA). NanoBiT live-cell substrate was added according to manufacturer's instructions and incubated for 5 minutes. Luminescence was measured using a Perkin-Elmer EnVision plate reader.

Whole-cell cross-linking.

HEK293T cells were transfected with 3xFlag-MRAP2. After 24 hours post-transfection, cells were washed with PBS and incubated with 1 mM disuccinimidyl suberate or disuccinimidyl glutarate (Thermo Fisher) in PBS for 30 minutes at room temperature. The cross-linking reaction was quenched with 30 mM Tris-HCl in PBS for 10 minutes. Cells were then pelleted and washed with 30 mM Tris-HCl in PBS. The washed cell pellet was lysed with 1% DDM in PBS and analyzed by SDS-PAGE and western blotting as described in the *co-immunoprecipitation and western blot* section.

Native protein gel electrophoresis and western blot.

HEK293T cells were transfected with 3xFlag-MRAP2. At 24 hours post-transfection, cells were washed with PBS and lysed with a native lysis buffer (50 mM BisTris pH 7.2, 50 mM NaCl, 10% glycerol) with protease inhibitors and varying concentrations of DDM for 30 minutes on ice. Lysates were clarified at 17,000 x g at 4°C for 25 minutes. Protein concentrations were determine using a BCA protein quantitation kit (Pierce Biotechnology, Rockford, IL) according to the manufacturer's instructions. A 10x loading dye (5% w/v Coomassie blue G-250, 500 mM 6-aminohexanoic acid) was added to lysates right before loading samples into a NativePAGE Bis-Tris gel 4-16% (Life Technologies). The proteins were separated according to Wittig et al.[24] and transferred onto a PVDF membrane using a standard Tris-glycine transfer buffer with 0.05% SDS. The membrane was de-stained in methanol for 3 minutes. The membrane

was blocked and immunoblotted as described in the *co-immunoprecipitation and western blot* section.

References

(1) Asai, M.; Ramachandrappa, S.; Joachim, M.; Shen, Y.; Zhang, R.; Nuthalapati, N.; Ramanathan, V.; Strochlic, D. E.; Ferket, P.; Linhart, K.; Ho, C.; Novoselova, T. V.; Garg, S.; Ridderstråle, M.; Marcus, C.; Hirschhorn, J. N.; Keogh, J. M.; O'Rahilly, S.; Chan, L. F.; Clark, A. J.; Farooqi, I. S.; Majzoub, J. A. Loss of Function of the Melanocortin 2 Receptor Accessory Protein 2 Is Associated with Mammalian Obesity. *Science* **2013**, *341* (6143), 275–278.

(2) Geets, E.; Zegers, D.; Beckers, S.; Verrijken, A.; Massa, G.; Van Hoorenbeeck, K.; Verhulst, S.; Van Gaal, L.; Van Hul, W. Copy Number Variation (CNV) Analysis and Mutation Analysis of the 6q14.1–6q16.3 Genes SIM1 and MRAP2 in Prader Willi like Patients. *Molecular Genetics and Metabolism* **2016**, *117* (3), 383–388.

(3) Schonnop, L.; Kleinau, G.; Herrfurth, N.; Volckmar, A.-L.; Cetindag, C.; Müller, A.; Peters, T.; Herpertz, S.; Antel, J.; Hebebrand, J.; Biebermann, H.; Hinney, A. Decreased Melanocortin-4 Receptor Function Conferred by an Infrequent Variant at the Human Melanocortin Receptor Accessory Protein 2 Gene. *Obesity* **2016**, *24* (9), 1976–1982.

(4) Baron, M.; Maillet, J.; Huyvaert, M.; Dechaume, A.; Boutry, R.; Loiselle, H.; Durand, E.; Toussaint, B.; Vaillant, E.; Philippe, J.; Thomas, J.; Ghulam, A.; Franc, S.;

Charpentier, G.; Borys, J.-M.; Lévy-Marchal, C.; Tauber, M.; Scharfmann, R.; Weill, J.; Aubert, C.; Kerr-Conte, J.; Pattou, F.; Roussel, R.; Balkau, B.; Marre, M.; Boissel, M.; Derhourhi, M.; Gaget, S.; Canouil, M.; Froguel, P.; Bonnefond, A. Loss-of-Function Mutations in MRAP2 Are Pathogenic in Hyperphagic Obesity with Hyperglycemia and Hypertension. *Nature Medicine* **2019**, *25* (11), 1733–1738.

(5) Sebag, J. A.; Zhang, C.; Hinkle, P. M.; Bradshaw, A. M.; Cone, R. D. Developmental Control of the Melanocortin-4 Receptor by MRAP2 Proteins in Zebrafish. *Science* **2013**, *341* (6143), 278–281.

(6) Farooqi, I. S.; Yeo, G. S. H.; Keogh, J. M.; Aminian, S.; Jebb, S. A.; Butler, G.; Cheetham, T.; O'Rahilly, S. Dominant and Recessive Inheritance of Morbid Obesity Associated with Melanocortin 4 Receptor Deficiency. *J Clin Invest* **2000**, *106* (2), 271–279.

(7) Vaisse, C.; Clement, K.; Durand, E.; Hercberg, S.; Guy-Grand, B.; Froguel, P. Melanocortin-4 Receptor Mutations Are a Frequent and Heterogeneous Cause of Morbid Obesity. *J Clin Invest* **2000**, *106* (2), 253–262.

(8) Bruschetta, G.; Kim, J. D.; Diano, S.; Chan, L. F. Overexpression of Melanocortin 2 Receptor Accessory Protein 2 (MRAP2) in Adult Paraventricular MC4R Neurons Regulates Energy Intake and Expenditure. *Molecular Metabolism* **2018**.

(9) Chaly, A. L.; Srisai, D.; Gardner, E. E.; Sebag, J. A. The Melanocortin Receptor Accessory Protein 2 Promotes Food Intake through Inhibition of the Prokineticin Receptor-1. *eLife Sciences* **2016**, *5*, e12397.

(10) Rouault, A. A. J.; Lee, A. A.; Sebag, J. A. Regions of MRAP2 Required for the Inhibition of Orexin and Prokineticin Receptor Signaling. *Biochimica et Biophysica Acta (BBA) - Molecular Cell Research* **2017**, *1864* (12), 2322–2329.

(11) Srisai, D.; Yin, T. C.; Lee, A. A.; Rouault, A. A. J.; Pearson, N. A.; Grobe, J. L.; Sebag, J. A. MRAP2 Regulates Ghrelin Receptor Signaling and Hunger Sensing. *Nature Communications* **2017**, *8* (1), 713.

(12) Rouault, A. A. J.; Rosselli-Murai, L. K.; Hernandez, C. C.; Gimenez, L. E.; Tall, G. G.; Sebag, J. A. The GPCR Accessory Protein MRAP2 Regulates Both Biased Signaling and Constitutive Activity of the Ghrelin Receptor GHSR1a. *Sci. Signal.* **2020**, *13* (613).

(13) Sebag, J. A.; Hinkle, P. M. Regions of Melanocortin 2 (MC2) Receptor Accessory Protein Necessary for Dual Topology and MC2 Receptor Trafficking and Signaling. *J Biol Chem* **2009**, *284* (1), 610–618.

(14) Hinkle, P. M.; Sebag, J. A. Structure and Function of the Melanocortin2 Receptor Accessory Protein MRAP. *Mol Cell Endocrinol* **2009**, *300* (1–2), 25–31.

(15) Sebag, J. A.; Hinkle, P. M. Melanocortin-2 Receptor Accessory Protein MRAP Forms Antiparallel Homodimers. *Proc Natl Acad Sci U S A* **2007**, *104* (51), 20244–20249.

(16) Sebag, J. A.; Hinkle, P. M. Regulation of G Protein–Coupled Receptor Signaling: Specific Dominant-Negative Effects of Melanocortin 2 Receptor Accessory Protein 2. *Sci Signal* **2010**, *3* (116), ra28.

(17) Chan, L. F.; Webb, T. R.; Chung, T.-T.; Meimaridou, E.; Cooray, S. N.; Guasti, L.; Chapple, J. P.; Egertová, M.; Elphick, M. R.; Cheetham, M. E.; Metherell, L. A.; Clark, A. J. L. MRAP and MRAP2 Are Bidirectional Regulators of the Melanocortin Receptor Family. *PNAS* **2009**, *106* (15), 6146–6151.

(18) von Heijne, G. The Distribution of Positively Charged Residues in Bacterial Inner Membrane Proteins Correlates with the Trans-Membrane Topology. *The EMBO Journal* **1986**, *5* (11), 3021–3027.

(19) Hartmann, E.; Rapoport, T. A.; Lodish, H. F. Predicting the Orientation of Eukaryotic Membrane-Spanning Proteins. *Proc Natl Acad Sci U S A* **1989**, *86* (15), 5786–5790.

(20) McLatchie, L. M.; Fraser, N. J.; Main, M. J.; Wise, A.; Brown, J.; Thompson, N.; Solari, R.; Lee, M. G.; Foord, S. M. RAMPs Regulate the Transport and Ligand Specificity of the Calcitonin-Receptor-like Receptor. *Nature* **1998**, *393* (6683), 333–339.

(21) Teese, M. G.; Langosch, D. Role of GxxxG Motifs in Transmembrane Domain Interactions. *Biochemistry* **2015**, *54* (33), 5125–5135.

(22) Senes, A.; Gerstein, M.; Engelman, D. M. Statistical Analysis of Amino Acid Patterns in Transmembrane Helices: The GxxxG Motif Occurs Frequently and in Association with β-Branched Residues at Neighboring Positions11Edited by G. von Heijne. *Journal of Molecular Biology* **2000**, *296* (3), 921–936.

(23) Rapp, M.; Granseth, E.; Seppälä, S.; Heijne, G. von. Identification and Evolution of Dual-Topology Membrane Proteins. *Nat Struct Mol Biol* **2006**, *13* (2), 112–116.

(24) Sonnhammer, E. L.; von Heijne, G.; Krogh, A. A Hidden Markov Model for Predicting Transmembrane Helices in Protein Sequences. *Proc Int Conf Intell Syst Mol Biol* **1998**, *6*, 175–182.

(25) Hilairet, S.; Bélanger, C.; Bertrand, J.; Laperrière, A.; Foord, S. M.; Bouvier, M. Agonist-Promoted Internalization of a Ternary Complex between Calcitonin Receptor-like Receptor, Receptor Activity-Modifying Protein 1 (RAMP1), and β-Arrestin. *J. Biol. Chem.* **2001**, *276* (45), 42182–42190.

(26) Malik, S.; Dolan, T. M.; Maben, Z. J.; Hinkle, P. M. Adrenocorticotropic Hormone (ACTH) Responses Require Actions of the Melanocortin-2 Receptor Accessory Protein on the Extracellular Surface of the Plasma Membrane. *J Biol Chem* **2015**, *290* (46), 27972–27985.

(27) Walters, R. F. S.; DeGrado, W. F. Helix-Packing Motifs in Membrane Proteins. *PNAS* **2006**, *103* (37), 13658–13663.

(28) Elbaz, Y.; Salomon, T.; Schuldiner, S. Identification of a Glycine Motif Required for Packing in EmrE, a Multidrug Transporter from Escherichia Coli. *J Biol Chem* **2008**, *283* (18), 12276–12283.

(29) Swanton, E.; Holland, A.; High, S.; Woodman, P. Disease-Associated Mutations Cause Premature Oligomerization of Myelin Proteolipid Protein in the Endoplasmic Reticulum. *PNAS* **2005**, *102* (12), 4342–4347.

(30) Bugge, K.; Lindorff-Larsen, K.; Kragelund, B. B. Understanding Single-Pass Transmembrane Receptor Signaling from a Structural Viewpoint—What Are We Missing? *The FEBS Journal* **2016**, *283* (24), 4424–4451.

(31) K.M. Schilling; C.K. Campilsson. Primer Designer https://primerdesigner.com/

(32) Wittig, I.; Braun, H.-P.; Schägger, H. Blue Native PAGE. *Nature Protocols* **2006**, *1* (1), 418–428.

Chapter 4

Conclusions

Behavioral responses to food deprivation are critical to survival and the circuitry that is responsible for the homeostatic maintenance of energetic state is centered around MC4R signaling. This hardwired system guarantees survival by preventing starvation. Unfortunately, in an environment of caloric abundance, such as the world we live in today, this hardwiring has led to an obesity epidemic. Not surprisingly, MC4R has been seen as a druggable target. Setmelanotide, an MC4R agonist, is on its way to FDA approval to treat POMC and LEPR deficiency [1]. To fully understand MC4R biology, we must also understand the role of MC4R's accessory proteins, syndecan-3 and MRAP2, in MC4R signaling.

Syndecans and AgRP-induced Long-term Feeding

Chapter 2 of this dissertation highlights the significance of AgRP's non-ICK segments as well as sheds light on alternative pathways and the involvement of accessory proteins in AgRP-driven orexigenic effects. We have shown that the duration of AgRP's orexigenic effects are positively correlated with AgRP's positive charge density and therefore, its affinity to heparan sulfate. These results strongly support the role of syndecans in potentiating AgRP signaling. Feeding experiments with SDC3 knock out mice treated with AgRP WT, 4K, and 4Q and imaging-based AgRP localization studies in PVH tissue slices from these mice would likely further support the involvement of syndecan-3. These experiments would allow direct testing of the proposed hypothesis [2].

Despite convincing evidence that syndecan-3 is a key modulator of AgRP's prolonged action, at this juncture, we are unable to completely rule out alternative mechanisms. It is well known that AgRP WT blocks the effects of MTII, an MC3/4R agonist, when co-administered in animals. However, if AgRP is injected 24 hours prior to MTII, AgRP is no longer effective at reversing the effects of MTII [3]. This points to alternative mechanisms for AgRP's prolonged action, other than just antagonism of melanocortin receptor activity. The additional lysine residues in AgRP 4K may have effects at the at the receptor level such as the stabilization of alternative active states of MC3/4R. AgRP 4K may act as a biased agonist at MC4R and enhance the effects of MC4R's regulation over Kir7.1 [4]. The concept of AgRP and its variants as biased agonists can also be extended to other MC4R-dependent mechanism. For example, AgRP 4K may promote endocytosis of MC3/4R through the recruitment of β-arrestins [5]. It is also possible that AgRP's non-ICK segments mediate interactions with an unknown receptor or allosteric site. Of course, additional experiments must be performed to validate these hypotheses.

While the experimental peptide concentrations used in chapter 2 of this dissertation do not reflect physiological concentrations released by AgRP neurons, this work sheds light on strategies for the design of potent orexigenic molecules for the treatment of wasting diseases like cachexia. This work will serve as a template for further studies

aimed at uncovering the molecular mechanisms behind AgRP's non-ICK sequence. Untangling the details of AgRP-driven feeding on a molecular and physiological level will not only aid in the understanding of metabolic dysfunction but also facilitate the design of pharmaceuticals that treat metabolic disease.

MRAP2 Structure and Function

MRAP2 is not only an important accessory protein for MC4R signaling but MRAP2 also regulates the trafficking and signaling of several other GPCRs that are essential for energy homeostasis. A unique feature of MRAP2 is that the protein can exist in the membrane in both orientations such that the N-terminus of the protein can be either intracellular or extracellular [6]. MRAP2 from native tissues also forms detergent resistant dimers [7]. In order to elucidate the mechanism by which MRAP2 modulates MC4R, we must first understand what dictates MRAP2's structure. In chapter 3 of this dissertation, we demonstrate that the conserved polybasic motif that dictates the membrane topology and dimerization of MRAP2's homolog MRAP1 does not control the membrane orientation or dimerization of MRAP2. Additionally, MRAP2 dimerizes through its transmembrane domain and can form higher order oligomers that arrange MRAP2 monomers in a parallel orientation. Through these experiments, we have gained valuable insight on the molecular mechanisms that dictate MRAP2's unusual structure. What still remains unknown is how these structural features of MRAP2 relate to its regulation over MC4R as well its promiscuity as a GPCR accessory protein.

Cell-based MC4R assays that measure cAMP response and ligand binding can be employed along with MRAP2 variants to determine which regions of MRAP2 are necessary for its modulation of MC4R. Hypothalamic AgRP mRNA levels are reduced in mice lacking MRAP2 [8]. It is also unclear whether the presence of MRAP2 changes MC4R's response to AgRP.

We and several others have provided biochemical characterization of MRAP2 structure in terms of membrane orientation and oligomeric state [6,7]. However, high resolution structures generated by either experimental or computational means are nonexistent when it comes to MRAP2. Structural information on single-pass transmembrane proteins has been limited despite the fact that this class of proteins makes up approximately 6% of human genes, which codes for roughly 1300 proteins [9]. Due to the conformational flexibility of single-pass transmembrane proteins, there are currently no high resolution structures of members of this protein family. Fortunately, there are a few high resolution structures of the transmembrane domains of these proteins solved through solution-state NMR [9]. Since we have shown that MRAP2 dimerizes through its transmembrane domain, a high resolution structure of the transmembrane domain in its dimeric state would provide valuable residue-specific information regarding MRAP2's inter-dimer contacts.

MRAP2 trafficking and folding are also of particular interest due to its unique conformation at the cell surface. From studies of MRAP1, it is assumed that MRAP2 trafficking is similar and MRAP2's orientation is fixed early on in biosynthesis [10]. However, the exact mechanisms in regard to MRAP2 folding, membrane threading and trafficking are unknown. Through whole-cell chemical cross-linking and LC-MS/MS peptide mapping, we identified proteins that mediate proper disulfide bond formation in the ER such as endoplasmic reticulum resident protein 44 and thioredoxin related transmembrane protein 1 [11,12] (unpublished, in collaboration with Mike Trnka, UCSF). MRAP2 contains two C-terminal cysteine residues and it possible that intermolecular disulfide bonds are important for MRAP2 oligomerization or that intramolecular disulfides mediate proper folding of the C-terminal domain. Understanding the features that dictate the structure of single-pass transmembrane protein such as MRAP2 will not only shed light on GPCR biology but also aid in deconstructing the complex neural circuit that drives hunger.

References

(1) Clément, K.; Biebermann, H.; Farooqi, I. S.; Ploeg, L.; Wolters, B.; Poitou, C.; Puder, L.; Fiedorek, F.; Gottesdiener, K.; Kleinau, G.; Heyder, N.; Scheerer, P.; Blume-Peytavi, U.; Jahnke, I.; Sharma, S.; Mokrosinski, J.; Wiegand, S.; Müller, A.; Weiß, K.; Mai, K.; Spranger, J.; Grüters, A.; Blankenstein, O.; Krude, H.; Kühnen, P. MC4R Agonism Promotes Durable Weight Loss in Patients with Leptin Receptor Deficiency. *Nature Medicine* **2018**, *24* (5), 551–555.

(2) Zheng, Q.; Zhu, J.; Shanabrough, M.; Borok, E.; Benoit, S. C.; Horvath, T. L.; Clegg, D. J.; Reizes, O. Enhanced Anorexigenic Signaling in Lean Obesity Resistant Syndecan-3 Null Mice. *Neuroscience* **2010**, *171* (4), 1032–1040.

(3) Hagan, M. M.; Benoit, S. C.; Rushing, P. A.; Pritchard, L. M.; Woods, S. C.; Seeley, R. J. Immediate and Prolonged Patterns of Agouti-Related Peptide-(83–132)-Induced c-Fos Activation in Hypothalamic and Extrahypothalamic Sites. *Endocrinology* **2001**, *142* (3), 1050–1056.

(4) Ghamari-Langroudi, M.; Digby, G. J.; Sebag, J. A.; Millhauser, G. L.; Palomino, R.; Matthews, R.; Gillyard, T.; Panaro, B. L.; Tough, I. R.; Cox, H. M.; Denton, J. S.; Cone, R. D. G-Protein-Independent Coupling of MC4R to Kir7.1 in Hypothalamic Neurons. *Nature* **2015**

(5) Breit, A.; Wolff, K.; Kalwa, H.; Jarry, H.; Büch, T.; Gudermann, T. The Natural Inverse Agonist Agouti-Related Protein Induces Arrestin-Mediated Endocytosis of Melanocortin-3 and -4 Receptors. *J. Biol. Chem.* **2006**, *281* (49), 37447–37456.

(6) Sebag, J. A.; Hinkle, P. M. Regulation of G Protein–Coupled Receptor Signaling: Specific Dominant-Negative Effects of Melanocortin 2 Receptor Accessory Protein 2. *Sci Signal* **2010**, *3* (116), ra28.

(7) Chan, L. F.; Webb, T. R.; Chung, T.-T.; Meimaridou, E.; Cooray, S. N.; Guasti, L.; Chapple, J. P.; Egertová, M.; Elphick, M. R.; Cheetham, M. E.; Metherell, L. A.; Clark, A. J. L. MRAP and MRAP2 Are Bidirectional Regulators of the Melanocortin Receptor Family. *PNAS* **2009**, *106* (15), 6146–6151.

(8) Asai, M.; Ramachandrappa, S.; Joachim, M.; Shen, Y.; Zhang, R.; Nuthalapati, N.; Ramanathan, V.; Strochlic, D. E.; Ferket, P.; Linhart, K.; Ho, C.; Novoselova, T. V.; Garg, S.; Ridderstråle, M.; Marcus, C.; Hirschhorn, J. N.; Keogh, J. M.; O'Rahilly, S.; Chan, L. F.; Clark, A. J.; Farooqi, I. S.; Majzoub, J. A. Loss of Function of the Melanocortin 2 Receptor Accessory Protein 2 Is Associated with Mammalian Obesity. *Science* **2013**, *341* (6143), 275–278.

(9) Bugge, K.; Lindorff-Larsen, K.; Kragelund, B. B. Understanding Single-Pass Transmembrane Receptor Signaling from a Structural Viewpoint—What Are We Missing? *The FEBS Journal* **2016**, *283* (24), 4424–4451.

(10) Maben, Z. J.; Malik, S.; Jiang, L. H.; Hinkle, P. M. Dual Topology of the Melanocortin-2 Receptor Accessory Protein Is Stable. *Front. Endocrinol.* **2016**, *7*.

(11) Anelli, T.; Alessio, M.; Mezghrani, A.; Simmen, T.; Talamo, F.; Bachi, A.; Sitia, R. ERp44, a Novel Endoplasmic Reticulum Folding Assistant of the Thioredoxin Family. *EMBO J* **2002**, *21* (4), 835–844.

(12) Anelli, T.; Alessio, M.; Bachi, A.; Bergamelli, L.; Bertoli, G.; Camerini, S.; Mezghrani, A.; Ruffato, E.; Simmen, T.; Sitia, R. Thiol-Mediated Protein Retention in the Endoplasmic Reticulum: The Role of ERp44. *EMBO J* **2003**, *22* (19), 5015–5022.